Exploring for New Physics using Charged Lepton Flavor Violation

Doug Glenzinski

Fermilab

May 2018

Outline

- Motivation & Introduction
- Experimental Summary
- Future Expectations
- Summary

Why Charged Lepton Flavor Violation (CLFV)?

- Quarks mix, ν mix… what about l^+?
  - CLFV : neutrino-less transitions of the type $\mu \rightarrow e$, $\tau \rightarrow e$, $\tau \rightarrow \mu$
- There is no known Global Symmetry that requires LF conservation
- Many extensions to the Standard Model predict large CLFV effects
- CLFV offers opportunity to probe Λ_{NP} ~ O(10^3 -10^4) TeV >> TeV

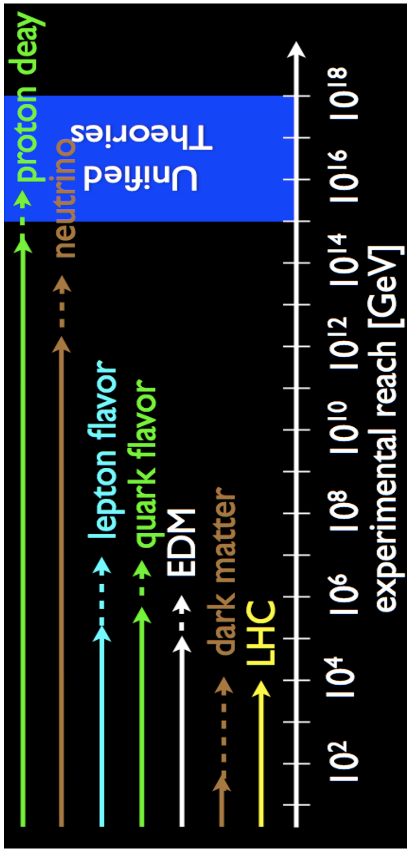

Some CLFV Processes

Process	Current Limit	Next Generation exp
$\tau \rightarrow \mu\eta$	BR < 6.5 E-8	10^{-9} - 10^{-10} (Belle II, LHCb)
$\tau \rightarrow \mu\gamma$	BR < 6.8 E-8	
$\tau \rightarrow \mu\mu\mu$	BR < 3.2 E-8	
$\tau \rightarrow eee$	BR < 3.6 E-8	
$K_L \rightarrow e\mu$	BR < 4.7 E-12	NA62
$K^+ \rightarrow \pi^+ e^- \mu^+$	BR < 1.3 E-11	
$B^0 \rightarrow e\mu$	BR < 7.8 E-8	LHCb, Belle II
$B^+ \rightarrow K^+ e\mu$	BR < 9.1 E-8	
$\mu^+ \rightarrow e^+\gamma$	BR < 4.2 E-13	10^{-14} (MEG)
$\mu^+ \rightarrow e^+e^+e^-$	BR < 1.0 E-12	10^{-16} (PSI)
$\mu^- N \rightarrow e^- N$	$R_{\mu e}$ < 7.0 E-13	10^{-17} (Mu2e, COMET)

(current limits from the PDG)

Expect significant progress in near future

Some CLFV Processes

Process	Current Limit	Next Generation exp
$\tau \rightarrow \mu\eta$	BR < 6.5 E-8	
$\tau \rightarrow \mu\gamma$	BR < 6.8 E-8	10^{-9} - 10^{-10} (Belle II, LHCb)
$\tau \rightarrow \mu\mu\mu$	BR < 3.2 E-8	
$\tau \rightarrow eee$	BR < 3.6 E-8	
$K_L \rightarrow e\mu$	BR < 4.7 E-12	NA62
$K^+ \rightarrow \pi^+ e^- \mu^+$	BR < 1.3 E-11	
$B^0 \rightarrow e\mu$	BR < 7.8 E-8	LHCb, Belle II
$B^+ \rightarrow K^+ e\mu$	BR < 9.1 E-8	
$\mu^+ \rightarrow e^+\gamma$	BR < 4.2 E-13	10^{-14} (MEG)
$\mu^+ \rightarrow e^+e^+e^-$	BR < 1.0 E-12	10^{-16} (PSI)
$\mu^- N \rightarrow e^- N$	$R_{\mu e}$ < 7.0 E-13	10^{-17} (Mu2e, COMET)

(current limits from the PDG)

Experiments using muons among the most sensitive

CLFV in the ν-Standard Model

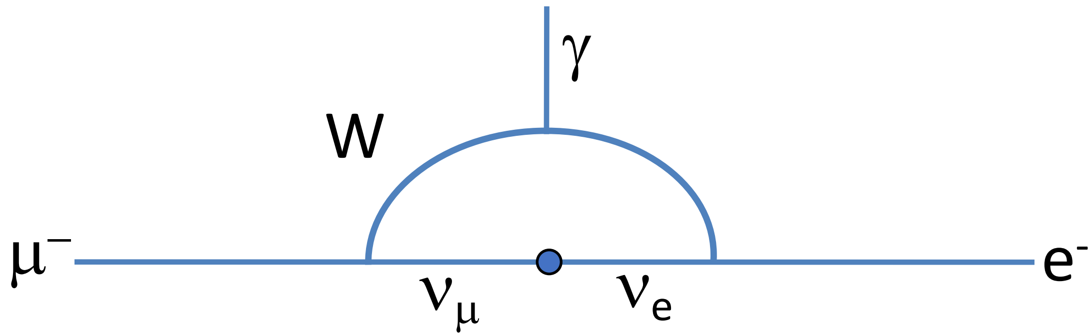

- Extremely suppressed in the Standard Model : rate ~ $\Delta m_{\nu}^{4} / M_{w}^{4} < 10^{-50}$
- Many New Physics models predict rates observable at next generation CLFV experiments
- No SM pollution : Observation is unambiguously New Physics

New Physics Contributions to CLFV

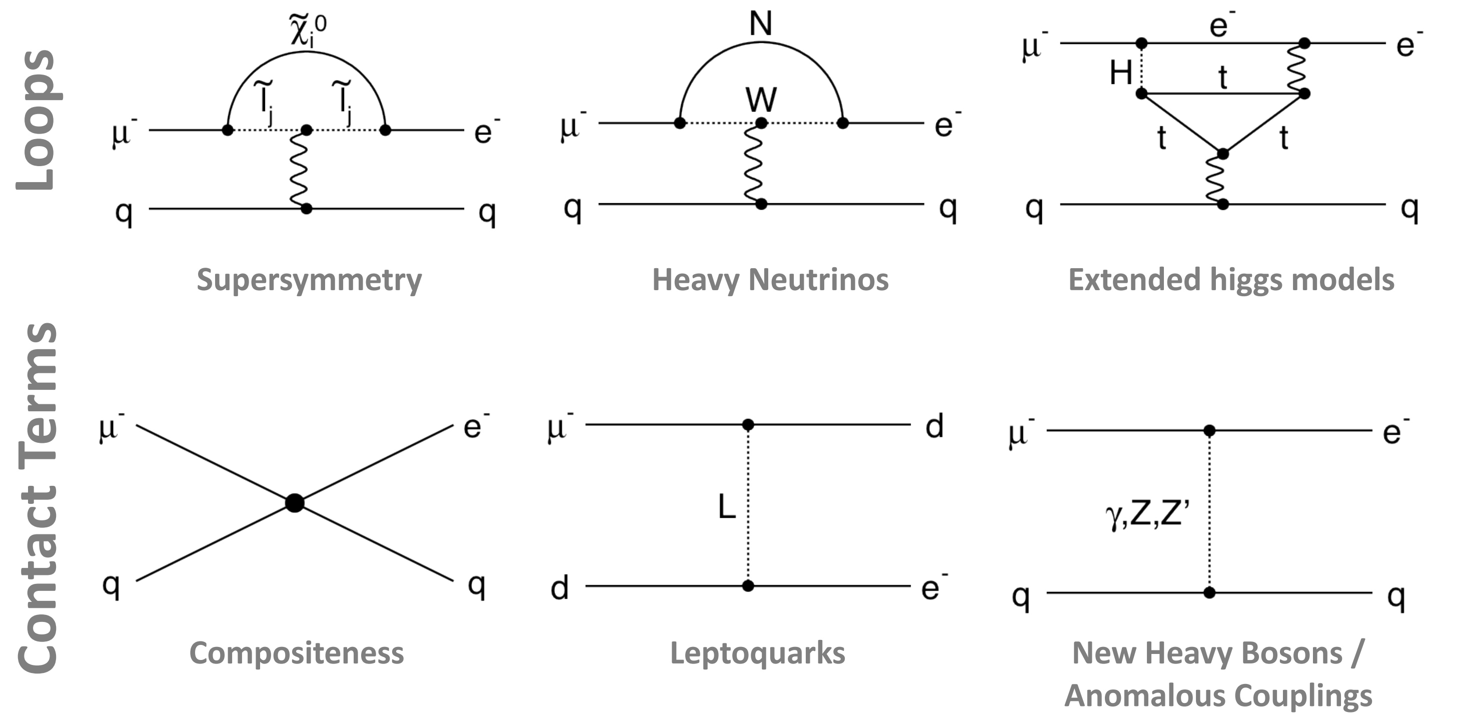

A broad array of New Physics models contribute to CLFV

CLFV Predictions

$\mu^+ \rightarrow e^+\gamma$

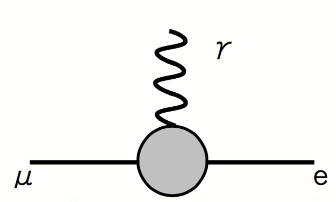

$\mu^+ \rightarrow e^+e^+e^-$

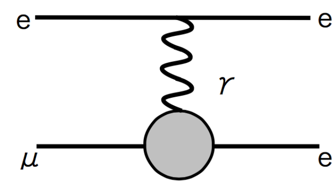

$\mu^- N \rightarrow e^- N$

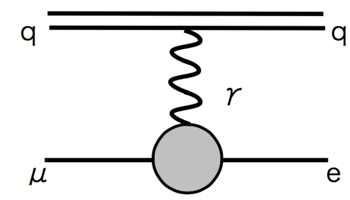

The different channels offer complementary sensitivity.
Their comparison is a powerful model discriminant.

CLFV Predictions

$\mu^+ \rightarrow e^+\gamma$

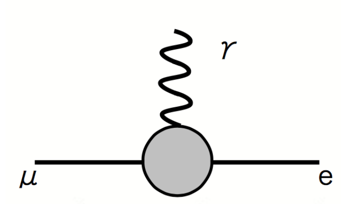

$\mu^+ \rightarrow e^+e^+e^-$

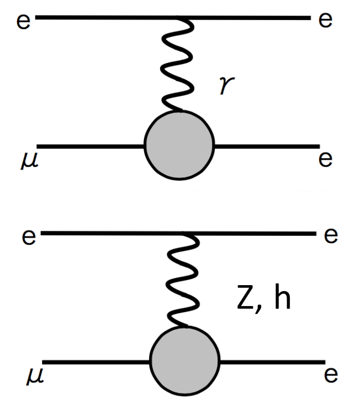

$\mu^-N \rightarrow e^-N$

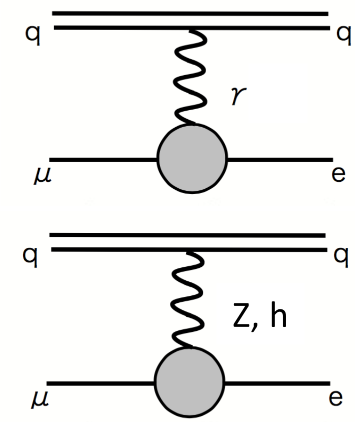

The different channels offer complementary sensitivity.
Their comparison is a powerful model discriminant.

CLFV Predictions

$\mu^+ \rightarrow e^+\gamma$

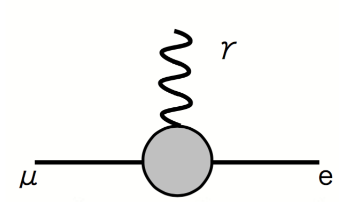

$\mu^+ \rightarrow e^+e^+e^-$

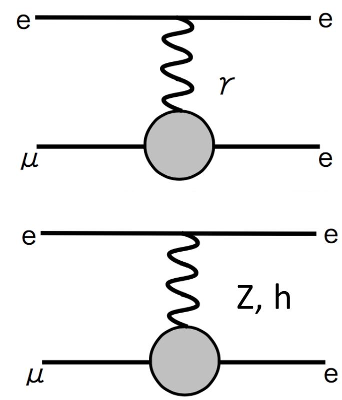

$\mu^- N \rightarrow e^- N$

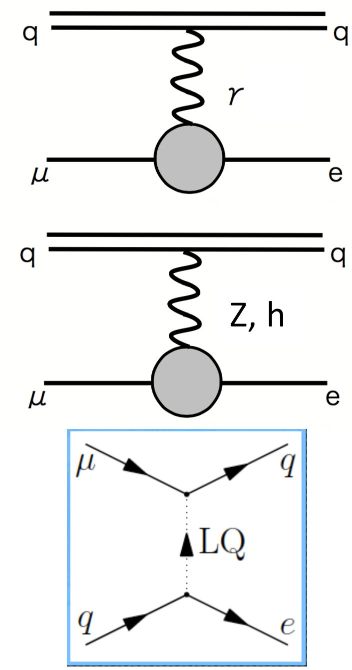

The different channels offer complementary sensitivity.
Their comparison is a powerful model discriminant.

Using CLFV to Determine New Physics

from L. Calibbi and G. Signorelli, Riv. Nuovo Cimento, 41 (2018) 71

Model	$\mu \to eee$	$\mu N \to eN$	$\frac{\mathrm{BR}(\mu\to eee)}{\mathrm{BR}(\mu\to e\gamma)}$	$\frac{\mathrm{CR}(\mu N\to eN)}{\mathrm{BR}(\mu\to e\gamma)}$
MSSM	Loop	Loop	$\approx 6\times 10^{-3}$	$10^{-3} - 10^{-2}$
Type-I seesaw	Loop*	Loop*	$3\times 10^{-3} - 0.3$	0.1–10
Type-II seesaw	Tree	Loop	$(0.1-3)\times 10^{3}$	$\mathcal{O}(10^{-2})$
Type-III seesaw	Tree	Tree	$\approx 10^{3}$	$\mathcal{O}(10^{3})$
LFV Higgs	Loop†	Loop*†	$\approx 10^{-2}$	$\mathcal{O}(0.1)$
Composite Higgs	Loop*	Loop*	$0.05-0.5$	$2-20$

arXiv:1709.00294v2[hep-ph]

TABLE VII. – *Pattern of the relative predictions for the $\mu \to e$ processes as predicted in several models (see the text for details). It is indicated whether the dominant contributions to $\mu \to eee$ and $\mu \to e$ conversion are at the tree or at the loop level; Loop* indicates that there are contributions that dominate over the dipole one, typically giving an enhancement compared to Eq. (40, 41). † A tree-level contribution to this process exists but it is subdominant.*

- The relative rates are model dependent
- Their ratios can be used to probe the underlying theory

CLFV Sensitivity

W. Altmannshofer, A.J.Buras, S.Gori, P.Paradisi, D.M.Straub

★★★ = Discovery Sensitivity

	AC	RVV2	AKM	δLL	FBMSSM	LHT	RS
$D^0-\bar{D}^0$	★★★	★	★	★	★	★★★	?
ϵ_K	★	★★★	★★★	★	★	★★	★★★
$S_{\psi\phi}$	★★★	★★★	★★★	★	★	★★★	★★★
$S_{\phi K_S}$	★★★	★★	★	★★★	★★★	★	?
$A_{\mathrm{CP}}(B\to X_s\gamma)$	★	★	★	★★★	★★★	★	?
$A_{7,8}(B\to K^*\mu^+\mu^-)$	★	★	★	★★★	★★★	★★	?
$A_9(B\to K^*\mu^+\mu^-)$	★	★	★	★	★	★	?
$B\to K^{(*)}\nu\bar{\nu}$	★	★	★	★	★	★	★
$B_s\to\mu^+\mu^-$	★★★	★★★	★★★	★★★	★★★	★	★
$K^+\to\pi^+\nu\bar{\nu}$	★	★	★	★	★	★★★	★★★
$K_L\to\pi^0\nu\bar{\nu}$	★	★	★	★	★	★★★	★★★
$\mu\to e\gamma$	★★★	★★★	★★★	★★★	★★★	★★★	★★★
$\tau\to\mu\gamma$	★★★	★★★	★	★★★	★★★	★★★	★★★
$\mu+N\to e+N$	★★★	★★★	★★★	★★★	★★★	★★★	★★★
d_n	★★★	★★★	★★★	★★	★★★	★	★★★
d_e	★★★	★★★	★★	★	★★★	★	★★★
$(g-2)_\mu$	★★★	★★★	★★	★★★	★★★	★	?

arXiv:0909.1333[hep-ph]

Table 8: "DNA" of flavour physics effects for the most interesting observables in a selection of SUSY and non-SUSY models ★★★ signals large effects, ★★ visible but small effects and ★ implies that the given model does not predict sizable effects in that observable.

CLFV Sensitivity

W. Altmannshofer, A.J.Buras, S.Gori, P.Paradisi, D.M.Straub

	AC	RVV2	AKM	δLL	FBMSSM	LHT	RS
$D^0 - \bar{D}^0$	★★★	★	★	★	★	★★★	?
ϵ_K	★	★★★	★★★	★	★	★★	★★★
$S_{\psi\phi}$	★★★	★★★	★★★	★	★	★★★	★★★
$S_{\phi K_S}$	★★★	★★	★	★★★	★★★	★	?
$A_{\rm CP}(B \to X_s\gamma)$	★	★	★	★★★	★★★	★	?
$A_{7,8}(B \to K^*\mu^+\mu^-)$	★	★	★	★★★	★★★	★★	?
$A_9(B \to K^*\mu^+\mu^-)$	★	★	★	★	★	★	?
$B \to K^{(*)}\nu\bar{\nu}$	★	★	★	★	★	★	★
$B_s \to \mu^+\mu^-$	★★★	★★★	★★★	★★★	★★★	★	★
$K^+ \to \pi^+\nu\bar{\nu}$	★	★	★	★	★	★★★	★★★
$K_L \to \pi^0\nu\bar{\nu}$	★	★	★	★	★	★★★	★★★
$\mu \to e\gamma$	★★★	★★★	★★★	★★★	★★★	★★★	★★★
$\tau \to \mu\gamma$	★★★	★★★	★	★★★	★★★	★★★	★★★
$\mu + N \to e + N$	★★★	★★★	★★★	★★★	★★★	★★★	★★★
d_n	★★★	★★★	★★★	★★	★★★	★	★★★
d_e	★★★	★★★	★★	★	★★★	★	★★★
$(g-2)_\mu$	★★★	★★★	★★	★★★	★★★	★	?

arXiv:0909.1333[hep-ph]

★★★ = Discovery Sensitivity

Table 8: "DNA" of flavour physics effects for the most interesting observables in a selection of SUSY and non-SUSY models ★★★ signals large effects, ★★ visible but small effects and ★ implies that the given model does not predict sizable effects in that observable.

The sensitivity of these experiments is exciting and compelling.

CLFV Experiments using muons

CLFV Experiments using muons

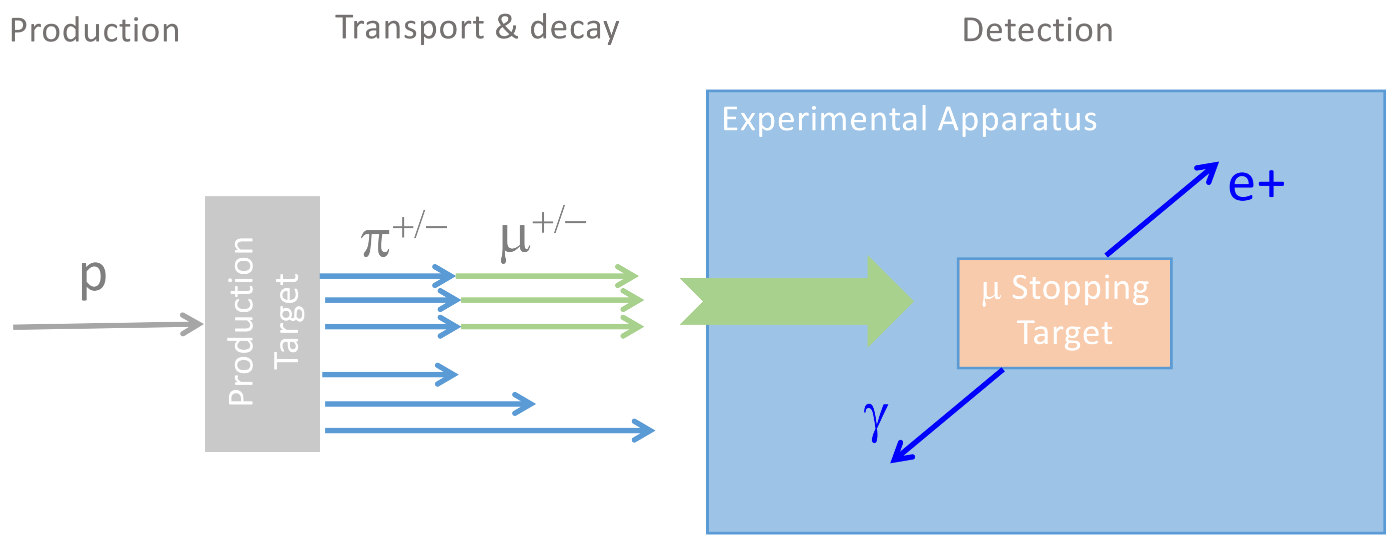

All 3 experiments use the same basic principles

CLFV Experiments using muons

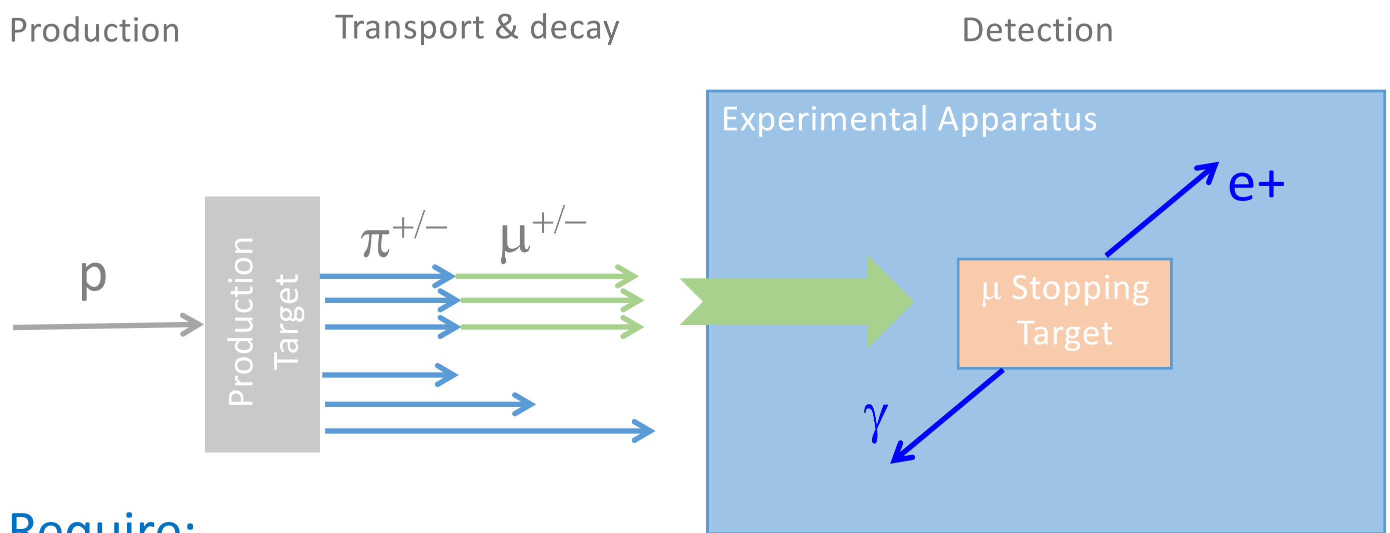

Require:

- High intensity, high purity μ source
- High μ stopping rate
- Detector to precisely measure particles consistent with having originated from stopping target

CLFV Experiments using muons

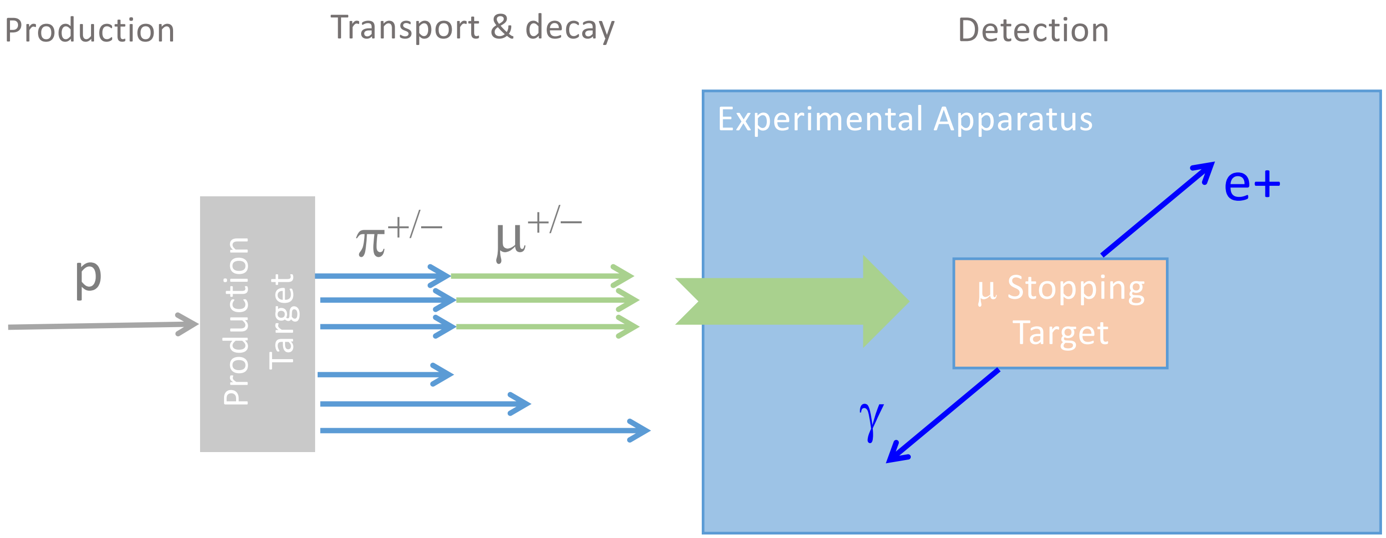

NB. In these experiments, 100 MeV/c is "high momentum"

	P (MeV/c)	E (MeV)	KE (MeV)
e :	100	100	100
μ :	100	145	40
π :	100	170	30

CLFV Experiments using μ^- :
Muon-to-Electron Conversion ($\mu^- N \rightarrow e^- N$)

Muon-to-electron Conversion ($\mu^- N \rightarrow e^- N$)

$$\mu^- N \longrightarrow e^- N$$

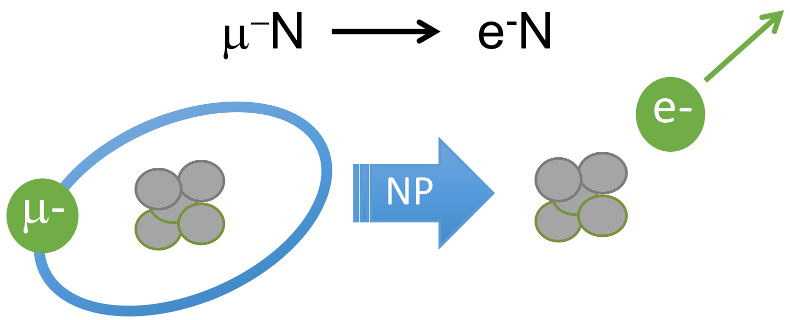

Current State-of-the-art (@ 90% CL) :

$$R_{\mu e} = \frac{\Gamma(\mu^- Au \rightarrow e^- Au)}{\Gamma(\mu^- Au\ capture)} < 7 \times 10^{-13}$$

W. Bertl, et al. (SINDRUM-II) Eur. Phys. J. C47 (2006) 337.

Muon-to-electron Conversion ($\mu^- N \rightarrow e^- N$)

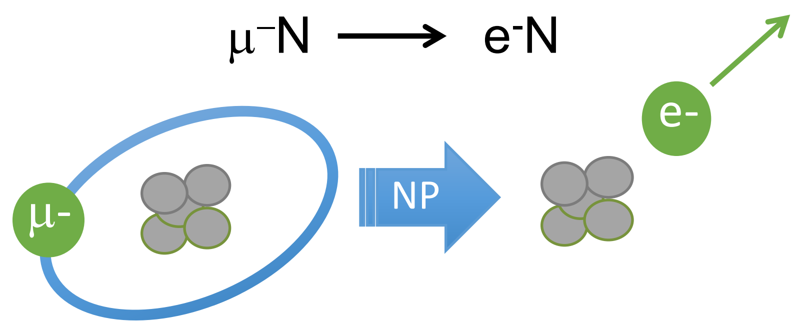

Next generation experiments:

– DeeMee (J-PARC, 3 GeV)	x10	
– Mu2e (Fermilab)	x10,000	Expected improvement (relative to current state-of-the-art)
– COMET (J-PARC, 8 GeV)		
• Phase-I	x10-100	
• Phase-II	x10,000	

Muon-to-electron Conversion ($\mu^{-}N \rightarrow e^{-}N$)

Signal

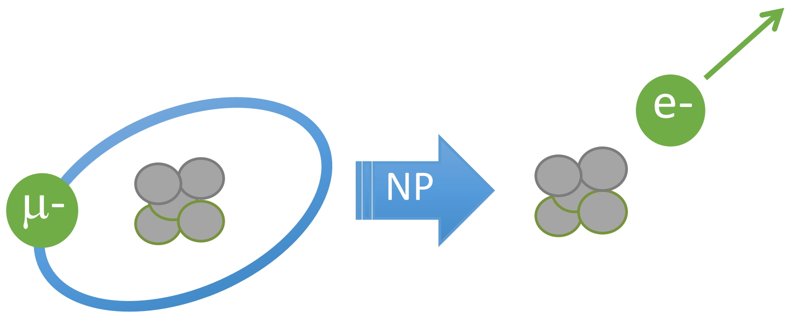

Mono-energetic electron

$E_{\mu e} = m_{\mu} - B(A,Z) - R(A,Z) \sim 105$ MeV

Coherent interaction with nucleus

Background

Decay in Orbit (DIO)
($\mu^{-}N \rightarrow e^{-}\nu\nu N$)

Radiative Pion Capture (RPC)
($\pi^{-}N \rightarrow \gamma N' \rightarrow e^{-}e^{+}N'$)

Cosmogenic

Aside : muonic atoms

- Stopped μ^- is captured in atomic orbit
  - Quickly (~fs) cascades to 1s state
- Bohr radius ~20 fm (for aluminum)
  - Significant overlap of μ^- and N wavefunctions
  - Lifetime of the μ-atom ~few 100 ns for stopping targets of interest
- Once in orbit, 3 things can happen
  - Decay : $\mu^- N(A,Z) \rightarrow e^-\nu\nu\, N(A,Z)$ (background)
  - Capture : $\mu^- N(A,Z) \rightarrow \nu\, N^*(A, Z\text{-}1)$ (normalization)
  - Conversion : $\mu^- N(A,Z) \rightarrow e^-\, N(A,Z)$ (signal)

Aside : muonic atoms

- Stopped μ^- is captured in atomic orbit
  - Quickly (~fs) cascades to 1s state
- Bohr radius ~20 fm (for aluminum)
  - Significant overlap of μ^- and N wavefunctions
  - Lifetime of the μ-atom ~few 100 ns for stopping targets of interest
- Once in orbit, 3 things can happen
  - Decay : $\mu^- N(A,Z) \rightarrow e^- \nu\nu\, N(A,Z)$ (39%)
  - Capture : $\mu^- N(A,Z) \rightarrow \nu\, N^*(A, Z-1)$ (61%)

for an aluminum stopping target

Aside : muonic atoms

- Stopped μ^- is captured in atomic orbit
  - Quickly (~fs) cascades to 1s state
- Bohr radius ~20 fm (for aluminum)
  - Significant overlap of μ^- and N wavefunctions
  - Lifetime of the μ-atom ~few 100 ns for stopping targets of interest
- Once in orbit, 3 things can happen
  - Decay : $\mu^- N(A,Z) \rightarrow e^- \nu\nu N(A,Z)$ (39%)
  - Capture : $\mu^- N(A,Z) \rightarrow \nu N^*(A, Z\text{-}1)$ (61%)

for an aluminum stopping target

Produces 1n, 2γ, 0.1p per capture

One Mu2e Event (500-1695 ns after proton pulse)

Stopping Target Straw Tracker Crystal Calorimeter

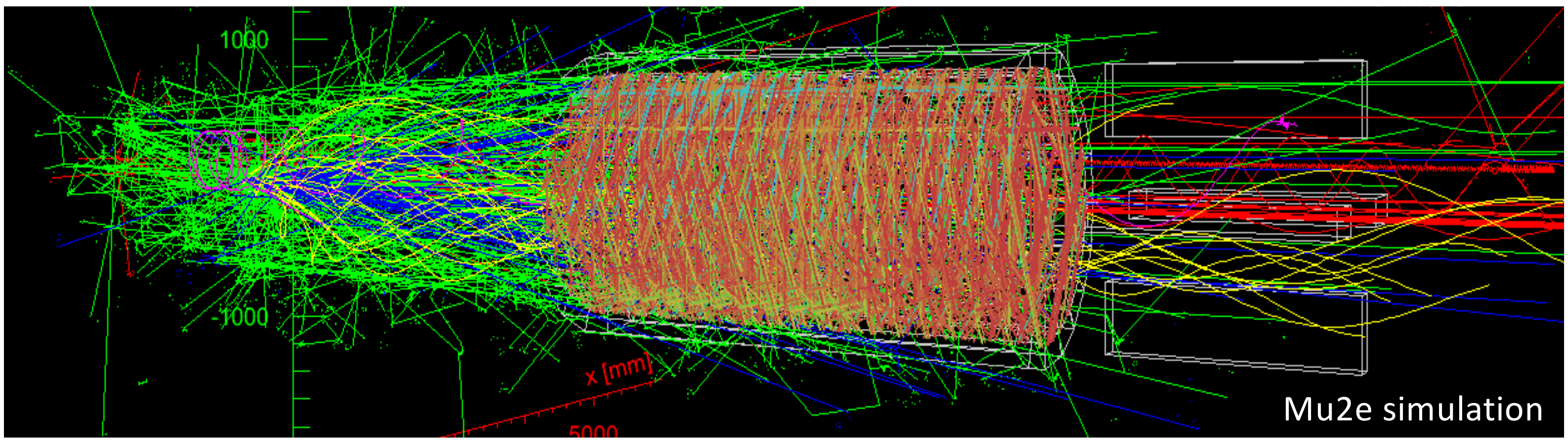

Timing information helps mitigate this

Decay in Orbit Background for ($\mu^{-}N \rightarrow e^{-}N$)

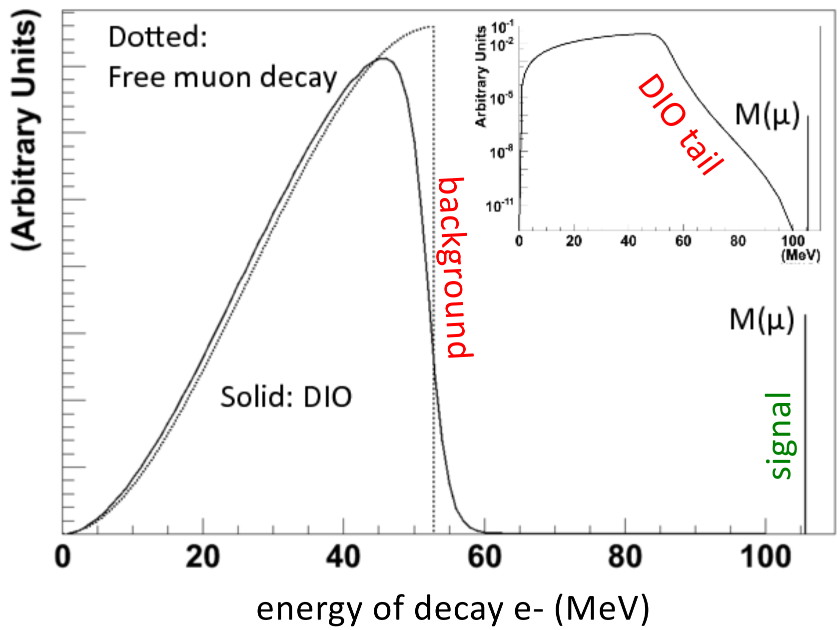

- E_e follows the Michel spectrum… but with a long tail from nuclear recoil $E_{max} = E_{\mu e}$
  - Requires excellent σ_p (<200 keV/c) & FWHM < 1 MeV/c to suppress

Radiative Pion Capture Background for ($\mu^- N \rightarrow e^- N$)

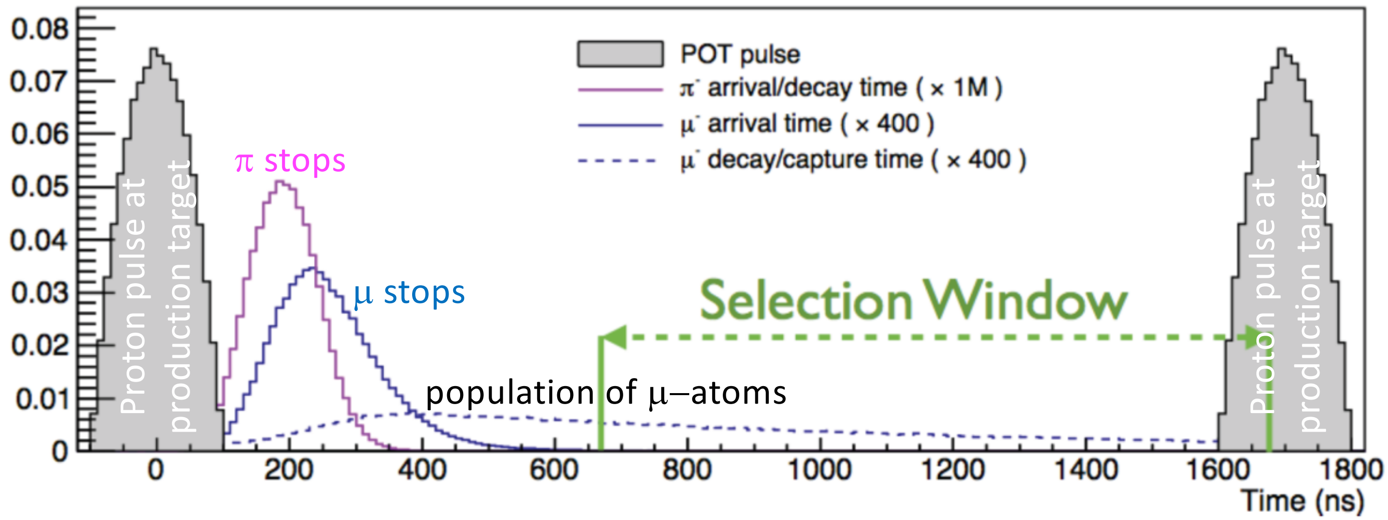

- Pions that survive to the stopping target are promptly captured on the nucleus
  - few% of the time, radiate γ with $E_\gamma \sim m_\mu$
  - Suppressed by 10^9-10^{10} with pulsed proton beam and utilizing a delayed search window while maintaining a high efficiency for signal (~50%)

Muon-to-electron Conversion ($\mu^- N \rightarrow e^- N$)

Signal

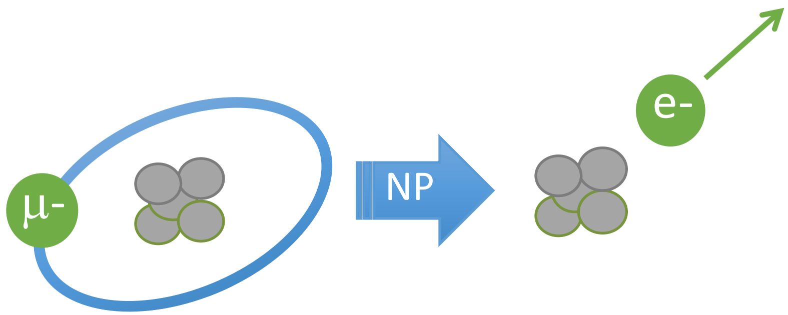

Background

Decay in Orbit (DIO)
($\mu^- N \rightarrow e^- \nu\nu N$)

Radiative Pion Capture (RPC)
($\pi^- N \rightarrow \gamma N'$)

Cosmogenic

Keys to success: excellent spectrometer resolution, pulsed proton beam, high efficiency cosmic veto

Proton Beams for Mu2e and COMET

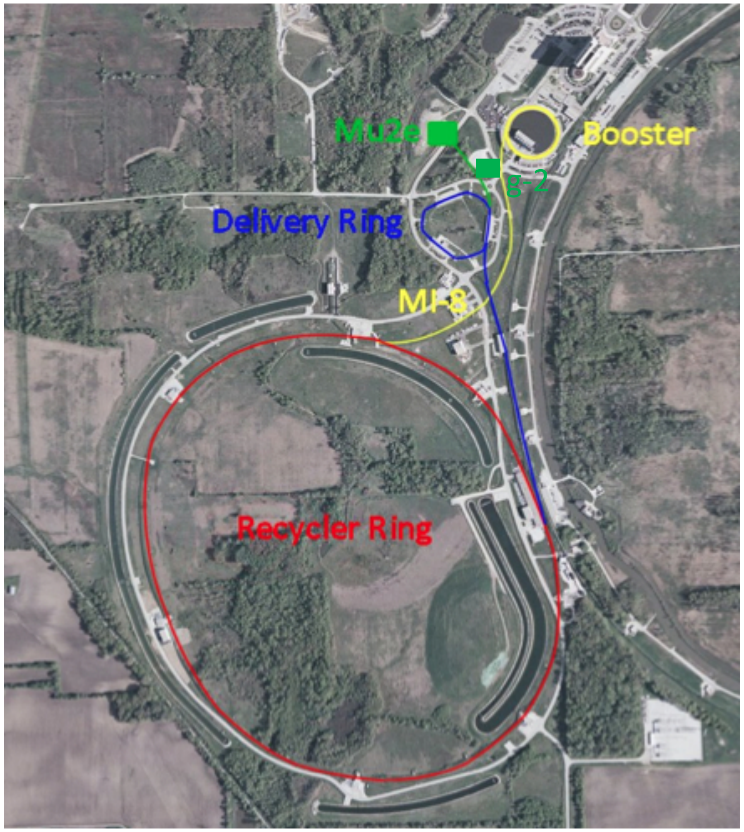

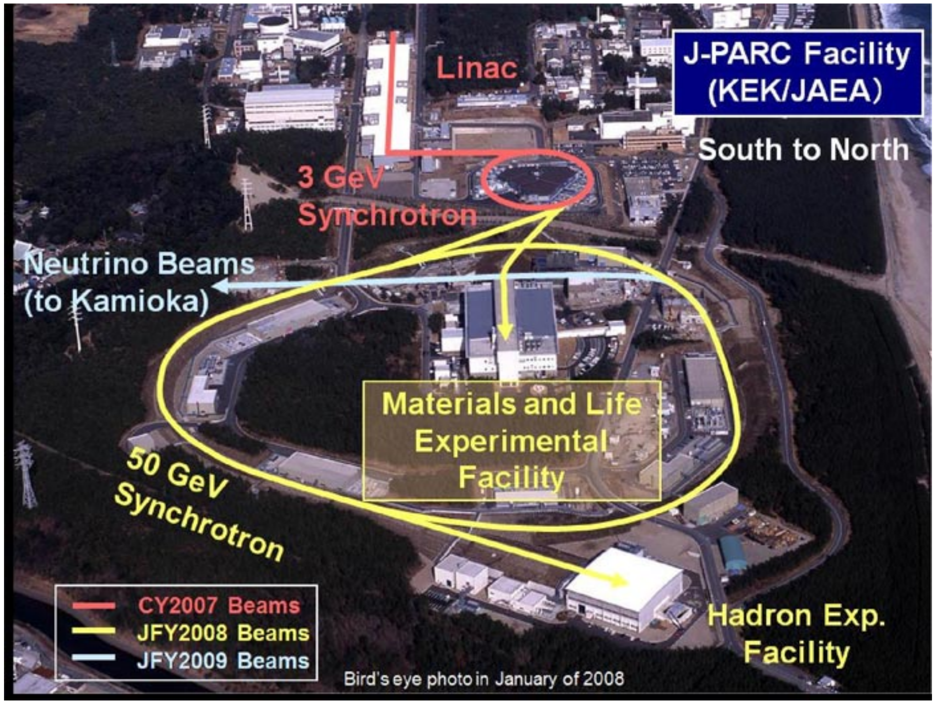

Proton Beams for Mu2e and COMET

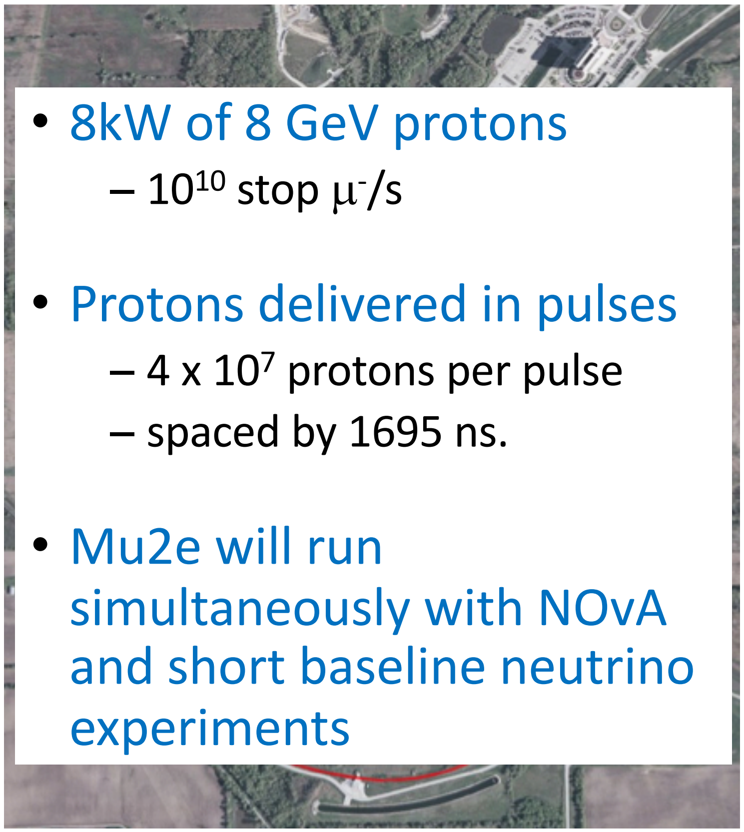

- 8kW of 8 GeV protons
  - 10^{10} stop μ^-/s
- Protons delivered in pulses
  - 4 x 10^7 protons per pulse
  - spaced by 1695 ns.
- Mu2e will run simultaneously with NOvA and short baseline neutrino experiments

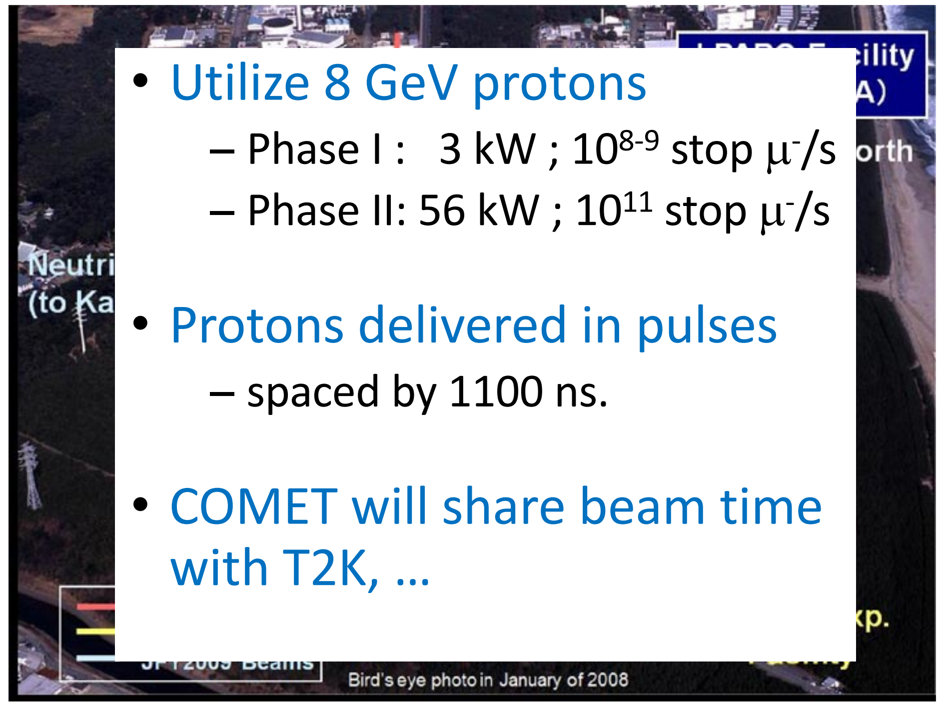

- Utilize 8 GeV protons
  - Phase I : 3 kW ; $10^{8\text{-}9}$ stop μ^-/s
  - Phase II: 56 kW ; 10^{11} stop μ^-/s
- Protons delivered in pulses
  - spaced by 1100 ns.
- COMET will share beam time with T2K, …

Mu2e Experimental Apparatus

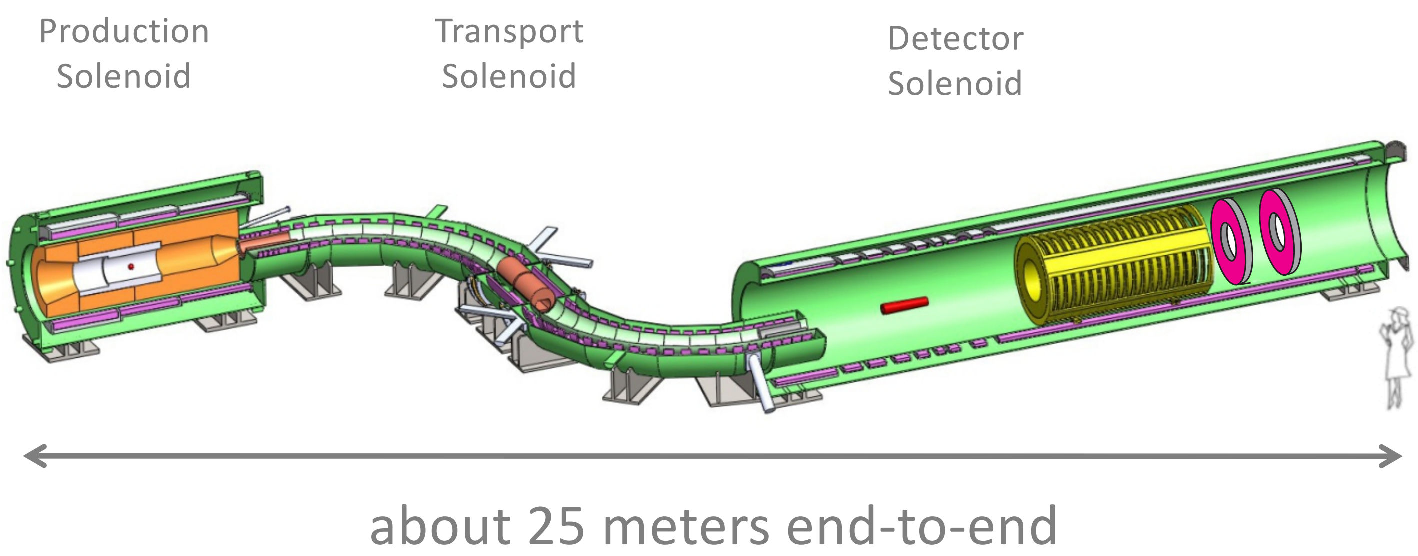

- Consists of 3 solenoid systems

Mu2e Experimental Apparatus

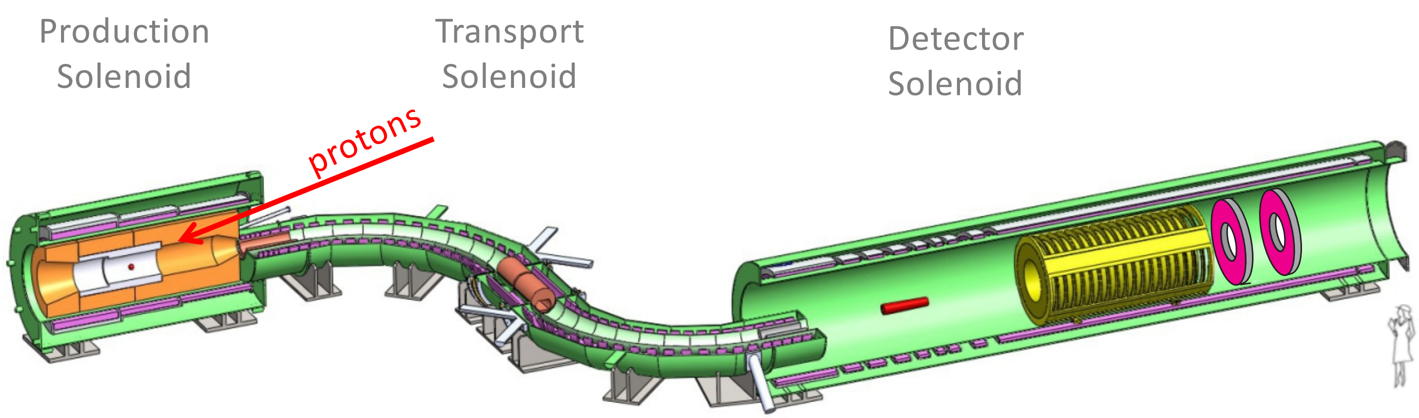

Production Solenoid:
8 GeV protons interact with a tungsten target to produce μ- (from π- decay)

- Consists of 3 solenoid systems

Mu2e Experimental Apparatus

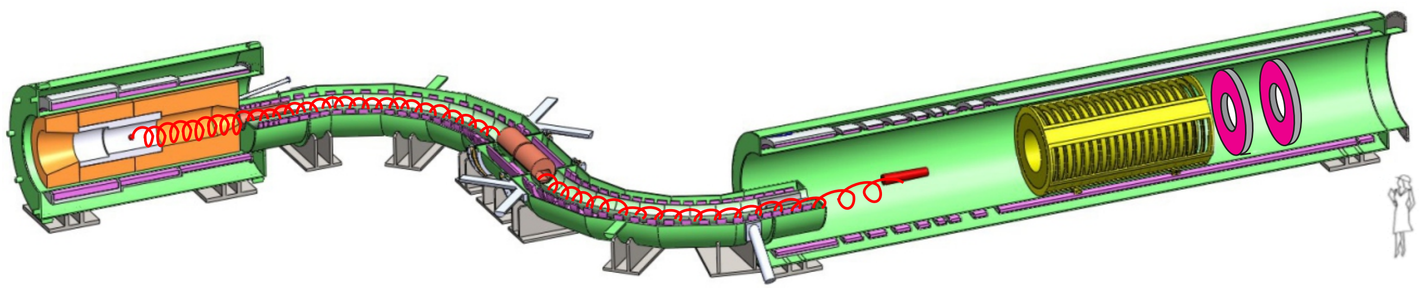

Transport Solenoid:
Captures π- and subsequent μ-; momentum- and sign-selects beam

- Consists of 3 solenoid systems

Mu2e Experimental Apparatus

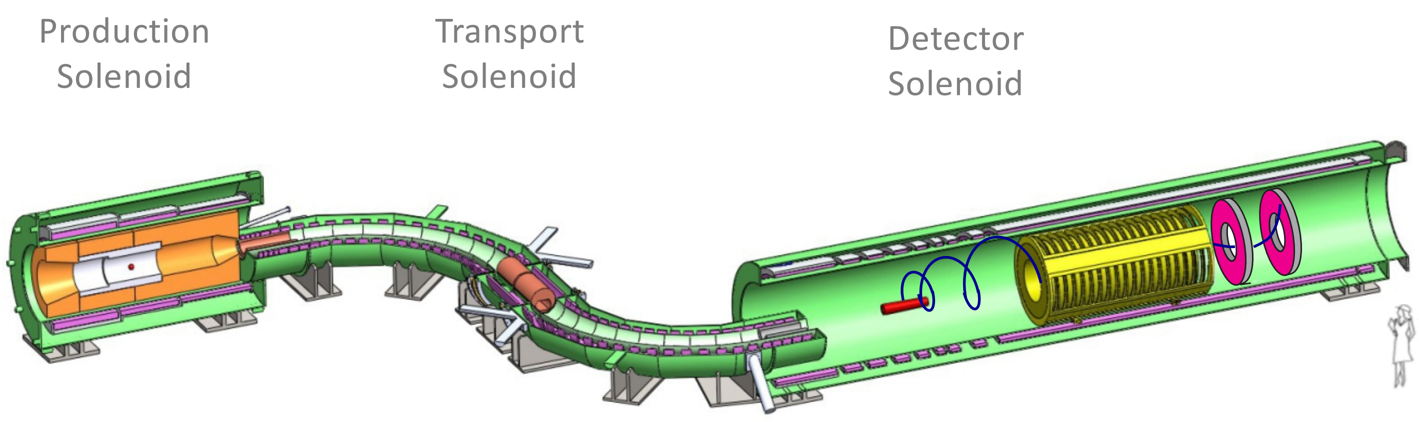

Detector Solenoid:

Upstream – Al. stopping target, Downstream – tracker, calorimeter

(not shown – cosmic ray veto system, proton-beam monitor, stopped-muon monitor)

- Consists of 3 solenoid systems

Mu2e Experimental Apparatus

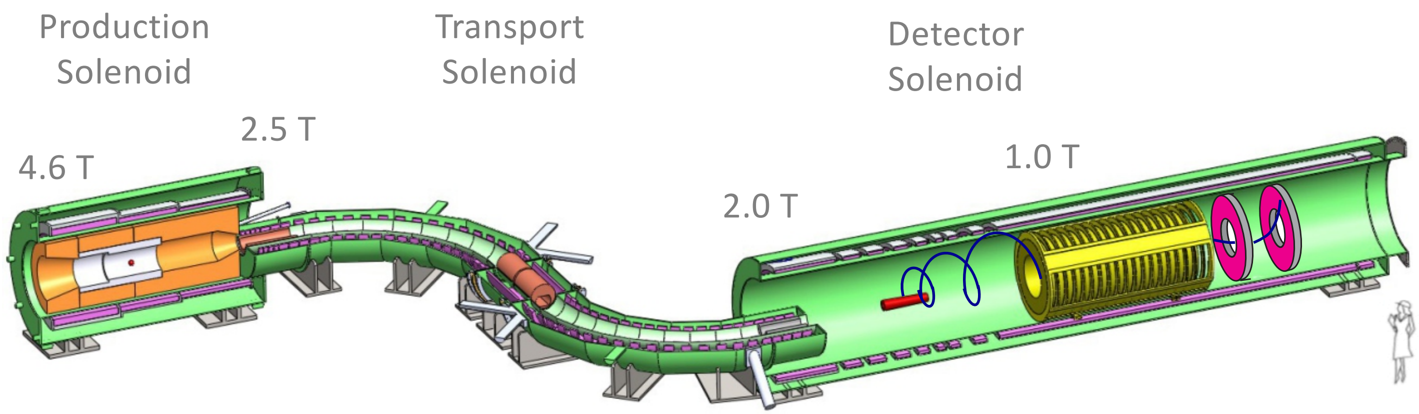

Graded fields important to suppress backgrounds, to increase muon yield, and to improve geometric acceptance for signal electrons

- Consists of 3 solenoid systems

Mu2e Experimental Apparatus

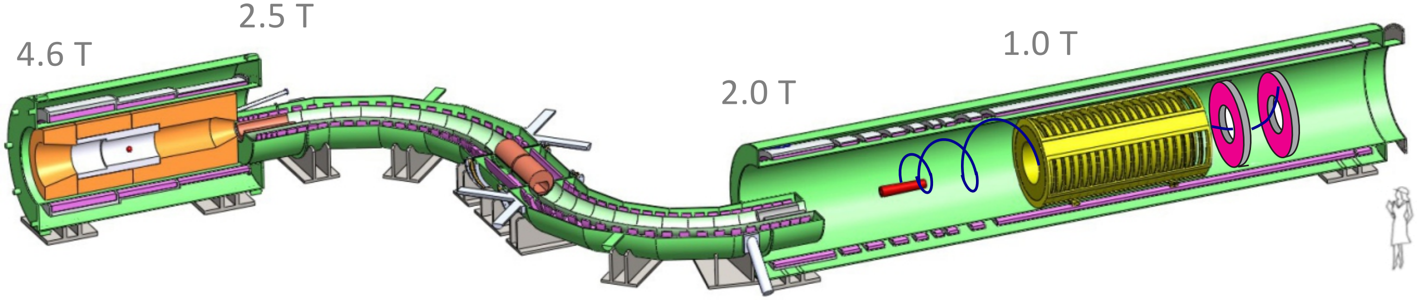

Graded fields important to suppress backgrounds, to increase muon yield, and to improve geometric acceptance for signal electrons

- Derived from MELC concept originated by Lobashev and Djilkibaev in 1989

COMET-II Apparatus

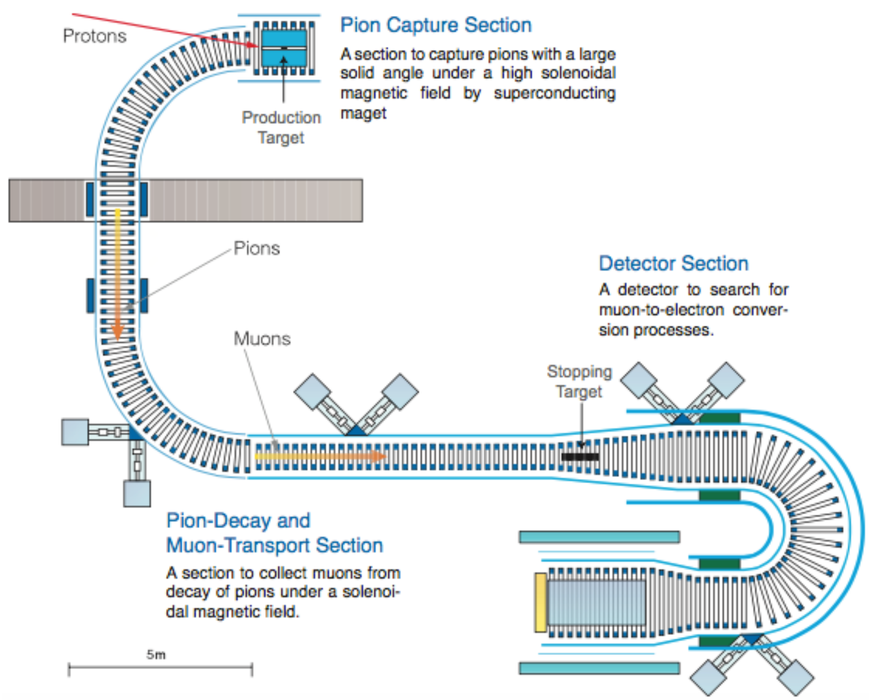

- Also inspired by Lobashev and Djilkibaev

COMET Evolution

Phase I

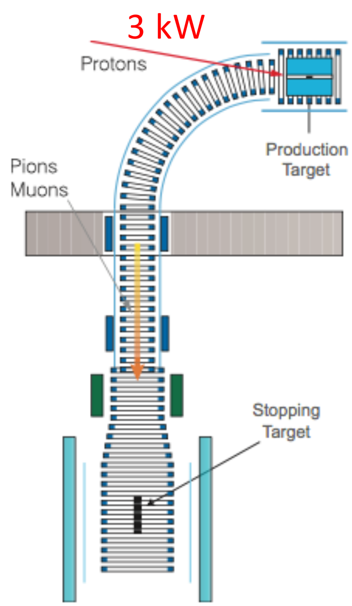

Starts ~2020

$R_{\mu e} < 10^{-14}$

Phase –II

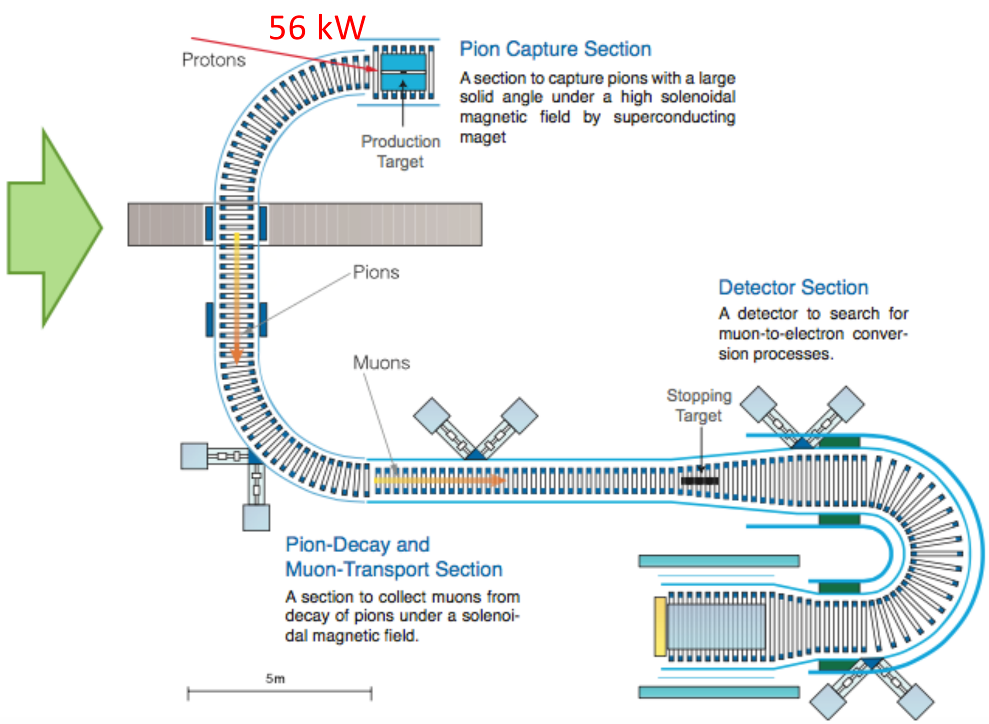

Mu2e Expected Background Yield (COMET Phase-II very similar)

Category	Source	Events
Intrinsic	μ Decay in Orbit	0.14
	Radiative μ Capture	<0.01
Late Arriving Beam	Radiative π Capture	0.02
	Beam electrons	<0.01
	μ Decay in Flight	<0.01
	π Decay in Flight	<0.01
Miscellaneous	Anti-proton induced	0.04
	Cosmic Ray induced	0.21
Total Background		0.41

(assuming 6.7E17 stopped muons in 6E7 s of beam time)

- Designed to be nearly background free

Detector development and prototypes

tracker

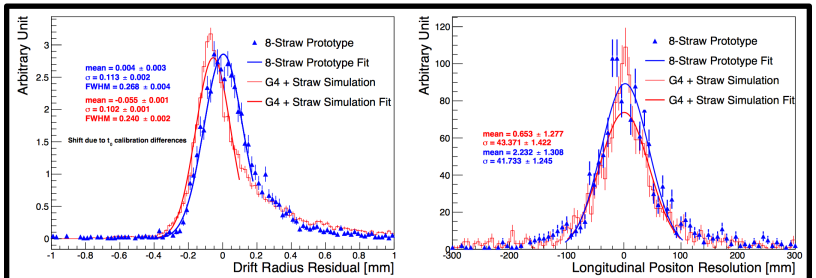

Transverse Resolution (Data vs MC)

$\sigma_{data} = 0.113 \pm 0.002$ mm

$\sigma_{MC} = 0.102 \pm 0.001$ mm

Longitudinal Resolution (Data vs MC)

$\sigma_{data} = 42 \pm 1$ mm

$\sigma_{MC} = 43 \pm 1$ mm

calorimeter

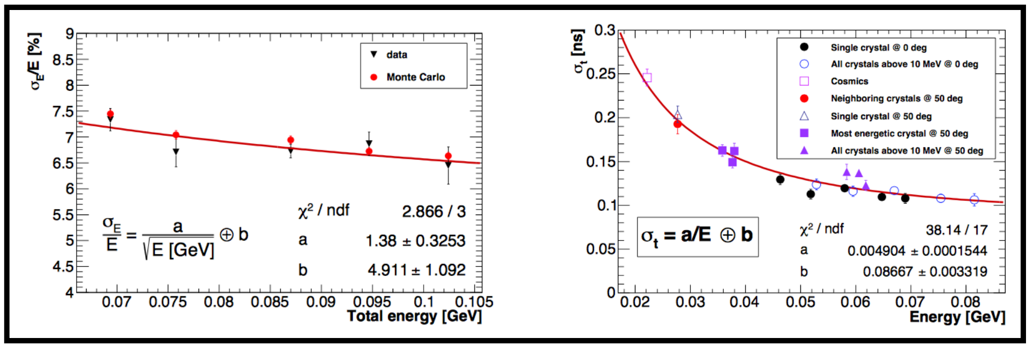

Cosmic veto

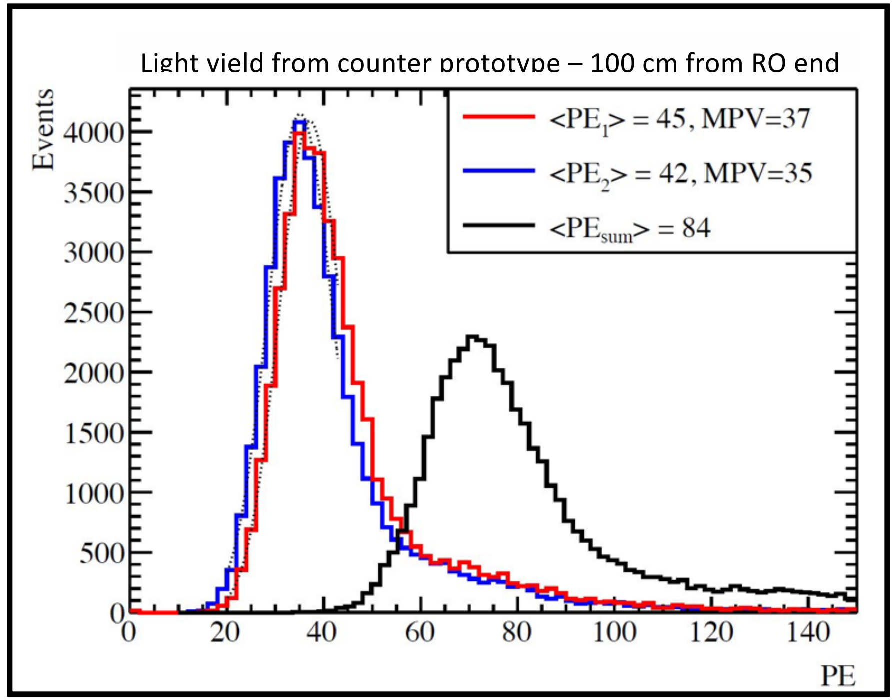

- Experiment designs finalized
- Required performance demonstrated in test beams

Construction well underway (Phase-I COMET, Mu2e)

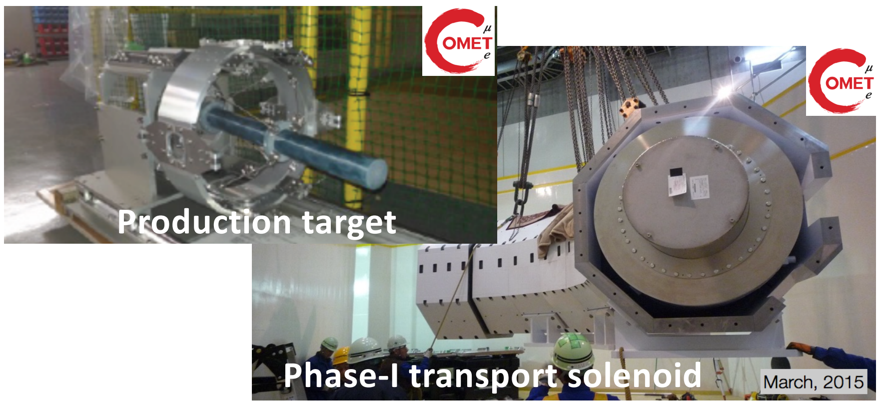

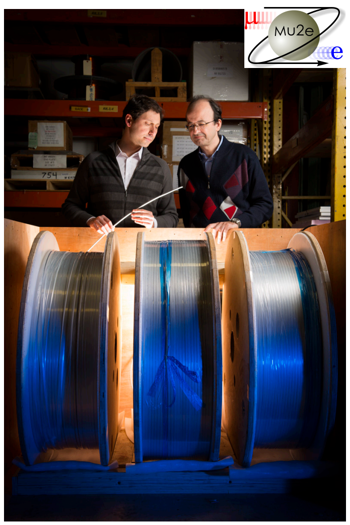

- Commissioning begins 2020-2021

CLFV Experiments using μ^+ :

Muon to e + gamma ($\mu^+ \rightarrow e^+\gamma$)

Muon to 3 electrons ($\mu^+ \rightarrow e^+e^+e^-$)

Muon to electron+gamma ($\mu^+ \rightarrow e^+\gamma$)

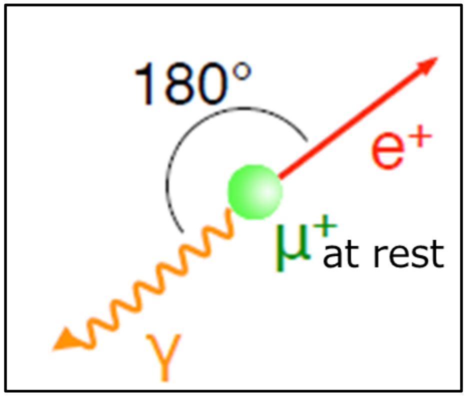

Current State-of-the-art (@ 90% CL) :

$$BF(\mu^+ \rightarrow e^+\gamma) < 4.2 \times 10^{-13}$$

A. M. Baldini, et al. (MEG) Eur. Phys. J. C76, 8 (2016) 434.

Muon to electron+gamma ($\mu^+ \rightarrow e^+\gamma$)

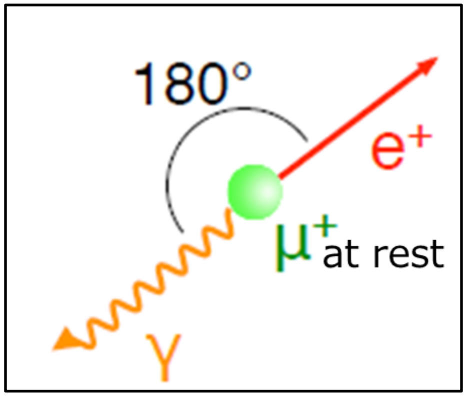

Next generation experiments:

– MEG-II (PSI) x10

Expected improvement (relative to current state-of-the-art)

MEG Experiment ($\mu^+ \rightarrow e^+\gamma$)

Signal

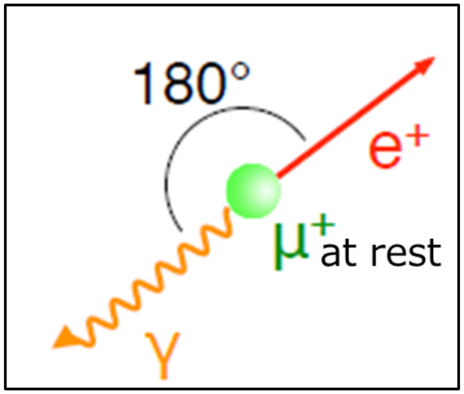

Back-to-back $e\gamma$

$E_e = E_\gamma = m_\mu/2$

Background

$\mu^+ \rightarrow e^+\nu\nu\gamma$

Radiative Muon Decay (RMD)

Accidentals (ACC)

MEG Experiment ($\mu^+ \rightarrow e^+\gamma$)

Signal

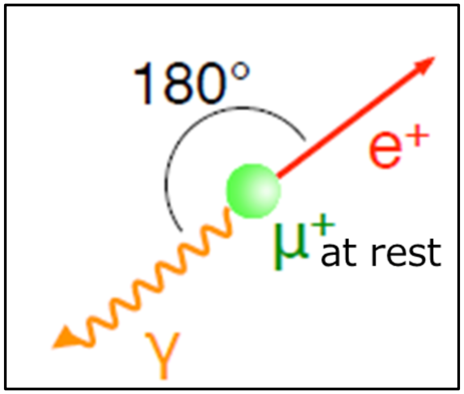

Background

$\mu^+ \rightarrow e^+\nu\nu\gamma$

Radiative Muon Decay (RMD)

Accidentals (ACC)

$$BF_{ACC} \propto \left(\frac{R_\mu}{D}\right)(\Delta t_{e\gamma})\frac{\Delta E_e}{m_\mu/2}\left(\frac{\Delta E_\gamma}{15m_\mu/2}\right)^2\left(\frac{\Delta\theta_{e\gamma}}{2}\right)^2$$

MEG Experiment ($\mu^+ \rightarrow e^+\gamma$)

Signal

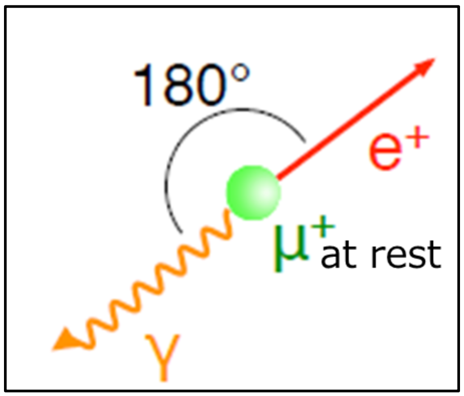

Background

$\mu^+ \rightarrow e^+\nu\nu\gamma$
Radiative Muon Decay (RMD)

Accidentals (ACC)

Keys to success: excellent energy, timing, angular resolutions, particularly ΔE_γ and $\Delta\theta_{e\gamma}$

MEG Proton Beam

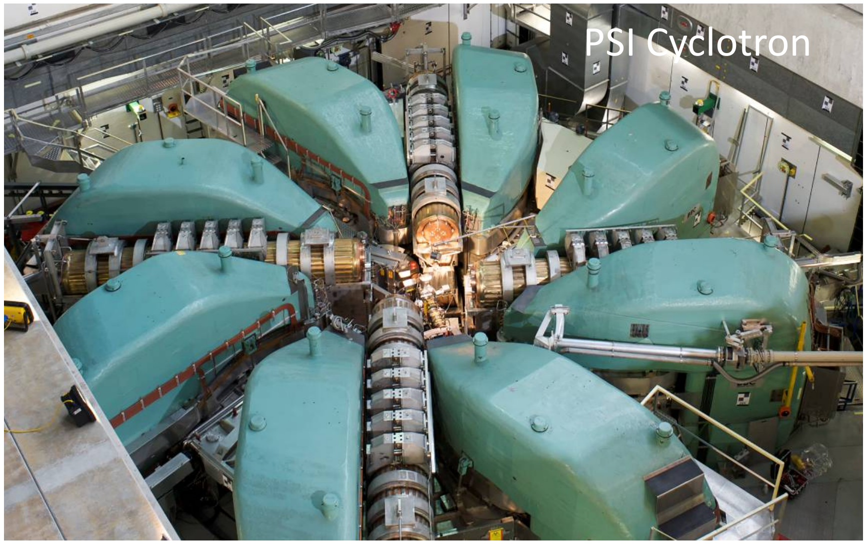

- 1.3 MW of 0.6 GeV protons
- DC muon beam using "surface" muons, $p_{\mu} \sim 28$ MeV/c
- MEG uses few 10^7 μ^+/s

MEG Detector

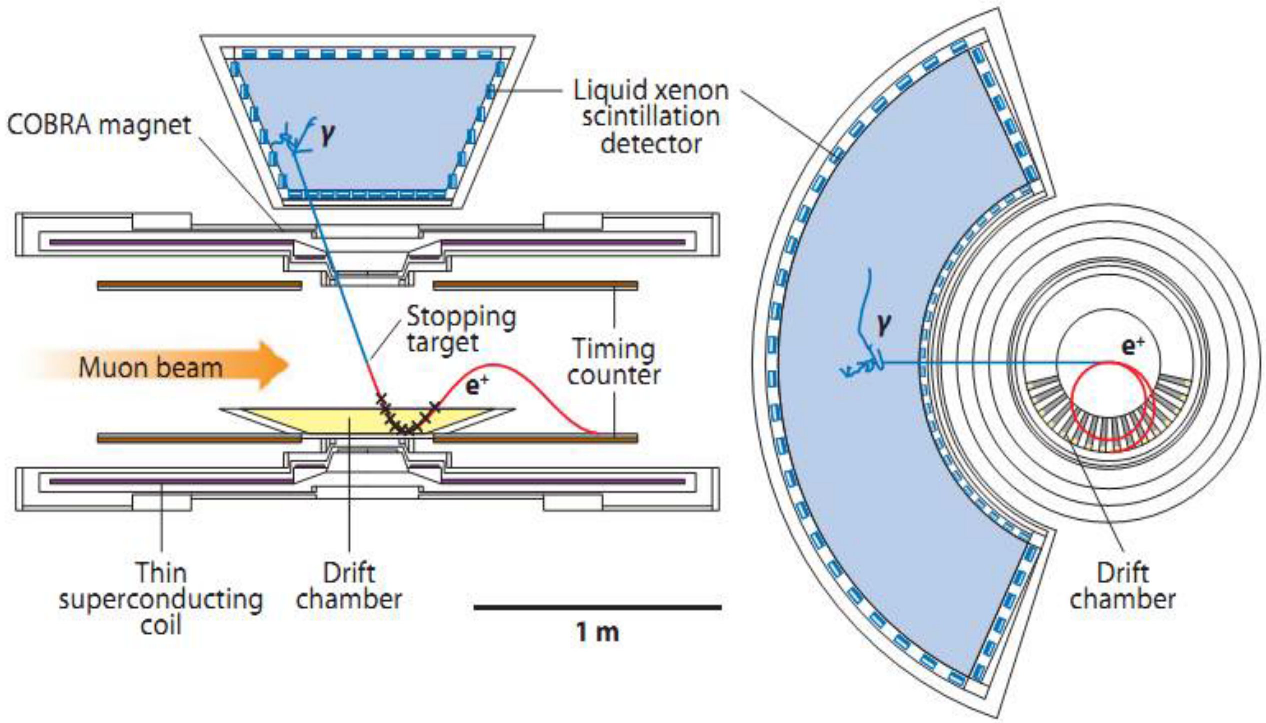

- Liquid Xe calorimeter
  - PMT readout
  - 11% of solid angle
- Drift Chamber (DC)
  - Radius : 19 - 28 cm
- Scintillator timing counters (TC)
- DC and TC inside graded solenoid field
- 205 μm polyethelene target

MEG Solenoid

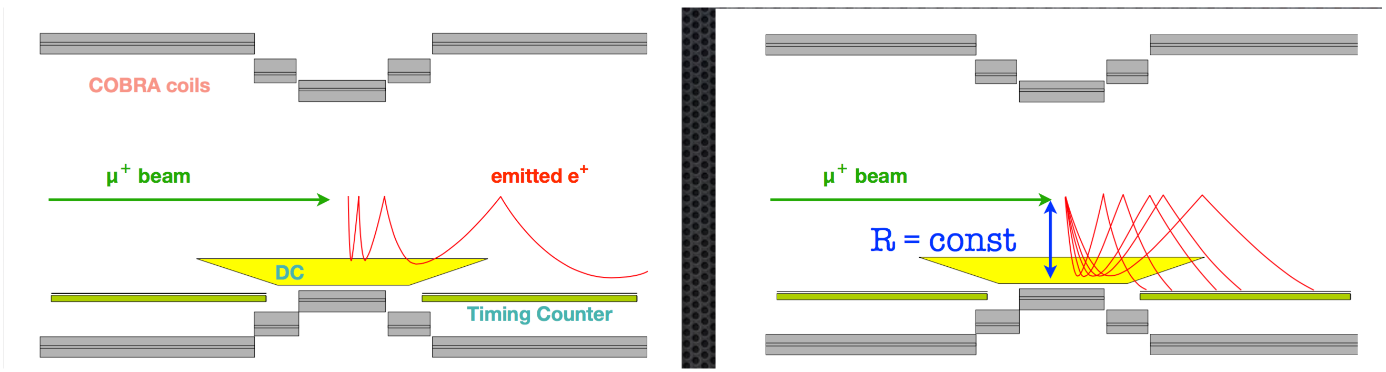

Sweeps e+ out of central region

Bending radius independent of pitch angle

COBRA = COnstant Bending Radius

– 1.3 T in central region
– 0.5 T in outer regions

MEG Analysis

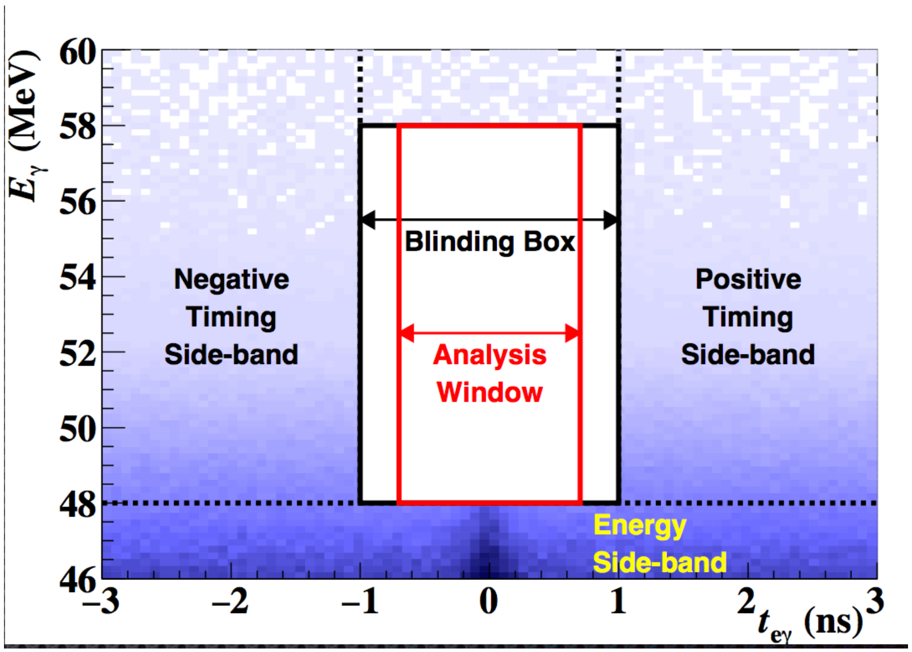

Utilizes 5 variables

- E_e, E_γ
- $t_{e\gamma} = t_e - t_\gamma$
- $\theta_{e\gamma}$
- $\phi_{e\gamma}$

Blind Analysis

Full Likelihood fit to data

- Published results uses full data set (2009-2013)
  - ~7.5 x 10^{14} stopped μ^+

MEG Analysis

$$\mathcal{L}\left(N_{\text{sig}}, N_{\text{RMD}}, N_{\text{ACC}}, \mathbf{t}\right) = \frac{e^{-N}}{N_{\text{obs}}!} C(N_{\text{RMD}}, N_{\text{ACC}}, \mathbf{t}) \times \prod_{i=1}^{N_{\text{obs}}} \left(N_{\text{sig}} S(\mathbf{x}_i, \mathbf{t}) + N_{\text{RMD}} R(\mathbf{x}_i) + N_{\text{ACC}} A(\mathbf{x}_i)\right)$$

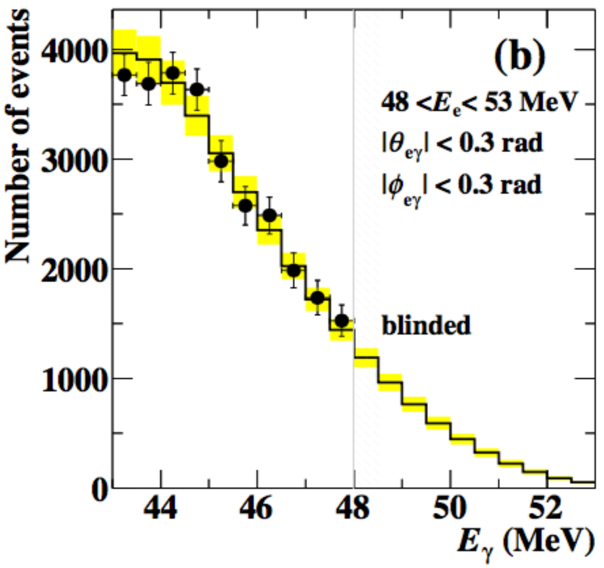

$x_i = (E_e, E_\gamma, t_{e\gamma}, \theta_{e\gamma}, \phi_{e\gamma})$

PDF_{ACC} : from sideband data

PDF_{SIG} & PDF_{RMD} : theory $\otimes$ resolution

MEG Calibrations

Table 1 The calibration tools of the MEG experiment.

	Process	Energy	Main Purpose	Frequency
Cosmic rays	$\mu^{\pm}$ from atmospheric showers	Wide spectrum $\mathcal{O}$(GeV)	LXe-DCH relative position	annually
			DCH alignment	
			TC energy and time offset calibration	
			LXe purity	on demand
Charge exchange	$\pi^- p \rightarrow \pi^0 n$ $\pi^0 \rightarrow \gamma\gamma$	55, 83, 129 MeV photons	LXe energy scale/resolution	annually
Radiative μ–decay	$\mu^+ \rightarrow e^+ \gamma\nu\bar{\nu}$	photons > 40 MeV,	LXe-TC relative timing	continuously
		positrons > 45 MeV	Normalisation	
Normal μ–decay	$\mu^+ \rightarrow e^+ \nu\bar{\nu}$	52.83 MeV end-point positrons	DCH energy scale/resolution	continuously
			DCH and target alignment	
			Normalisation	
Mott positrons	e^+ target $\rightarrow e^+$ target	$\approx$ 50 MeV positrons	DCH energy scale/resolution	annually
			DCH alignment	
Proton accelerator	^{7}Li(p, γ)^{8}Be	14.8, 17.6 MeV photons	LXe uniformity/purity	weekly
	^{11}B(p, γ)^{12}C	4.4, 11.6, 16.1 MeV photons	TC interbar/ LXe–TC timing	weekly
Neutron generator	^{58}Ni(n, γ)^{59}Ni	9 MeV photons	LXe energy scale	weekly
Radioactive source	^{241}Am(α, γ)^{237}Np	5.5 MeV α's, 56 keV photons	LXe PMT calibration/purity	weekly
Radioactive source	^{9}Be($\alpha_{^{241}\mathrm{Am}}$, n)^{12}C* ^{12}C*($\gamma$)^{12}C	4.4 MeV photons	LXe energy scale	on demand
LED			LXe PMT calibration	continuously

from Eur. Phys. J. C76, 8 (2016) 434 [arXiv:1605.05081]

Scale and resolutions determined with high degree of confidence

MEG Final Result

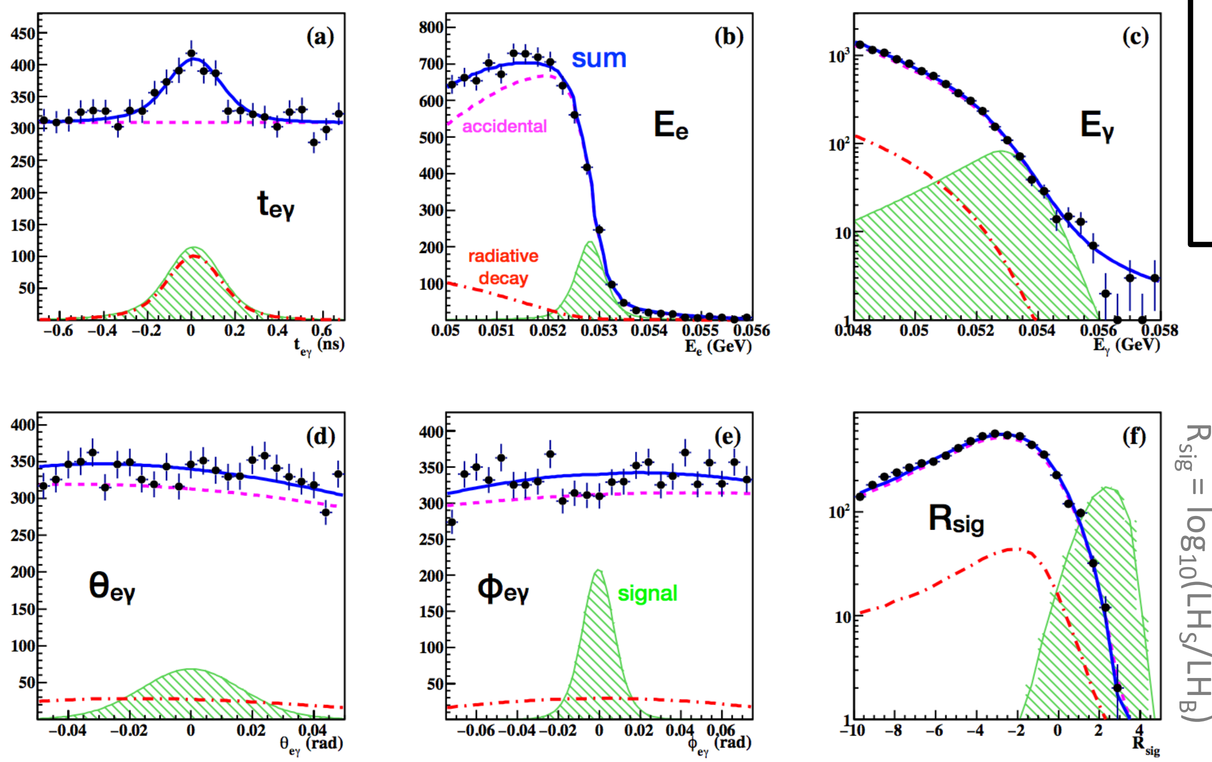

Best fit BF($\mu^+ \rightarrow e^+\gamma$) = -2.2 x 10^{-13}

BF($\mu^+ \rightarrow e^+\gamma$) < 4.2 x 10^{-13} @ 90% CL

(< 5.3 x 10^{-13} expected)

Eur. Phys. J. C76, 8 (2016) 434 [arXiv:1605.05081]

MEG-II Upgrade – another x10 better

Aiming for (3y physics run)
~6×10^{-14} sensitivity
@ 90% CL

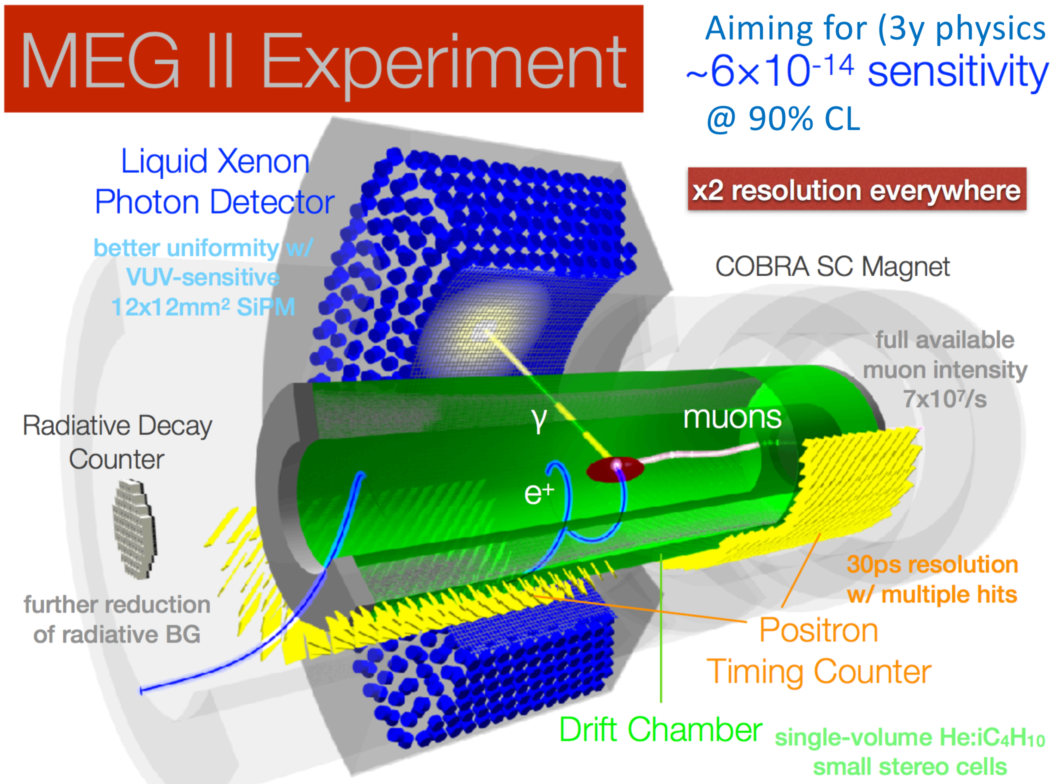

PDF parameters	MEG	MEG II
E_{e^+} (keV)	380	130
θ_{e^+} (mrad)	9.4	5.3
ϕ_{e^+} (mrad)	8.7	3.7
z_{e^+}/y_{e^+} (mm) core	2.4/1.2	1.6/0.7
E_γ(%) (w>2 cm)/(w<2 cm)	2.4/1.7	1.1/1.0
$u_\gamma, v_\gamma, w_\gamma$ (mm)	5/5/6	2.6/2.2/5
$t_{e^+\gamma}$ (ps)	122	84
Efficiency (%)		
Trigger	≈ 99	≈ 99
Photon	63	69
e$^+$(tracking × matching)	30	70

resolutions

- Commissioning with beam has begun!
- Physics data taking will begin late 2018 – early 2019

Muon to three electrons ($\mu^+ \rightarrow e^+e^+e^-$)

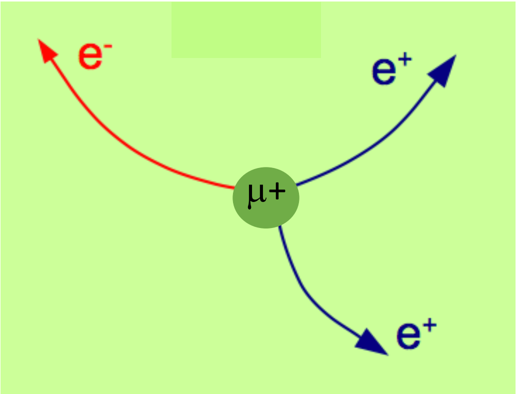

Current State-of-the-art (@ 90% CL) :

$$BF(\mu^+ \rightarrow e^+e^+e^-) < 1 \times 10^{-12}$$

U. Bellgardt, et al. (SINDRUM) Nucl.Phys. B299 (1988) 1.

Muon to three electrons ($\mu^+ \rightarrow e^+e^+e^-$)

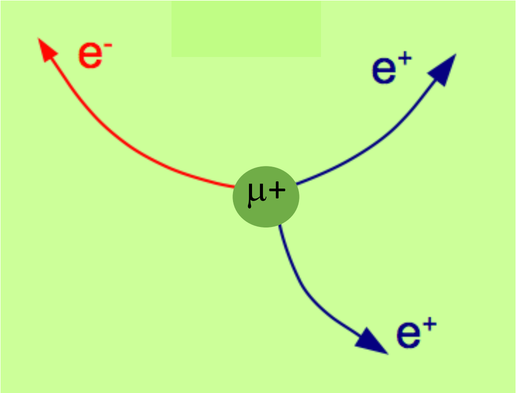

Next generation experiments:

– Mu3e (PSI)
- Phase Ia x20
- Phase Ib x400
- Phase II x10,000

Expected improvement
(relative to current state-of-the-art)

Mu3e Experiment ($\mu^+ \rightarrow e^+e^+e^-$)

Signal

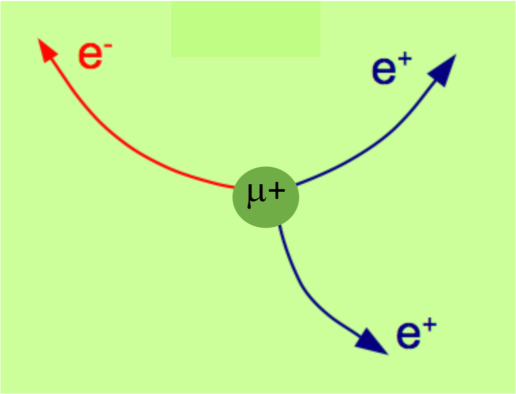

$\Sigma\, p = 0$

$E_e < m_\mu/2$

$\Sigma\, E_e = m_\mu$

Background

$\mu^+ \rightarrow e^+\nu\nu\gamma \rightarrow e^+\nu\nu e^+e^-$

Radiative Muon Decay (RMD)

Accidentals

Mu3e Experiment ($\mu^+ \rightarrow e^+e^+e^-$)

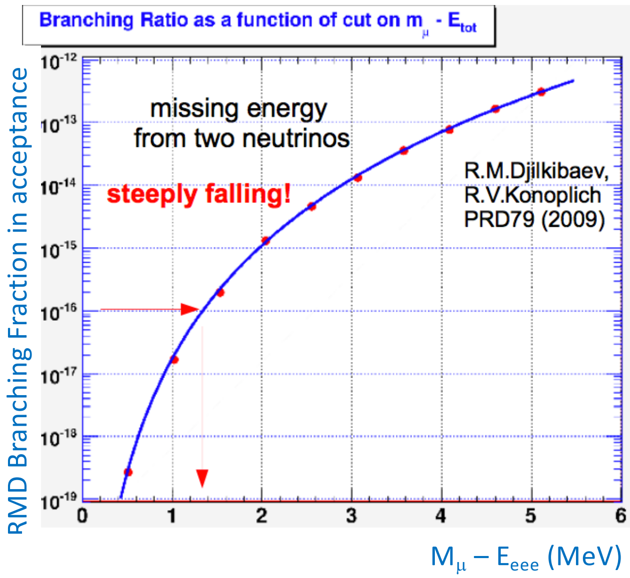

Background

$\mu^+ \rightarrow e^+\nu\nu\gamma \rightarrow e^+\nu\nu e^+e^-$

Radiative Muon Decay (RMD)

Accidentals

- **Keys to success:** excellent momentum, timing, and vertex resolutions

Mu3e Experiment ($\mu^+ \rightarrow e^+e^+e^-$)

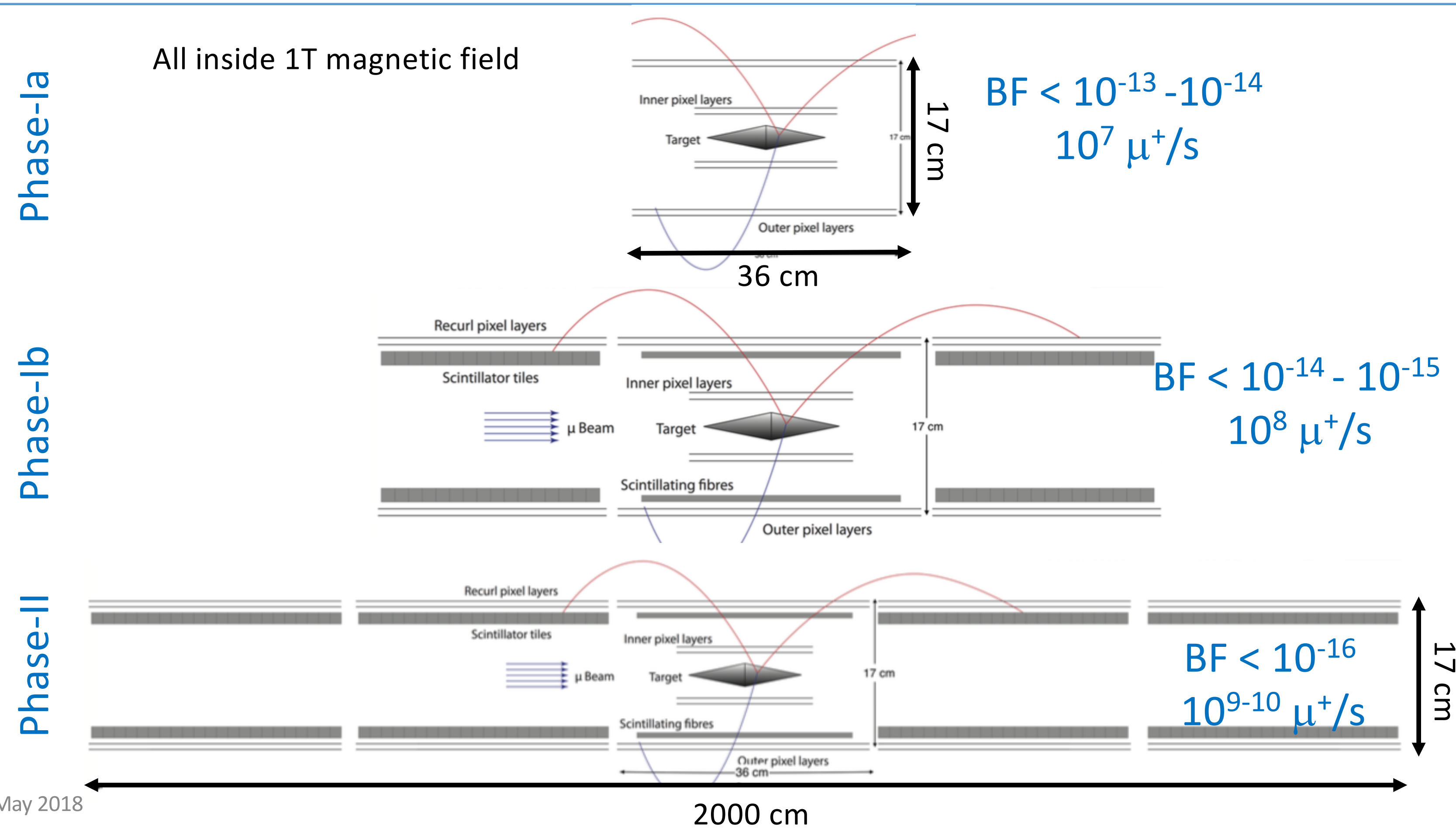

Mu3e (Phase-I) beam

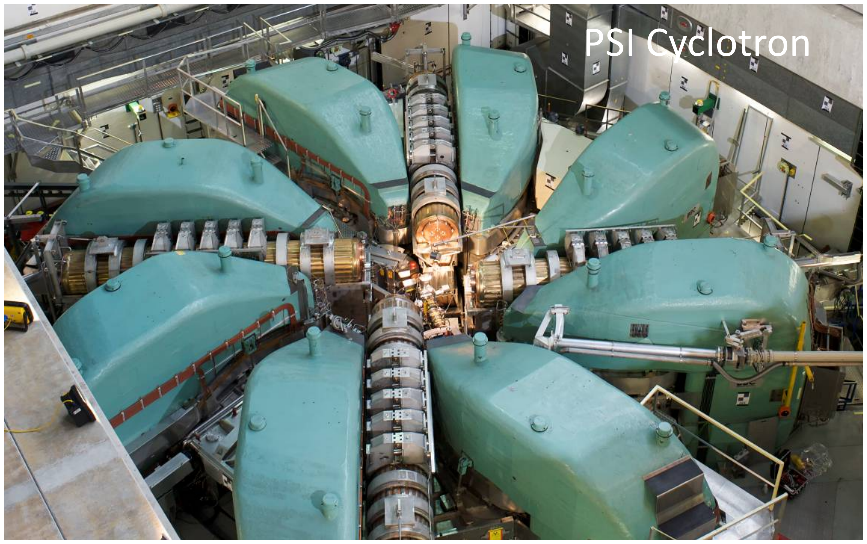

- 1.3 MW of 0.6 GeV protons
- DC muon beam using "surface" muons, p_{μ} ~ 28 MeV/c
- Mu3e will use $10^7 - 10^8\ \mu^+/s$
- Utilizes same beam line as MEG

Mu3e (Phase-II) beam

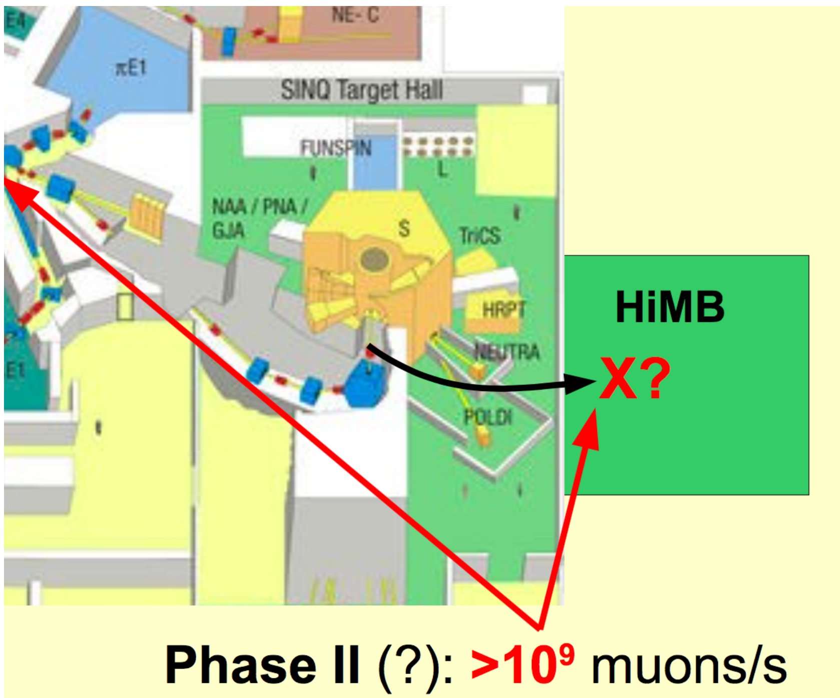

To achieve Phase-II sensitivity requires an upgraded facility at PSI: High Intensity Muon Beam

- Currently under development
- Not (yet) approved

Mu3e Detector development

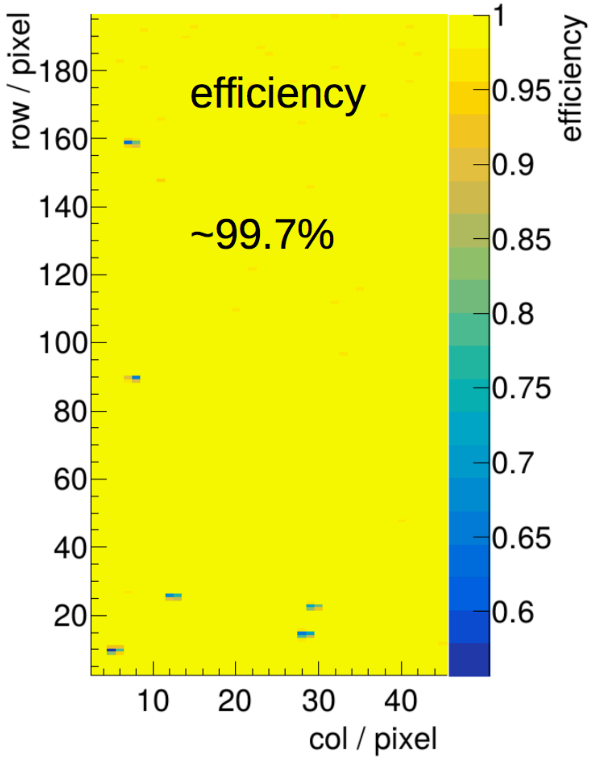

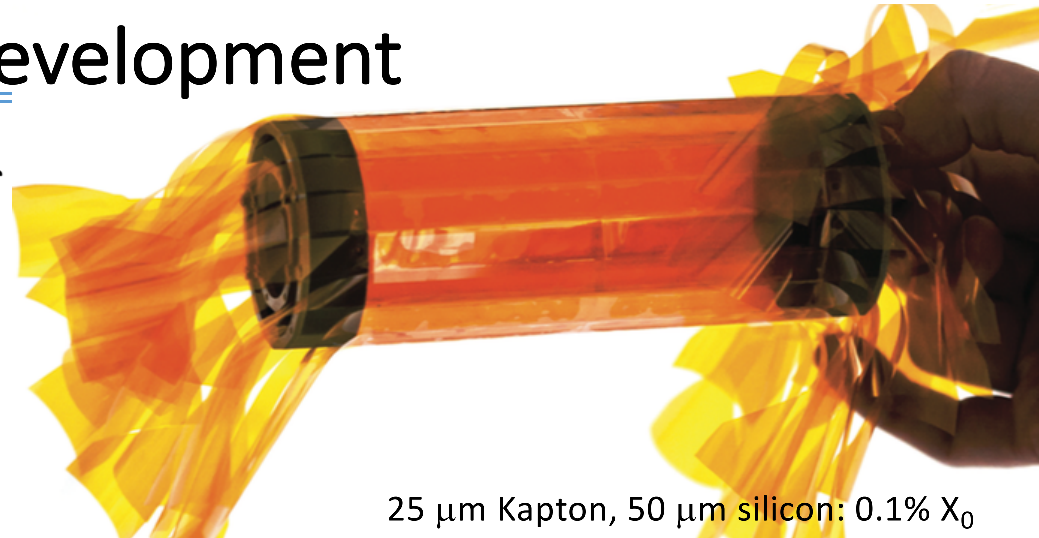

25 μm Kapton, 50 μm silicon: 0.1% X_0

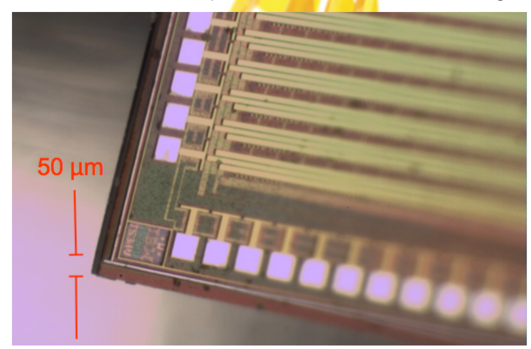

- Low mass pixel array (HV-MAPS thinned to 50 μm)

Mu3e Detector development (for Phase-Ib, II)

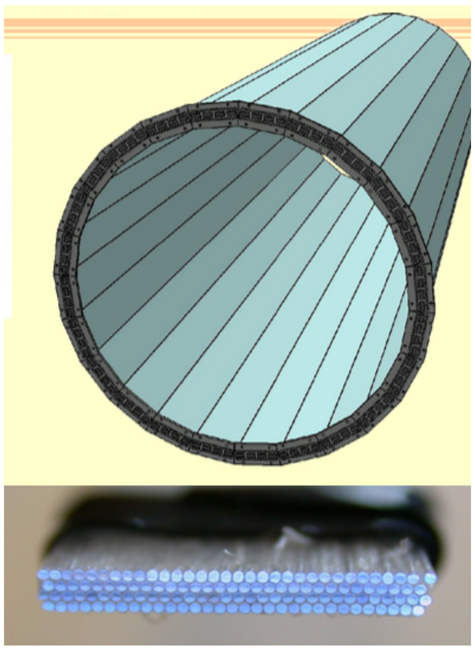

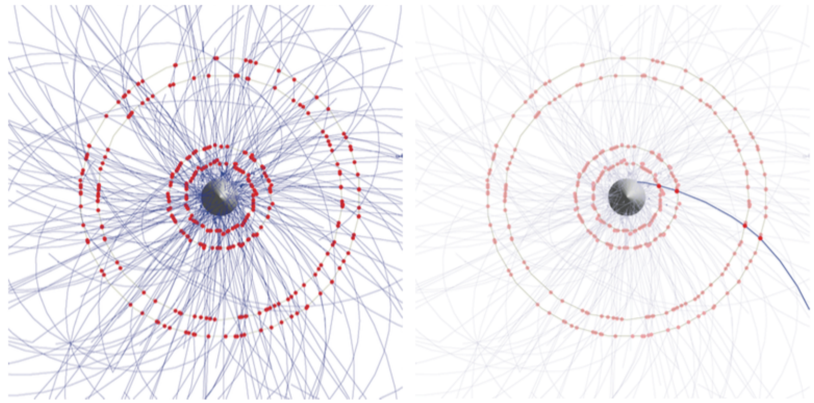

Pixels: O(50 ns)

Scintillating fibres O(1 ns);
Scintillating tiles O(100 ps)

- Scintillating arrays for <100ps timing
  - Will help suppress accidental background by x100
  - Fibers & tiles utilizing demonstrated technologies

- Finalizing experiment design & prototyping. Aim to have Phase 1a detector ready for data taking by end of MEG-II running.

Future Expectations

Expected data taking schedule

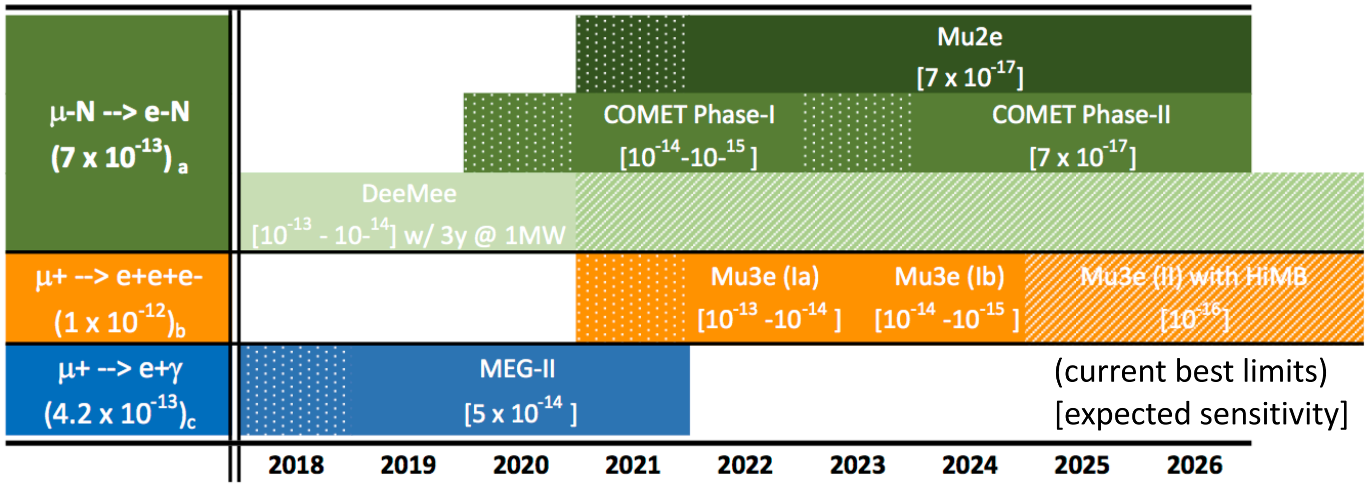

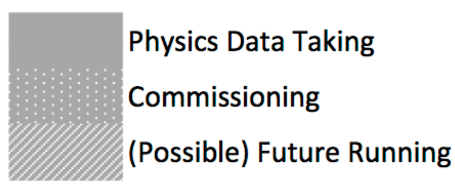

a) W. Bertl, et al. (SINDRUM-II), Eur. Phys. J. C47 (2006) 337.
b) U. Bellgardt, et al. (SINDRUM), Nucl. Phys. B299 (1988) 1.
c) A. Baldini, et al. (MEG), Eur. Phys. J. C76, 8 (2016) 434.

- Significant progress in all three μ channels in next 5-7 years

Comparing sensitivities

Constraints from μ→e Experiments

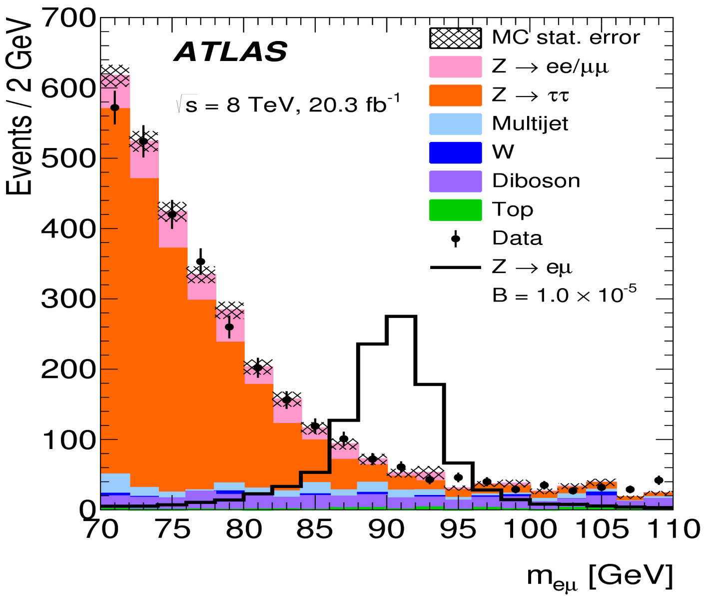

Constraints on LFV Z couplings

From CLFV experiments*

μ→eee: BF(Z→μe) <5x10^{-13} (today)

Collider experiments

CMS : BF(Z→μe) < 7.3 x 10^{-7}

ATLAS: BF(Z→μe) < 7.5 x 10^{-7} (today)

* S. Nussinov, R.D. Peccei, and X.M. Zhang, Phys. Rev. D63 (2001) 016003; (arXiv:0004153 [hep-ph]).

Constraints from μ→e Experiments

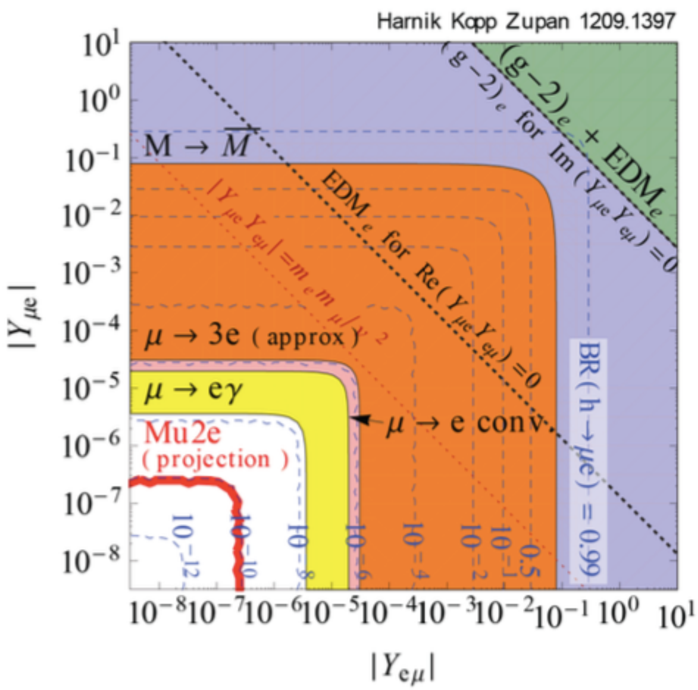

Constraints on LFV Yukawa couplings

From CLFV experiments*

$\mu \to e\gamma$: $B(h \to \mu e) < 10^{-8}$ (today)

$\mu N \to eN$: $B(h \to \mu e) < 10^{-10}$ (future)

Collider experiments

LHC : $B(h \to \mu e) < 10^{-2}$ - 10^{-3} (today – future)

* R. Harnik, J. Kopp, and J. Zupan, JHEP 03 (2013) 026; (arXiv:1209.1397 [hep-ph]).

Examples of CLFV and LHC sensitivity

Only Bino & RH Sleptons are light

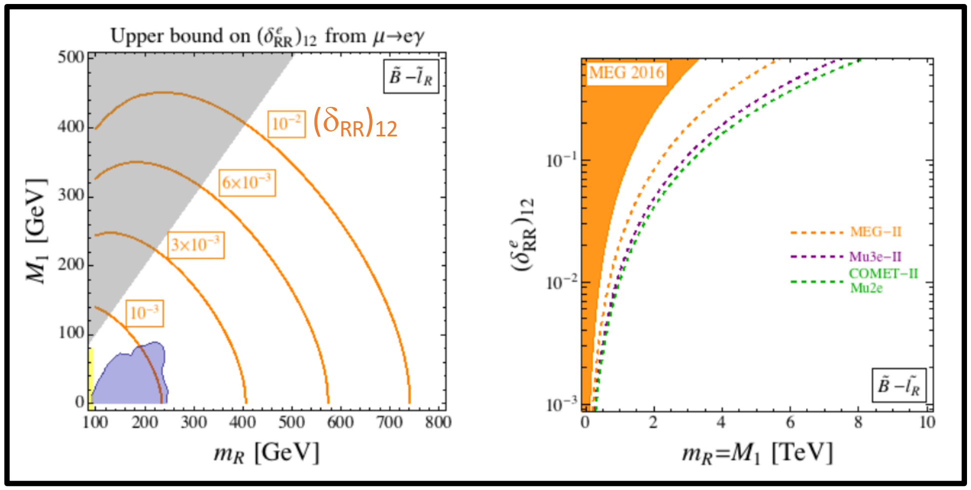

Only Wino, Higgino & LH Sleptons are light

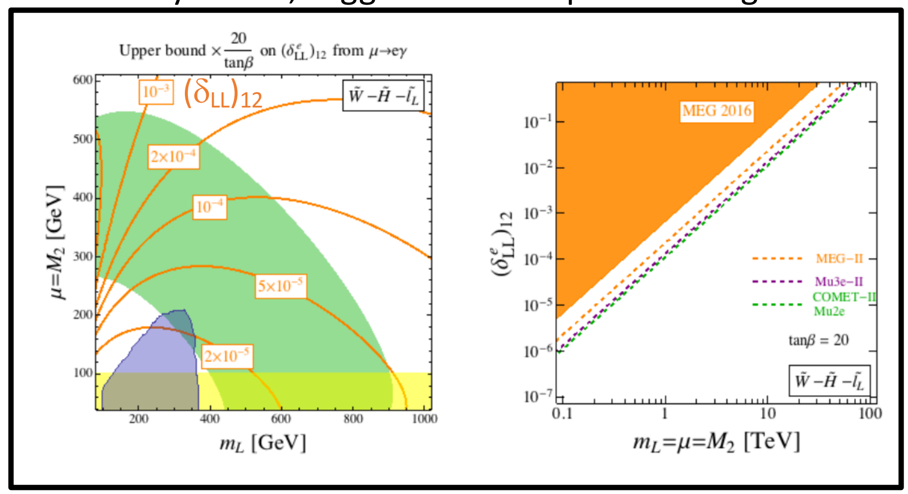

Excluded by LHC   Excluded by MEG   Excluded by LEP   Consistent with a_μ Theory disallowed

(from L. Calibbi and G. Signorelli, Riv. Nuovo Cimento, 41 (2018) 71)

- CLFV experiments probe parts of NP parameter space LHC does not

Constraints from τ→e,μ Experiments

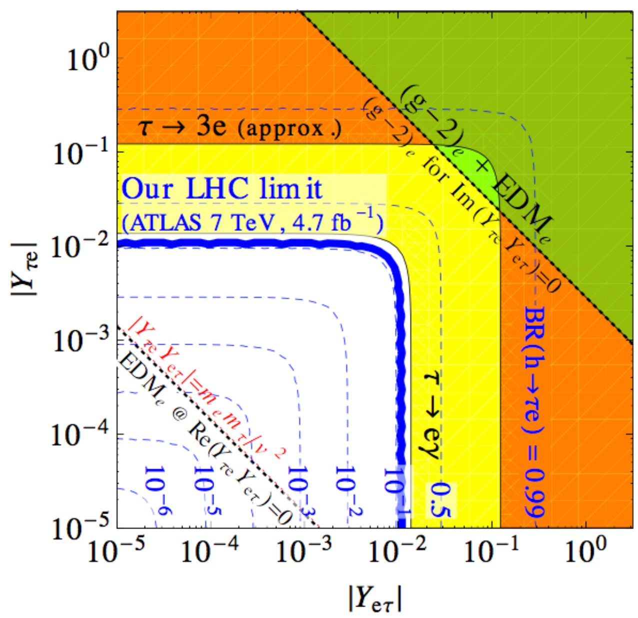

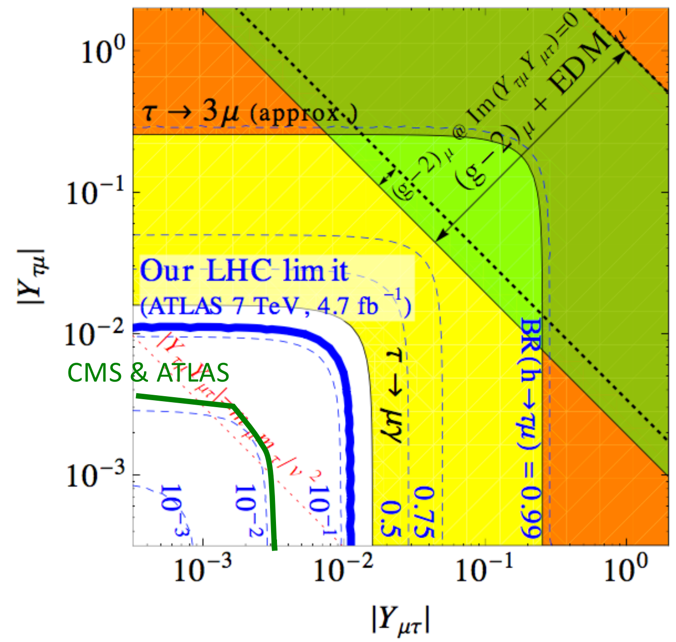

- Results using CLFV τ decays correspond to B(h→τe, τμ) ~ 10%
  - CMS and ATLAS already exploring B(h→τμ) ~ 1%

Summary

- CLFV experiments provide deep, broad probes of New Physics parameter space
  - Will probe $\Lambda_{NP} \sim O(10^3 - 10^4)$ TeV >> LHC
- Near future experiments have compelling discovery sensitivity over a broad range of New Physics models (SUSY, GUT, ED, LHT, 2HDM,…)
- Combining information from >1 CLFV channel can allow a determination of underlying New Physics mechanism
- The next ~5 years promise to be very exciting for CLFV searches!

For more information

- Useful reviews
  - L. Calibbi and G. Signorelli, Riv. Nuovo Cimento, 41 (2018) 71
  - T. Gorringe & D. Hertzog, Prog.Part.Nucl. Phys. 84 (2015) 73.
  - S. Mihara, J.P. Miller, P. Paradisi, G. Piredda, Annu.Rev.Nucl.Part.Sci. 63 (2013) 552.
  - R.H. Bernstein & P.S. Cooper, Phys. Rept. 532 (2013) 27.
  - Y. Kuno & Y. Okada, Rev.Mod.Phys. 73 (2001) 151.
- About the experiments
  - MEG: http://meg.icepp.s.u-tokyo.ac.jp (MEG-II TDR: arXiv:1801.04688)
  - Mu2e: http://mu2e.fnal.gov (TDR: arXiv:1501.05241)
  - COMET: http://comet.kek.jp/Introduction.html (Proposal: http://comet.kek.jp/Documents_files/Phase-I-Proposal-v1.2.pdf)
  - DeeMee: http://deeme.hep.sci.osaka-u.ac.jp (Proposal: http://deeme.hep.sci.osaka-u.ac.jp/documents/deeme-proposal-r28.pdf/view)
  - Mu3e: https://www.psi.ch/mu3e/mu3e (Proposal: https://www.psi.ch/mu3e/documents)

Backup Slides

Using CLFV to Determine New Physics

Can use ratio of rates to determine dominant operator contribution

- multiple ratios can determine multiple operators and the ratio of their couplings

e.g. ($\mu \rightarrow e\gamma$) / ($\mu N \rightarrow eN$)

e.g. $\mu N \rightarrow eN$ with different nuclei

- Also information in angular distributions
  - $\mu \rightarrow eee$, τ chnls

V. Cirigliano, R. Kitano, Y. Okada, P. Tuzon, Phys. Rev. **D80** 013002 (2009)

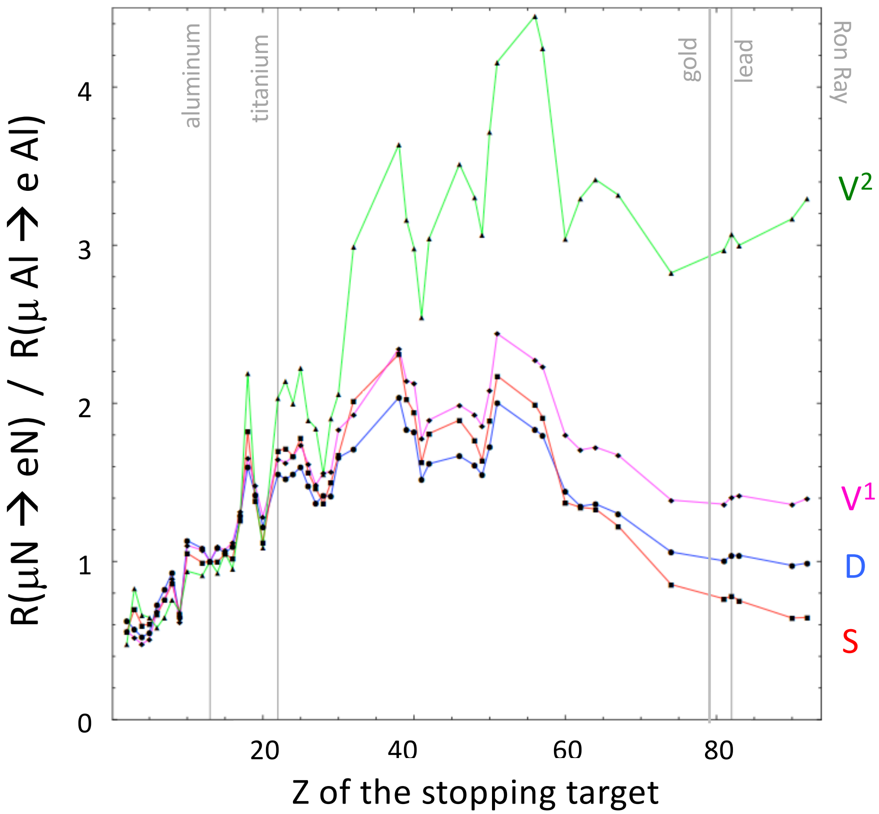

μ→eγ, μ→eee, μN→eN have complementary sensitivities to new physics

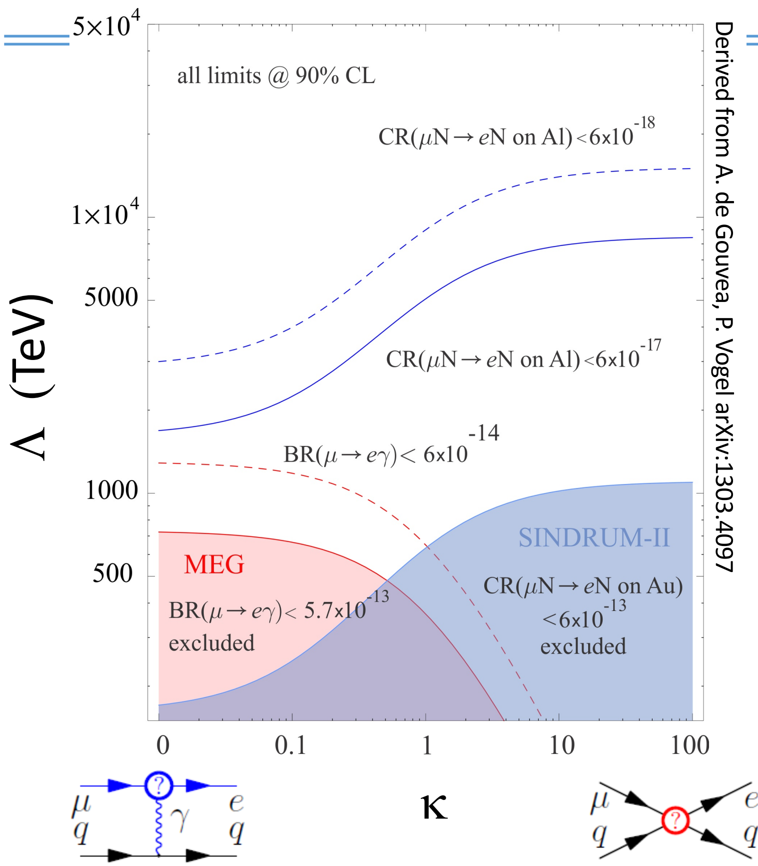

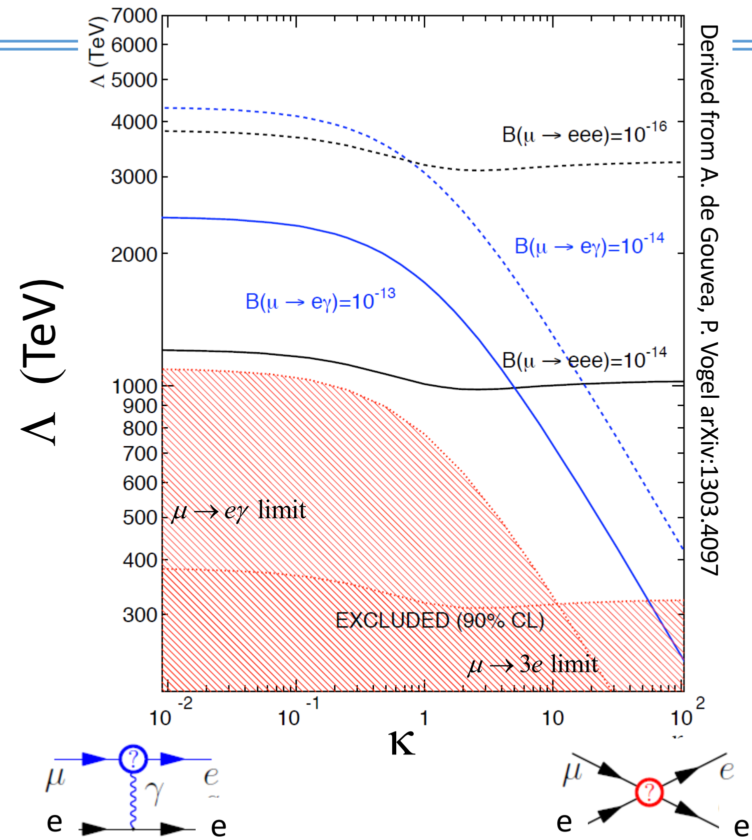

$$L_{CLFV} = \frac{m_\mu}{(1+\kappa)\Lambda^2}\bar{\mu}_R\sigma_{\mu\nu}e_L F^{\mu\nu} + \frac{\kappa}{(1+\kappa)\Lambda^2}\bar{\mu}_L\gamma_\mu e_L(\bar{u}_L\gamma^\mu u_L + \bar{d}_L\gamma^\mu d_L)$$

$$L_{CLFV} = \frac{m_\mu}{(1+\kappa)\Lambda^2}\bar{\mu}_R\sigma_{\mu\nu}e_L F^{\mu\nu} + \frac{\kappa}{(1+\kappa)\Lambda^2}\bar{\mu}_L\gamma_\mu e_L(\bar{e}\gamma^\mu e)$$

CLFV Sensitivity

★★★ = Discovery Sensitivity

W. Altmannshofer, A.J.Buras, S.Gori, P.Paradisi, D.M.Straub

	AC	RVV2	AKM	δLL	FBMSSM	LHT	RS
$D^0 - \bar{D}^0$	★★★	★	★	★	★	★★★	?
ϵ_K	★	★★★	★★★	★	★	★★	★★★
$S_{\psi\phi}$	★★★	★★★	★★★	★	★	★★★	★★★
$S_{\phi K_S}$	★★★	★★	★	★★★	★★★	★	?
$A_{\rm CP}(B \to X_s\gamma)$	★	★	★	★★★	★★★	★	?
$A_{7,8}(B \to K^*\mu^+\mu^-)$	★	★	★	★★★	★★★	★★	?
$A_9(B \to K^*\mu^+\mu^-)$	★	★	★	★	★	★	?
$B \to K^{(*)}\nu\bar{\nu}$	★	★	★	★	★	★	★
$B_s \to \mu^+\mu^-$	★★★	★★★	★★★	★★★	★★★	★	★
$K^+ \to \pi^+\nu\bar{\nu}$	★	★	★	★	★	★★★	★★★
$K_L \to \pi^0\nu\bar{\nu}$	★	★	★	★	★	★★★	★★★
$\mu \to e\gamma$	★★★	★★★	★★★	★★★	★★★	★★★	★★★
$\tau \to \mu\gamma$	★★★	★★★	★	★★★	★★★	★★★	★★★
$\mu + N \to e + N$	★★★	★★★	★★★	★★★	★★★	★★★	★★★
d_n	★★★	★★★	★★★	★★	★★★	★	★★★
d_e	★★★	★★★	★★	★	★★★	★	★★★
$(g-2)_\mu$	★★★	★★★	★★	★★★	★★★	★	?

Table 8: "DNA" of flavour physics effects for the most interesting observables in a selection of SUSY and non-SUSY models ★★★ signals large effects, ★★ visible but small effects and ★ implies that the given model does not predict sizable effects in that observable.

AC	U(1) flavor symmetry
RVV2	Non-abelian SU(3)-flavored MSSM
AKM	SU(3)-flavored SUSY
δLL	LH CKM-like currents
FBMSSM	Flavor-blind MSSM
LHT	Little Higgs w/T parity
RS	Randall-Sundrum

MEG Calibration

- E_e calibrated using Michel edge
- E_γ calibrated during special runs using a liquid hydrogen target
  - $\pi^- p \rightarrow \pi^0 n \rightarrow \gamma\gamma n$ (pion charge exchange)
  - Tag opposite side γ using a small movable BGO array dedicated to this calibration
  - The angle and energy of the opposite side tag can be used to define a mono-energetic source of γ in the LXe (~55 MeV)

MEG Calibration

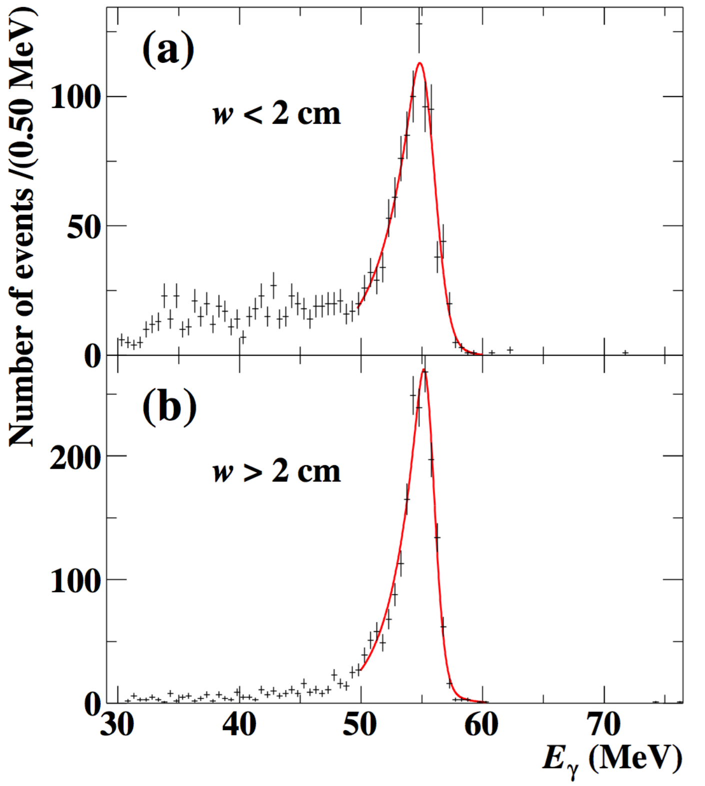

- Photon energy scale determined to <1% using special runs with a pion beam, a custom target, and exploiting charge exchange processes to identify monoenergetic photons with energies ~55 MeV

- Monitor stability of $E\gamma$ with short special runs that use a <1 MeV proton beam and a $Li_2B_4O_7$ target to produce photons at 18, 12, & 4 MeV

MEG Calibration

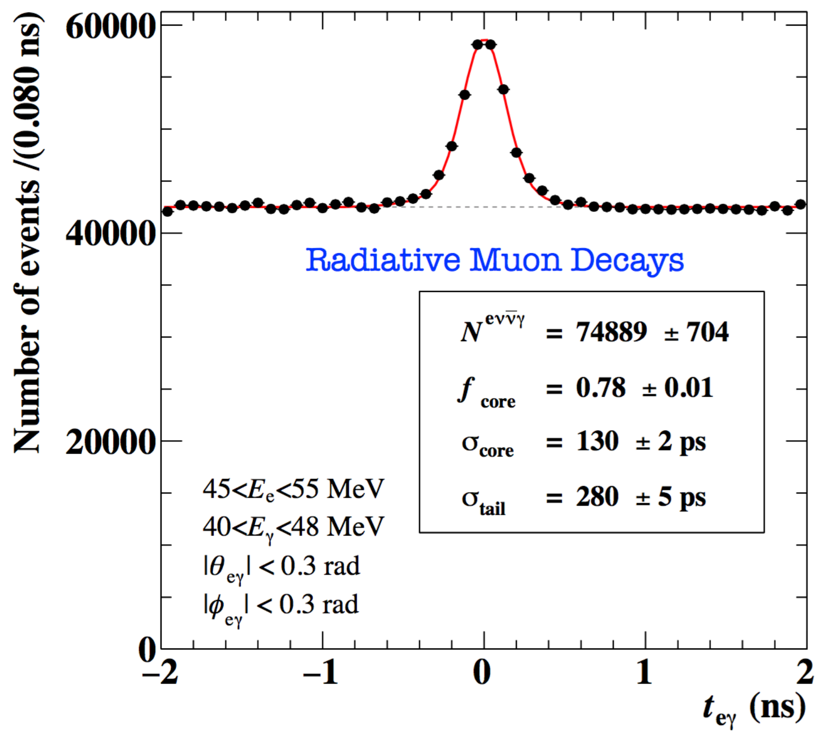

- Relative e-γ timing calibrated using radiative muon decays

MEG Backgrounds

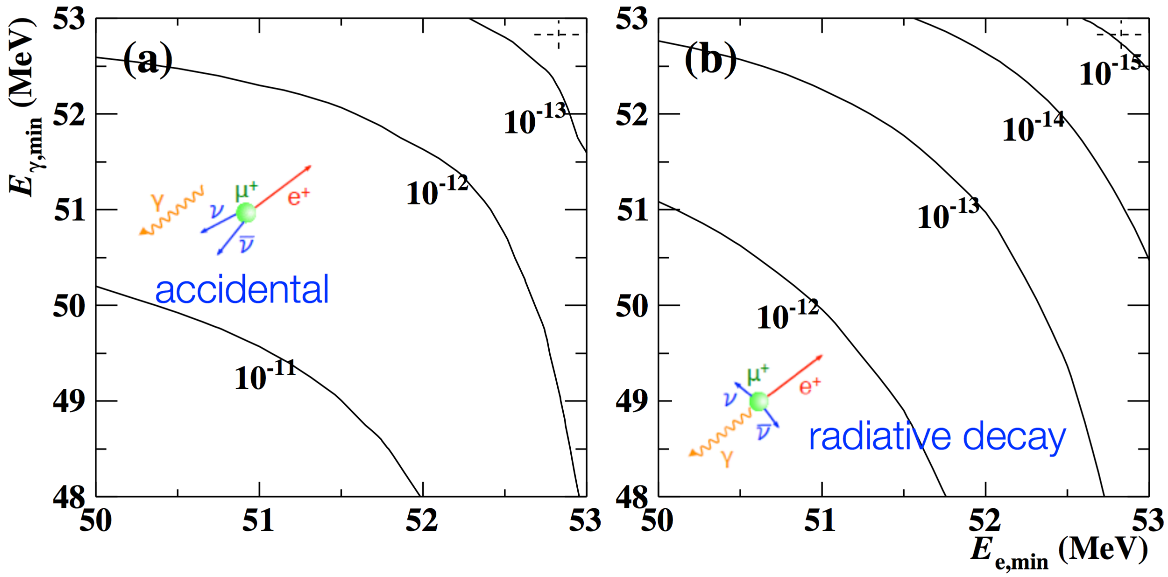

- Accidental backgrounds dominate.

MEG Accidental Background

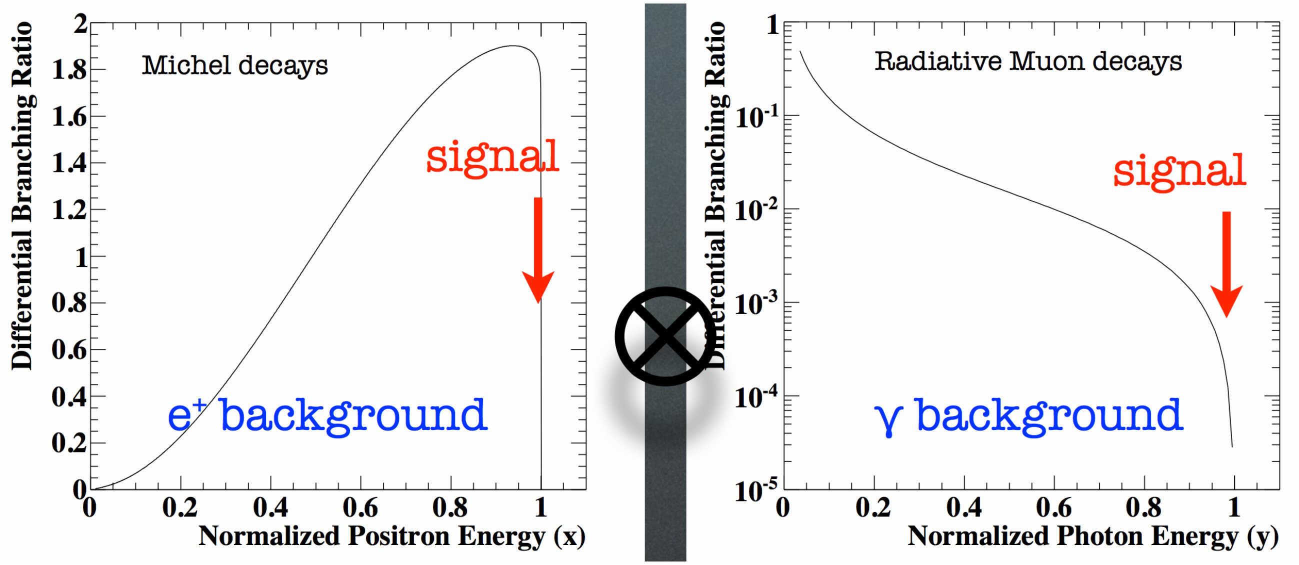

- Both curves are steeply falling in region of interest… sensitivity strong function of σ_E

MEG-II Upgrade : aim for x10 improvement

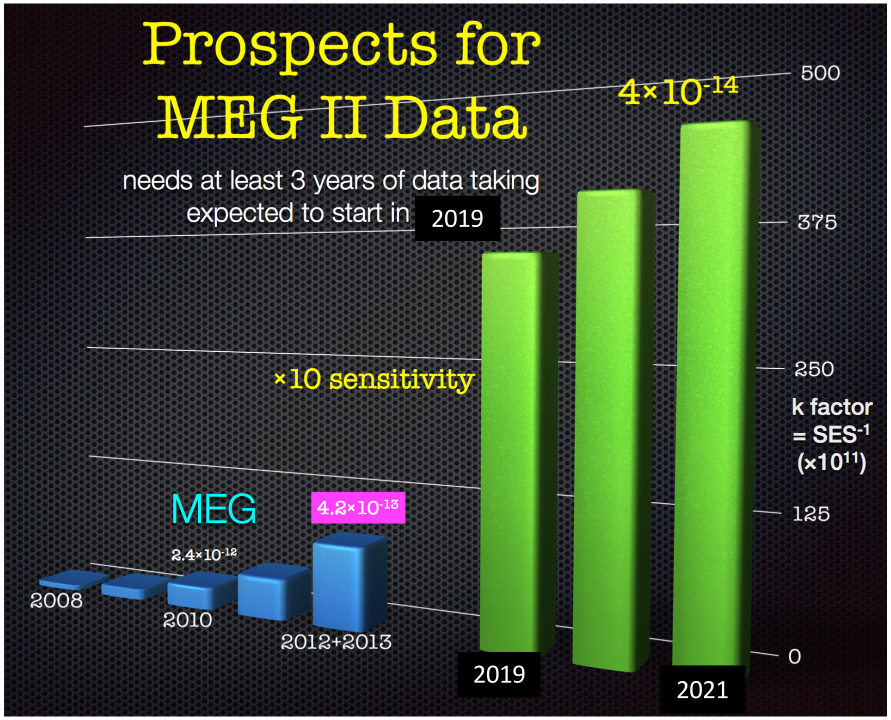

- Expect to begin 3y data taking in 2019
  - Aim to improve sensitivity by x10

Mu3e acceptance

- Inner bore of detector solenoid large enough to fully contain tracks with momenta up to ~50 MeV/c
- Central pixels fully fiducial for track momenta down to ~12 MeV/c
- Forward pixels provide additional hits from “recurl”

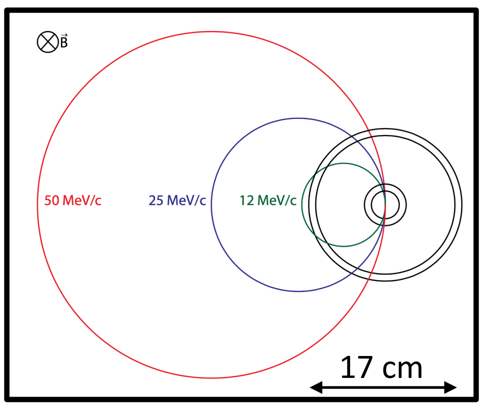

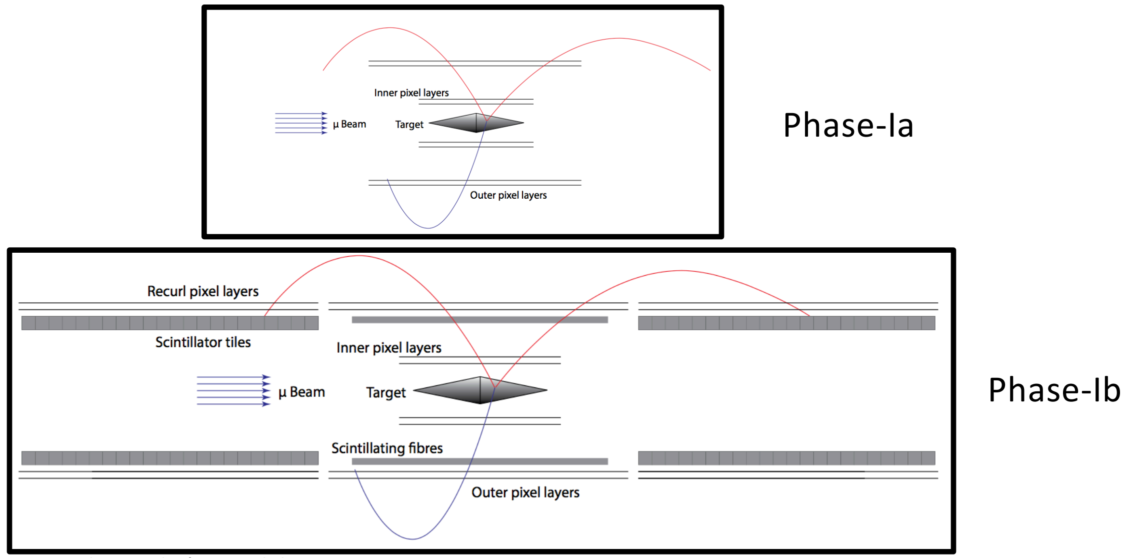

DeeMee ($\mu^- N \rightarrow e^- N$)

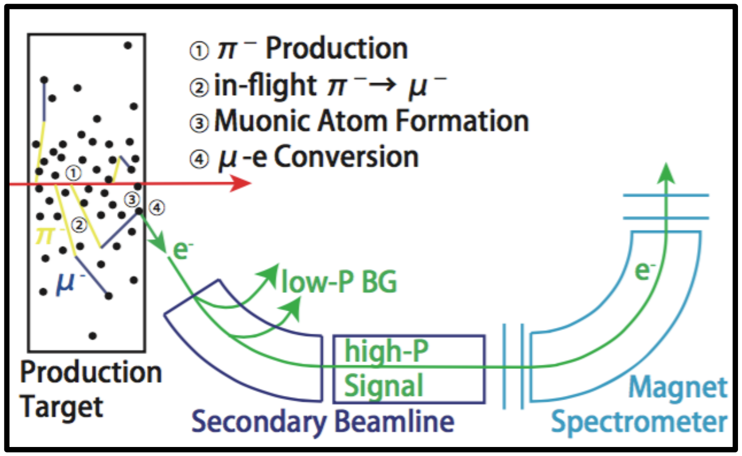

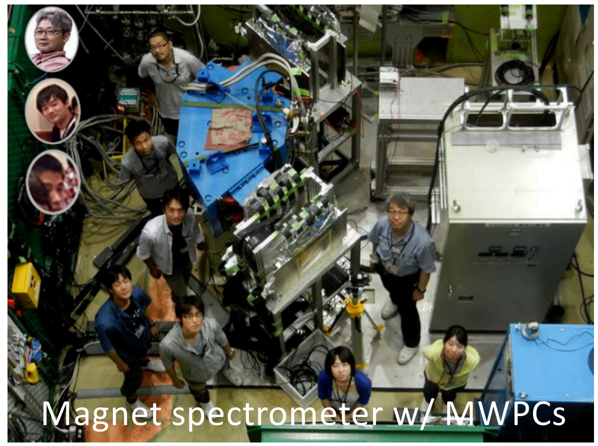

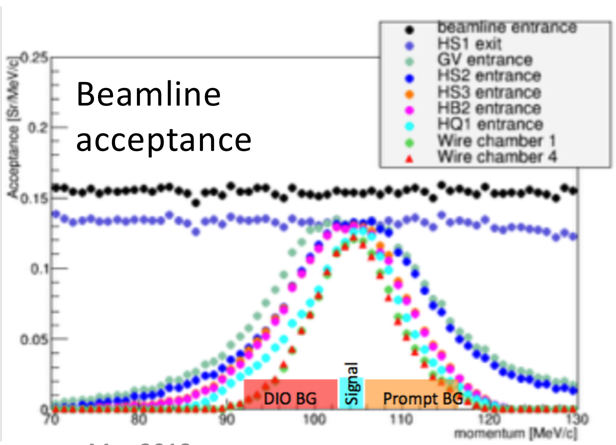

Simulated results with full data set

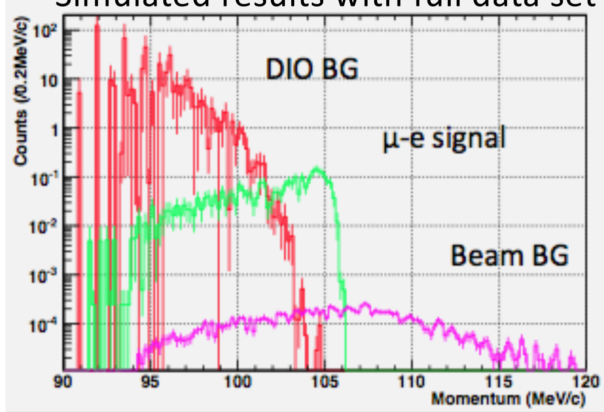

Signal Region: 102.0 -- 105.6 MeV/c

- New concept at JPARC
  - 3 GeV from RCS H-Line
- Use thick target as production, decay, and stopping volumes (graphite, SiC)
- Customize beam line to select momentum bite near $E_{\mu e} \sim m_\mu$ so that you're sensitive to $\mu N \rightarrow eN$ that occurs near the target surface
- Goal: $R_{\mu e} < 2 \times 10^{-14}$ @ 90%CL
  - 2-3y of running at 1 MW
  - Currently operating at ~400 kW

COMET Phase I & II

Summary of COMET phase-I/II

	COMET-Phase-I	COMET-Phase-II
experiment starts (*)	2020	~2022
beam intensity	3.2kW (8GeV)	56kW (8GeV)
running time	1.5×10^{6} (sec)	2.0×10^{7} (sec)
# of protons	3.8×10^{18}	8.5×10^{20}
# of muon stops	8.7×10^{15}	2.0×10^{18}
muon rate	5.8×10^{9}	1.0×10^{11}
# of muon stops / proton	0.0023	0.0023
# of BG	0.03	0.3
S.E.S.	3.1×10^{-15}	2.6×10^{-17}
U.L. (90%CL.)	7.0×10^{-15}	6.0×10^{-17}

(*) Engineering runs and Physics runs

The Mu2e Tracker

- Will employ straw technology
  - Low mass
  - Can reliably operate in vacuum
  - Robust against single-wire failures

- 5 mm diameter straw
- Spiral wound
- Walls: 12 μm Mylar + 3 μm epoxy + 200 Å Au + 500 Å Al
- 25 μm Au-plated W sense wire
- 33 – 117 cm in length
- 80/20 Ar/CO2 with HV < 1500 V

The Mu2e Tracker

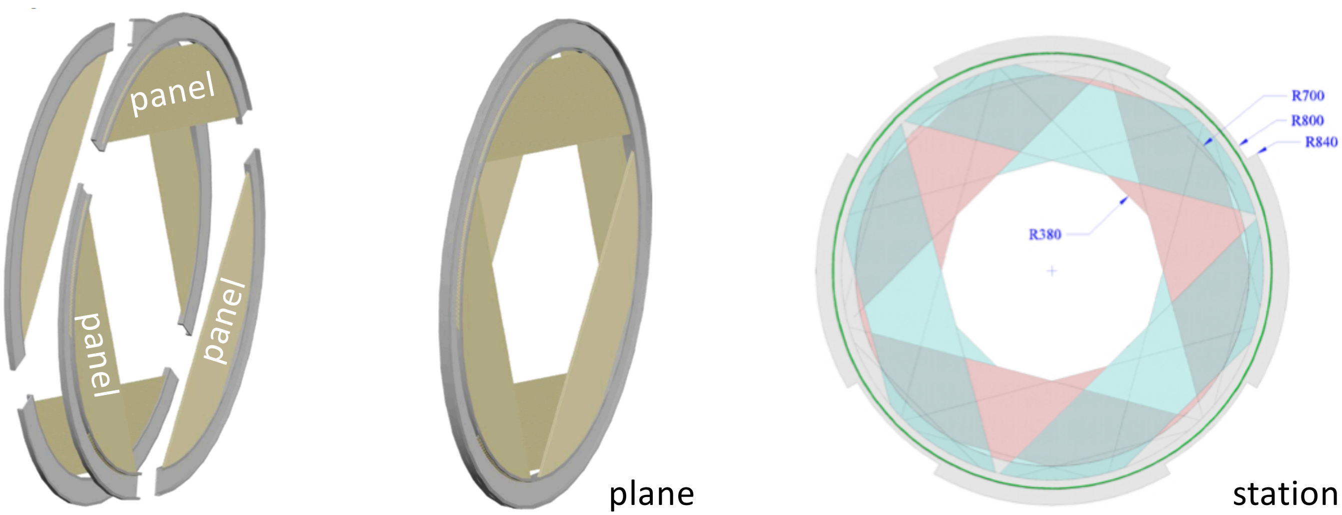

- Self-supporting "panel" consists of 100 straws
- 6 panels assembled to make a "plane"
- 2 planes assembled to make a "station"
- Rotation of panels and planes improves stereo information
- >20k straws total

The Mu2e Tracker

- 18 “stations” with straws transverse to the beam
- Naturally moves readout and support to large radii, out of the active volume

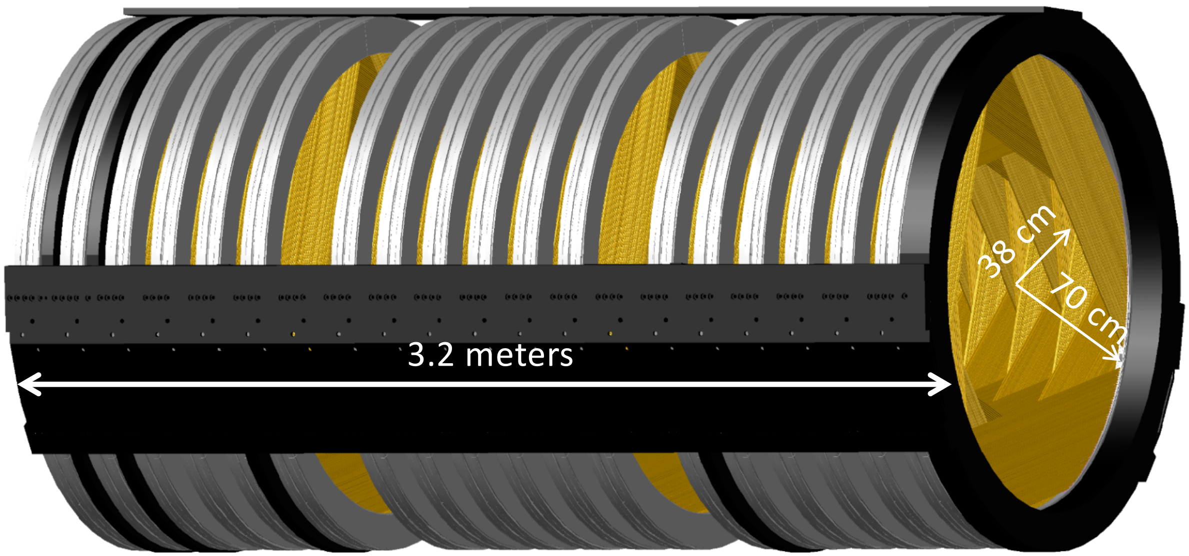

The Mu2e Tracker

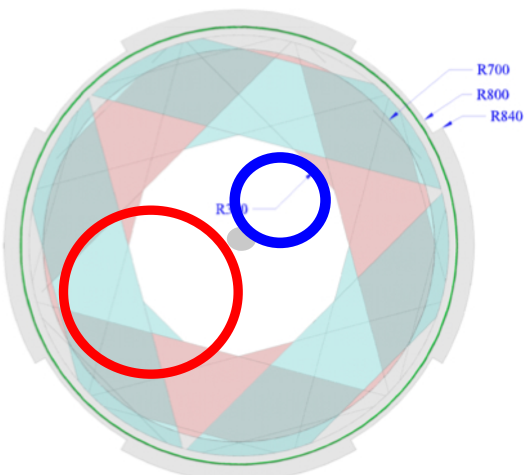

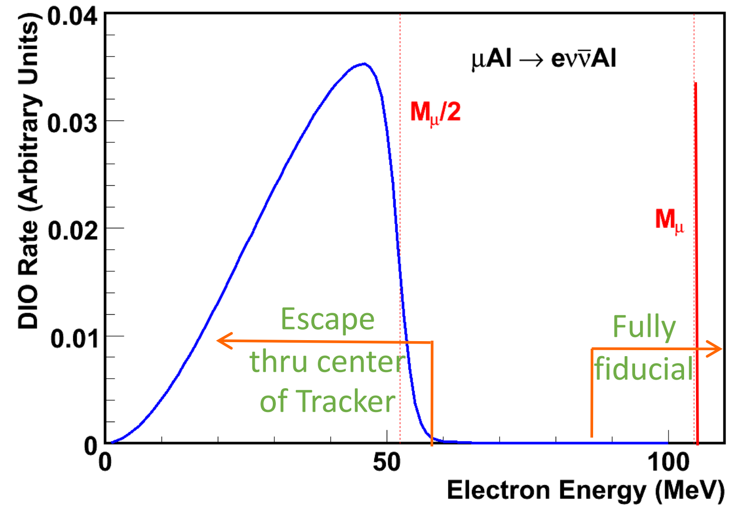

- Inner 38 cm is purposefully un-instrumented
  - Blind to beam flash
  - Blind to >99% of DIO spectrum

Mu2e Spectrometer Performance

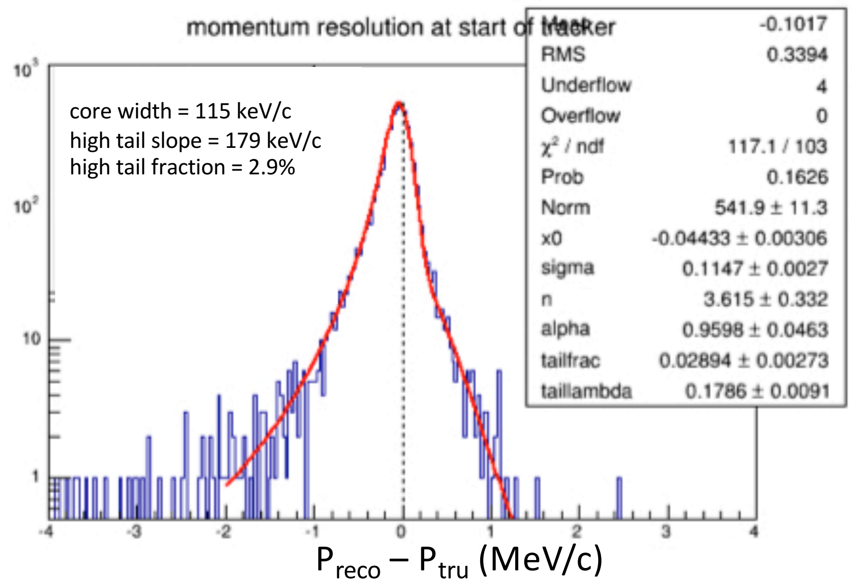

- Performance well within physics requirements

Mu2e Track Reconstruction and Selection

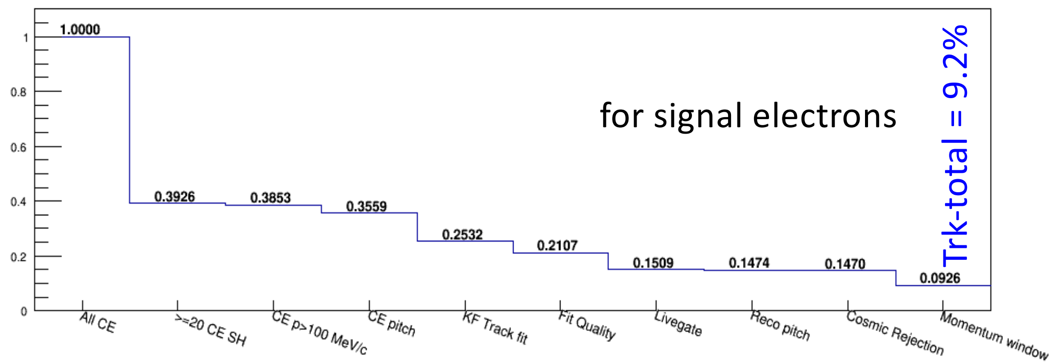

Inefficiency dominated by geometric acceptance

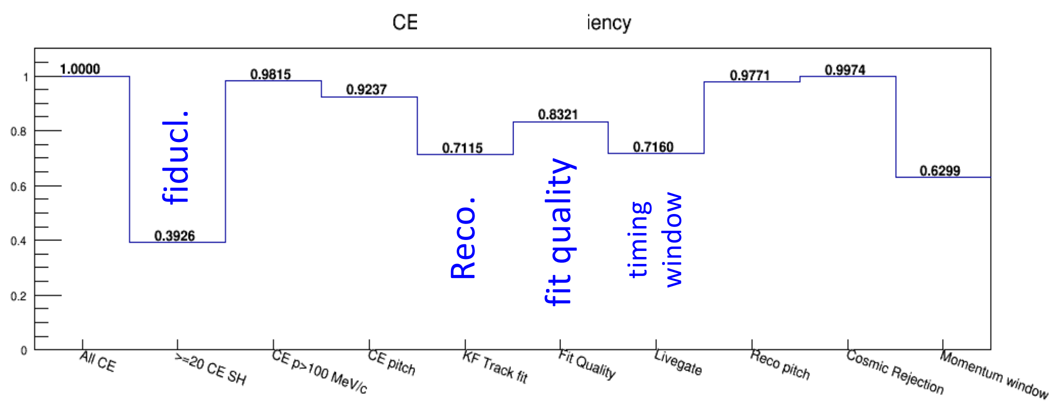

After calorimeter PID and CRV deadtime, Total = 8.5%

Mu2e Performance

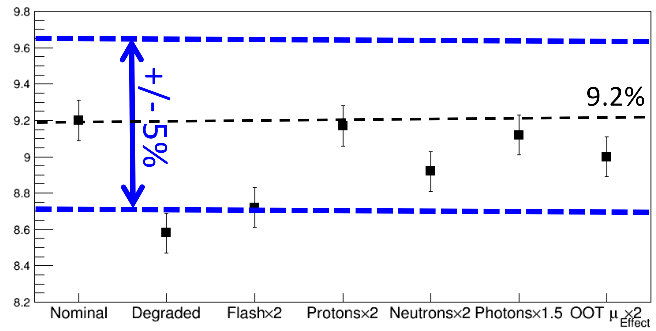

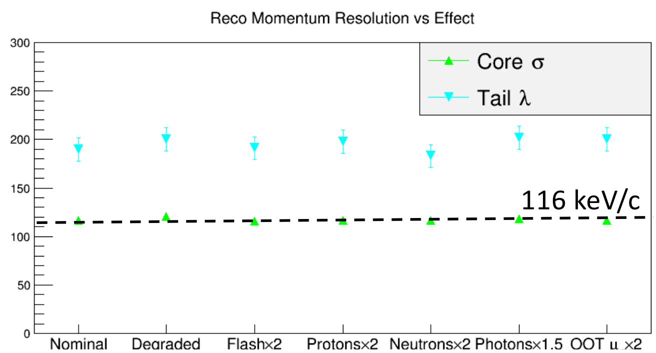

- Robust against increases in rate

Mu2e Calorimeter

- Baseline design : Cesium Iodide (CsI)
  - Radiation hard, fast, compact

	CsI
Density (g/cm3)	4.51
Radiation length (cm)	1.86
Moliere Radius (cm)	3.57
Interaction length (cm)	39.3
dE/dX (MeV/cm)	5.56
Refractive index	1.95
Peak luminescence (nm)	310
Decay time (ns)	26
Light yield (rel. to NaI)	3.6%
Variation with temperature	-1.4% / deg-C

Mu2e Calorimeter

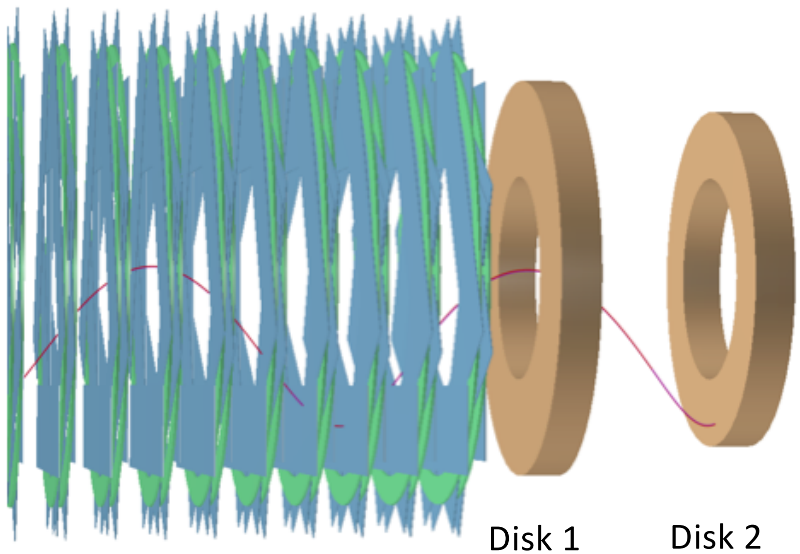

- Will employ 2 disks (radius = 36-70 cm)
- ~1400 crystals with square cross-section
  - ~3 cm diameter, ~20 cm long (10 X_0)
- Two photo-sensors/crystal on back (SiPMs)

Mu2e Calorimeter

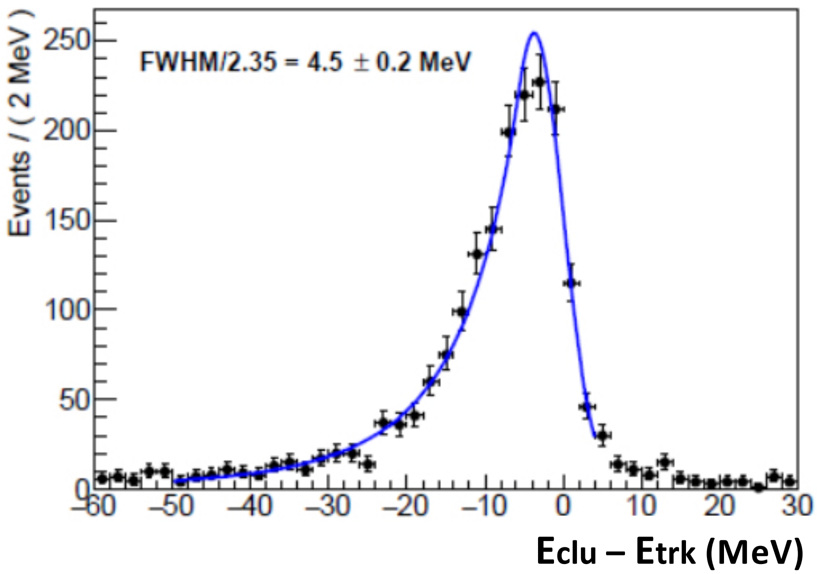

- With 60 ns integration, expect to achieve an energy resolution ~5% for 105 MeV electrons
  - Performance a weak function of rate in relevant range

Mu2e Cosmic-Ray Veto

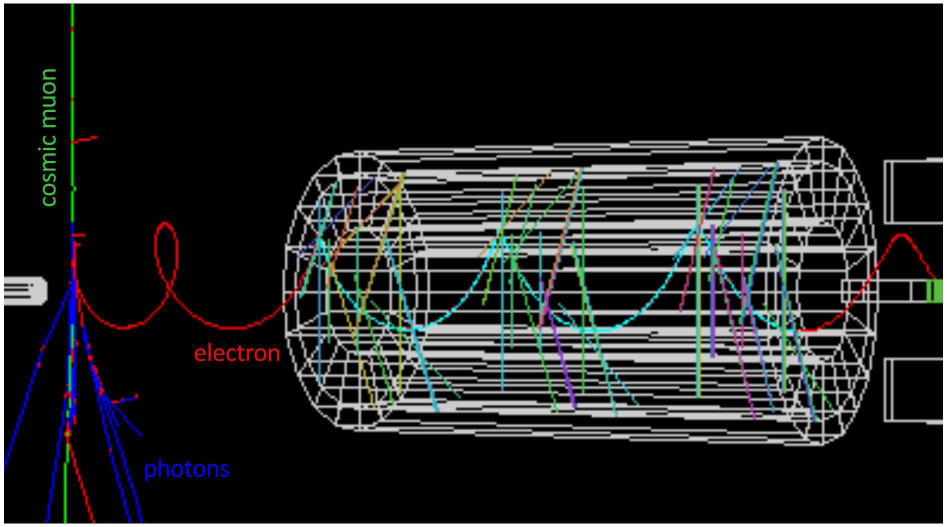

- Cosmic μ can generate background events via decay, scattering, or material interactions

Mu2e Cosmic-Ray Veto

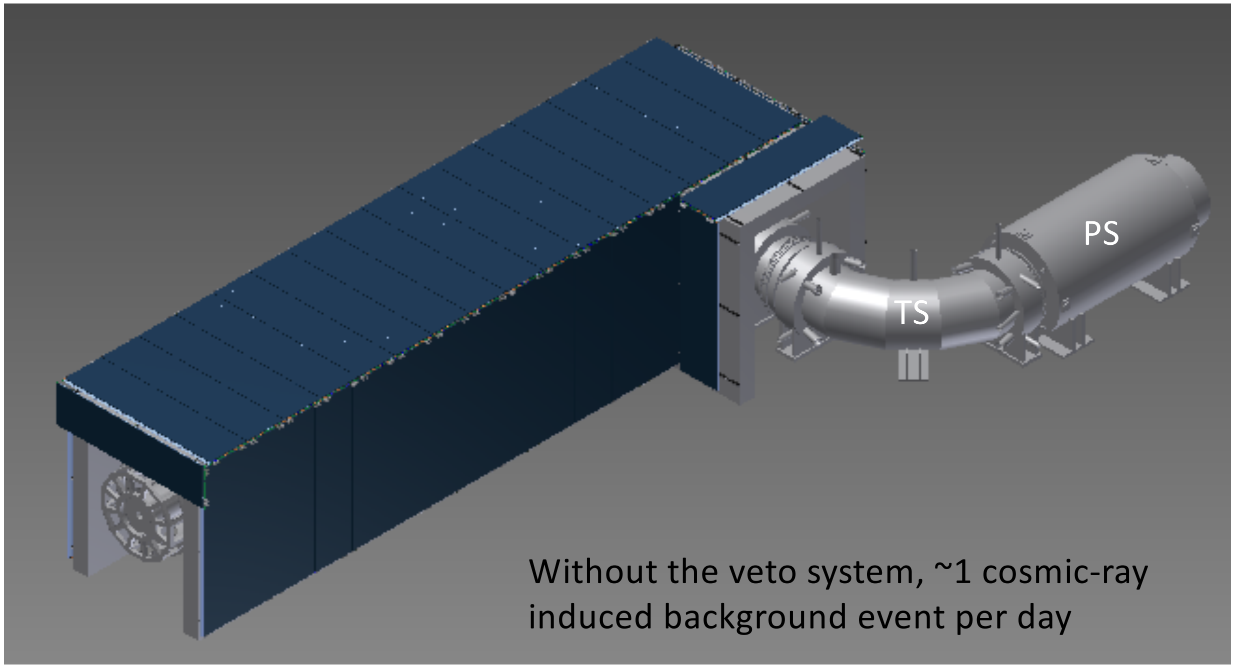

- Veto system covers entire DS and half TS

Mu2e Cosmic-Ray Veto

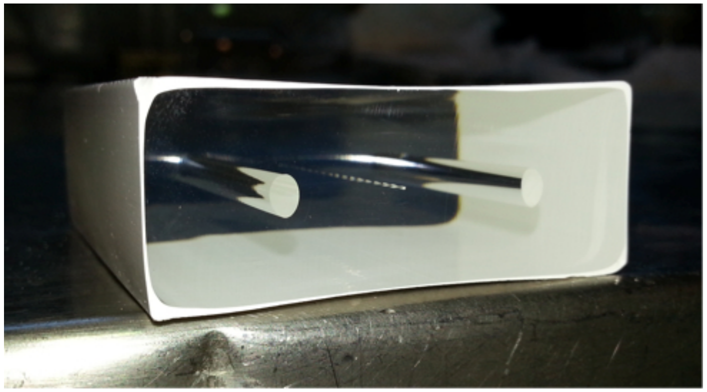

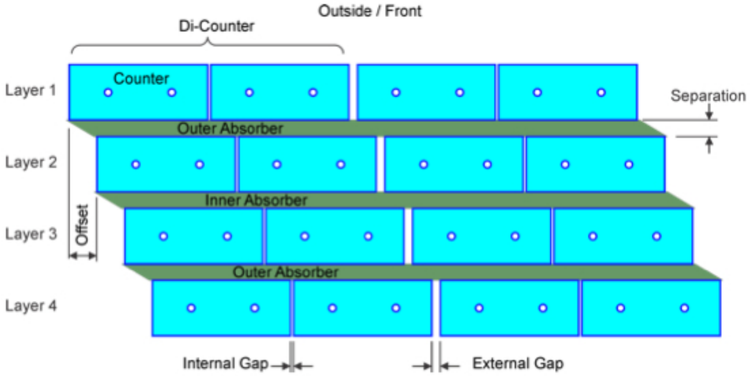

- Will use 4 overlapping layers of scintillator
  - Each bar is 5 x 2 x ~450 cm^3
  - 2 WLS fibers / bar
  - Read-out both ends of each fiber with SiPM
  - Have achieved $\varepsilon > 99.4\%$ (per layer) in test beam

Cosmic Ray Veto

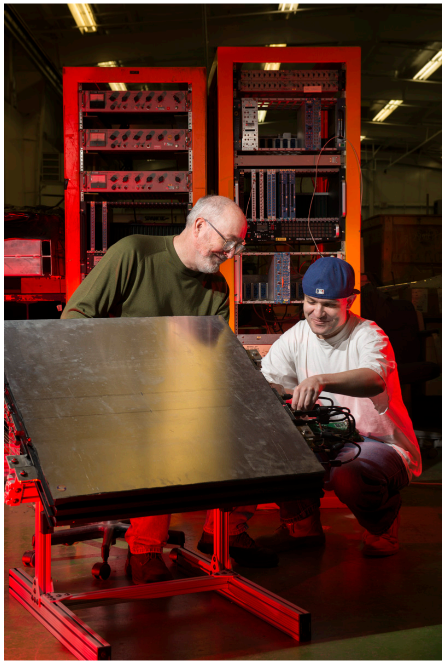

Typical light yield from CRV counter prototype – 20 cm from RO end

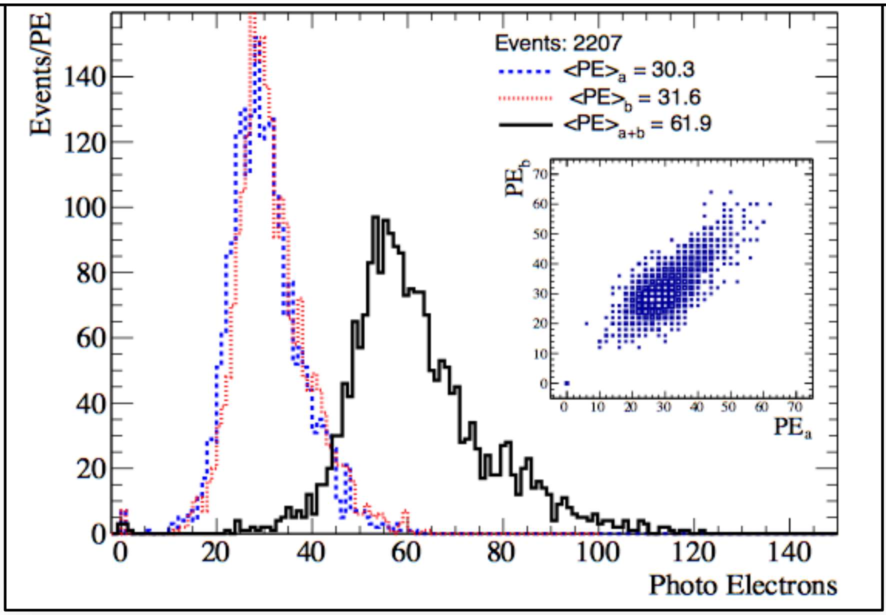

- Test beam data to vet design/performance

Mu2e Selection Requirements

Parameter	Requirement
Track quality and background rejection criteria	
Kalman Fit Status	Successful Fit
Number of active hits	$N_{active} \geq 25$
Fit consistency	$\chi 2$ consistency > $2x10^{-3}$
Estimated reconstructed momentum uncertainty	$\sigma_p < 250$ keV/c
Estimated track t_0 uncertainty	$\sigma_t < 0.9$ nsec
Track t_0 (livegate)	700 ns < t_0 < 1695 ns
Polar angle range (pitch)	$45° < \theta < 60°$
Minimum track transverse radius	-80 mm < d_0 < 105 mm
Maximum track transverse radius	450 mm < d_0+2/ω < 680 mm
Track momentum	103.75 < p < 105.0 MeV/c
Calorimeter matching and particle identification criteria	
Track match to a calorimeter cluster	$E_{cluster} > 10$ MeV $\chi 2$ (track-calo match) < 100
Ratio of cluster energy to track momentum	E/P < 1.15
Difference in track t_0 to calorimeter t_0	$\Delta t = \lvert t_{track} - t_{calo} \rvert < 3$ ns from peak
Particle identification	$\log(L(e)/L(\mu)) < 1.5$

- Full set of selection criteria employed to estimate backgrounds and sensitivity reported in TDR (Summer 2014)

Mu2e Systematic Uncertainties

Effect	Uncertainty in DIO background yield	Uncertainty in CE single-event-sensitivity ($\times 10^{-17}$)
MC Statistics	±0.02	±0.07
Theoretical Uncertainty	±0.04	-
Tracker Acceptance	±0.002	±0.03
Reconstruction Efficiency	±0.01	±0.15
Momentum Scale	+0.09, -0.06	±0.07
μ-bunch Intensity Variation	±0.007	±0.1
Beam Flash Uncertainty	±0.011	±0.17
μ-capture Proton Uncertainty	±0.01	±0.016
μ-capture Neutron Uncertainty	±0.006	±0.093
μ-capture Photon Uncertainty	±0.002	±0.028
Out-Of-Target μ Stops	±0.004	±0.055
Degraded Tracker	-0.013	+0.191
Total (in quadrature)	+0.10, -0.08	+0.35, -0.29

- Evaluated for all background sources

Mu2e Tracker Occupancy

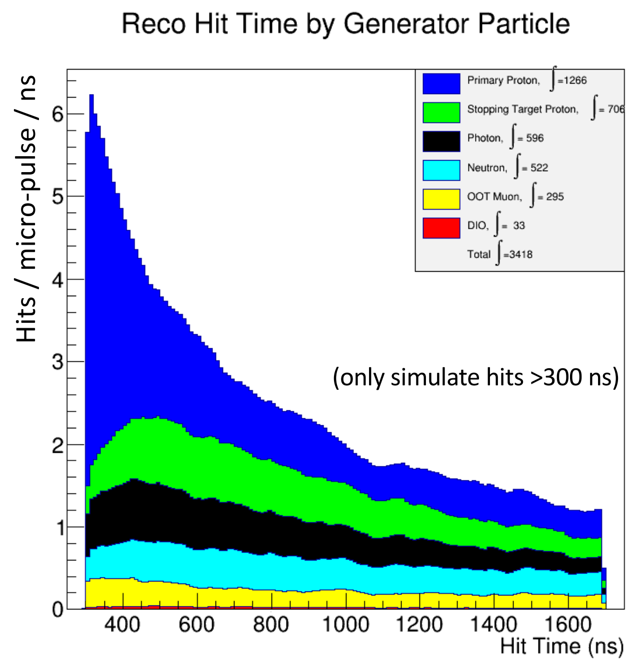

- Accidental occupancy from beam flash, μ capture products, out-of-target μ stops, etc.

Mu2e Signal Momentum Spectrum

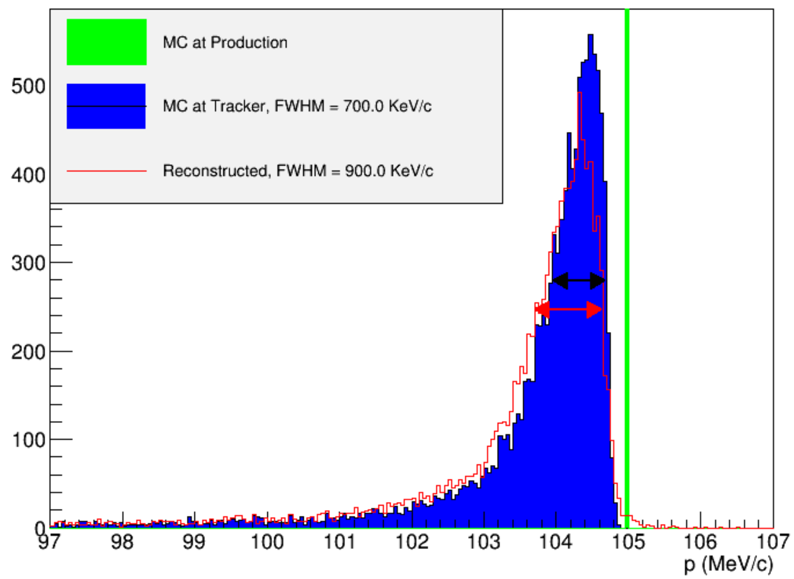

- Smearing dominated by interactions in stopping target and in (neutron/proton) absorbers upstream of tracker

False vetoes in Mu2e Cosmic Veto Counters

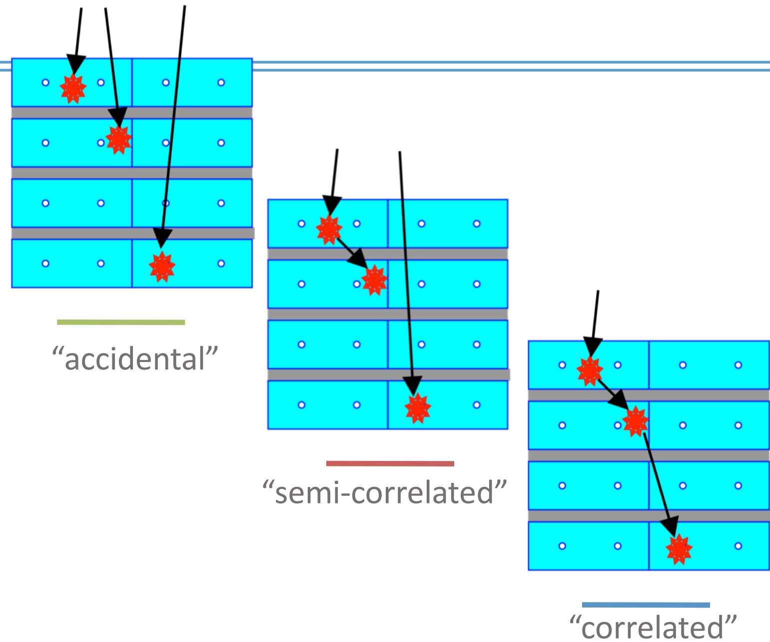

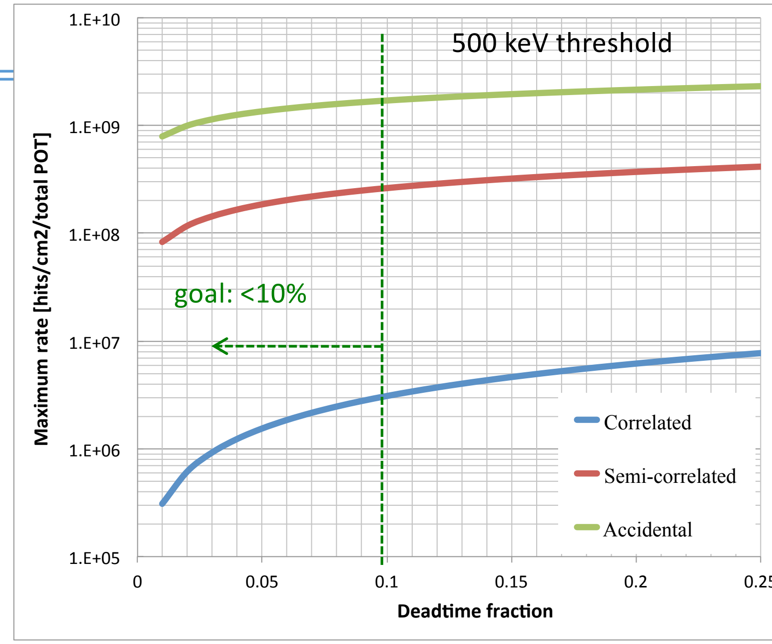

- We need to understand contributions from accidentals and correlated-accidentals
  - For neutrons and photons as a function of time, energy, timing resolution, and read-out threshold

Muon momentum distribution

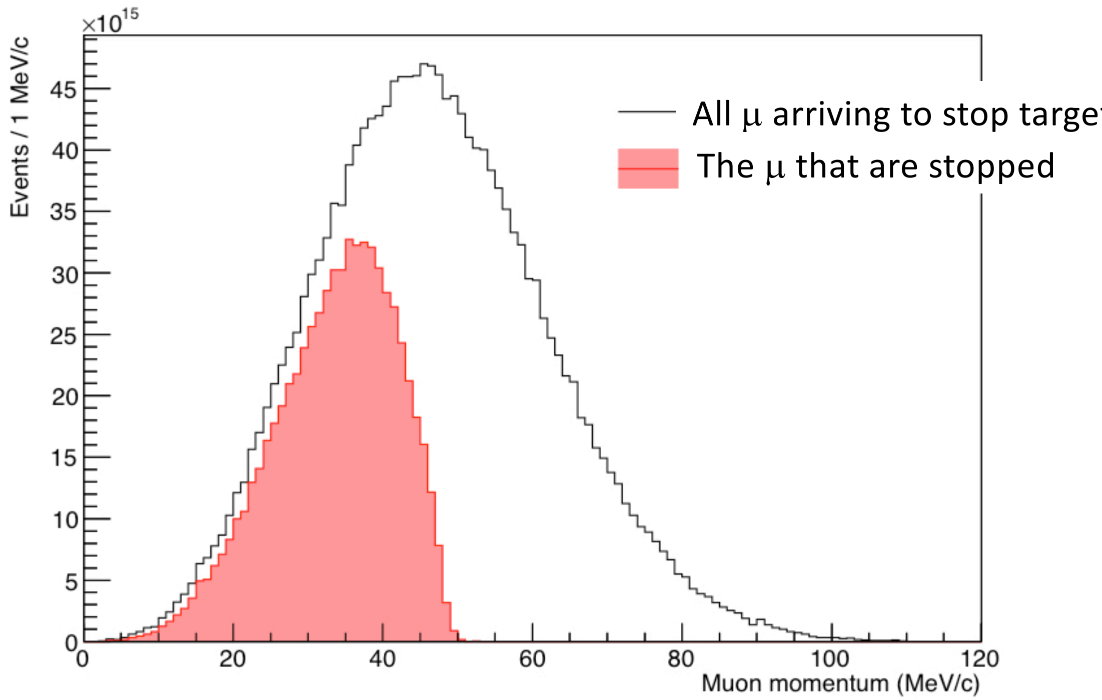

- The muons that stop are low momentum

Improving the Previous Experiment

- Current world's best limit on $\mu N \rightarrow eN$ is from SINDRUM-II:
  - W. Bertl, et al. (SINDRUM II Collaboration), Euro. Phys. C47 (2006) 337.
  - $R_{\mu e}(\mu N_{Au} \rightarrow eN_{Au}) < 7 \times 10^{-13}$ @ 90% CL (2006)
  - Limited by
    - Backgrounds from prompt pions
    - Stopped-μ rate (~10^7 μ/s using ~1 MW beam)
- Any improvement to SINDRUM-II needs to address these limitations

Improving the Previous Experiment

- In 1989 Lobashev and Djilkabaev published a paper proposing an experiment that solved these two problems by

  1. Utilizing a pulsed proton beam
  2. Employing solenoids to collect muons

- Mu2e is the realization of their proposed technique
  - Pulsed beam from the Fermilab accelerator complex
  - Solenoid system capable of delivering high intensity stopped-muon beam

Using Solenoids to Collect Muons

Courtesy of Andrei Gaponenko

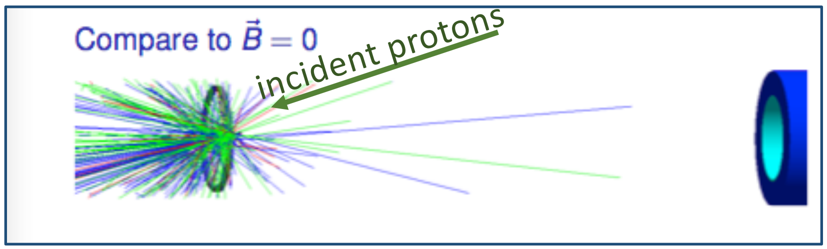

π production target

Transport & decay

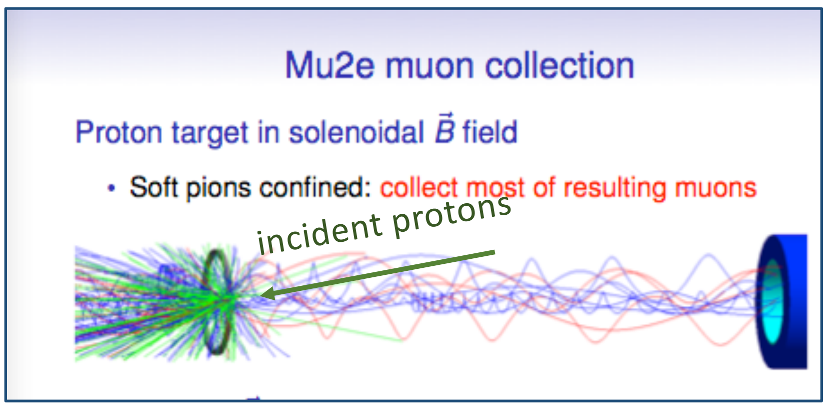

π production target

Transport & decay

- SINDRUM-II used ~1 MW beam to produce ~10^7 stopped μ/s

- Solenoids enable us to collect ~10^{10} μ/s using an 8kW beam.

Fermilab's Muon Campus

- New facilities to host muon experiments
  - Two new experimental halls and the associated beam lines
  - Will produce the world's highest intensity muon beams
  - Physics data taking has begun for Muon (g-2) experiment

Mu2e Solenoid Summary

	PS	TS	DS
Length (m)	4	13	11
Diameter (m)	1.7	0.4	1.9
Field @ start (T)	4.6	2.5	2.0
Field @ end (T)	2.5	2.0	1.0
Number of coils	3	52	11
Conductor (km)	14	44	17
Operating current (kA)	10	3	6
Stored energy (MJ)	80	20	30
Cold mass (tons)	11	26	8

- PS, DS is being built by General Atomics
- TS is being built by ASG + Fermilab

Mu2e Schedule

- Full scale solenoid construction has started
- Full scale detector construction ramping-up in 2018
- Solenoid and detector installation in 2019-2020
- Initial commissioning in 2021
- First physics running in 2022

- At full intensity
  - Reach Sindrum-II sensitivity in 100 min
  - x10 in 17 hours running
  - x100 in 7 days running
  - x10000 in 700 days running

Mu2e Collaboration

Spokespersons: Jim Miller (Boston), DG (Fermilab)

Over 200 Scientists from 37 Institutions

Argonne National Laboratory, Boston University, University of California Berkeley, University of California Davis, University of California Irvine, California Institute of Technology, City University of New York, Joint Institute of Nuclear Research Dubna, Duke University, Fermi National Accelerator Laboratory, Laboratori Nazionale di Frascati, University of Houston, Helmholtz-Zentrum Dresden-Rossendorf, INFN Genova, Institute for High Energy Physics, Protvino, Kansas State University, Lawrence Berkeley National Laboratory, INFN Lecce, University Marconi Rome, Lewis University, University of Liverpool, University College London, University of Louisville, University of Manchester, University of Minnesota, Muon Inc., Northwestern University, Institute for Nuclear Research Moscow, INFN Pisa, Northern Illinois University, Purdue University, Rice University, Sun Yat-Sen University, University of South Alabama, Novosibirsk State University/Budker Institute of Nuclear Physics, University of Virginia, University of Washington, Yale University

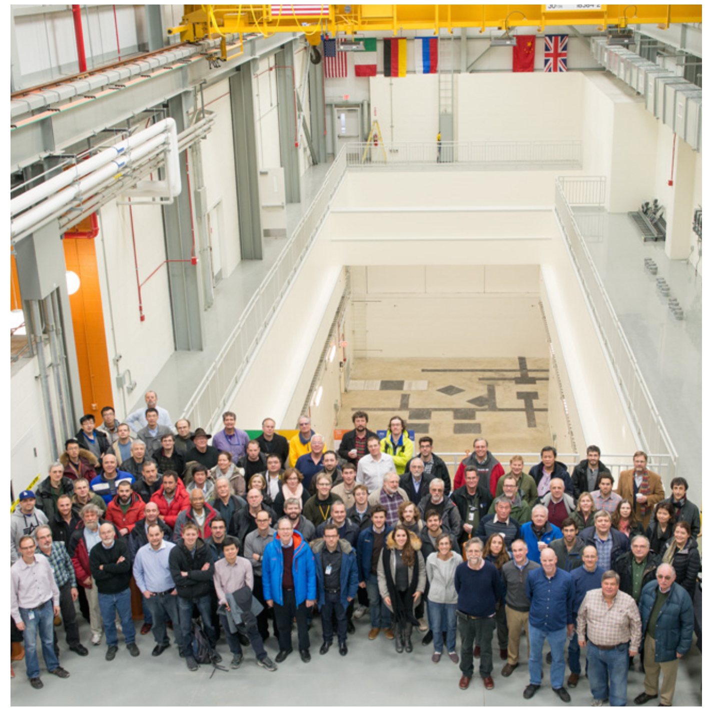

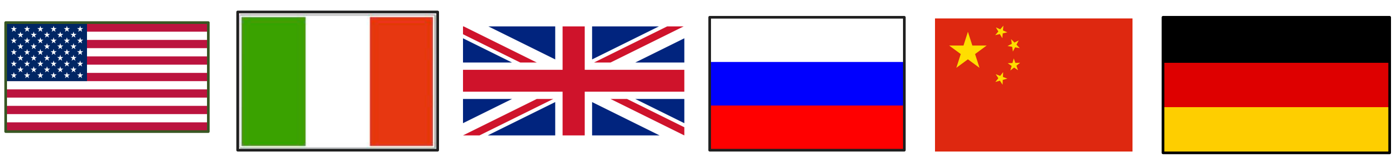

$h \rightarrow \tau$ constraints from $\mu \rightarrow e$ CLFV

$\tau\mu$-τe couplings can contribute to $\mu \rightarrow e$ transitions. As an example:

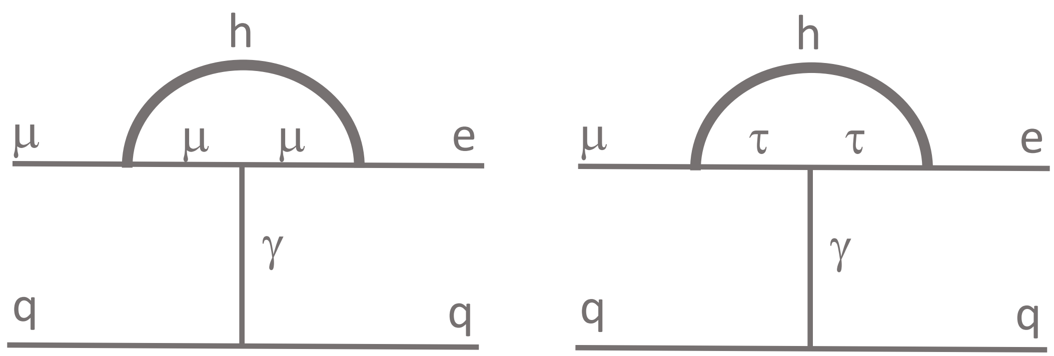

- $\mu \rightarrow e\gamma$ constrains dipole contributions
- $\mu^- N \rightarrow e^- N$ constrains vector contributions
- Future improvements in $\mu^- N \rightarrow e^- N$ will probe $B(h \rightarrow \tau\mu)B(h \rightarrow \tau e) < 10^{-7}$

cf. I.Dorsner, S. Fajfer, A. Greljo, J. Kamenik, N, Kosnik, I. Nisandzic, JHEP 1506 (2015) 108; (1502.07784).
R. Harnik, J. Kopp, J. Supan (1209.1397).

Direct Searches for CLFV h decays

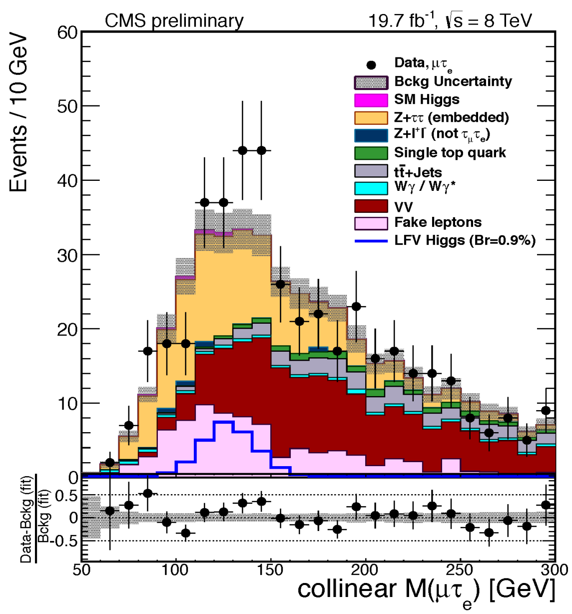

CMS

B(h→τμ) < 1.51 x 10^{-2}

Best fit : (0.84 +/- 0.40)%

ATLAS

B(h→τμ) < 1.43 x 10^{-2}

Best fit : (0.53 +/- 0.51)%

- Looking forward to the updated analysis…

NP Contributions to CLFV

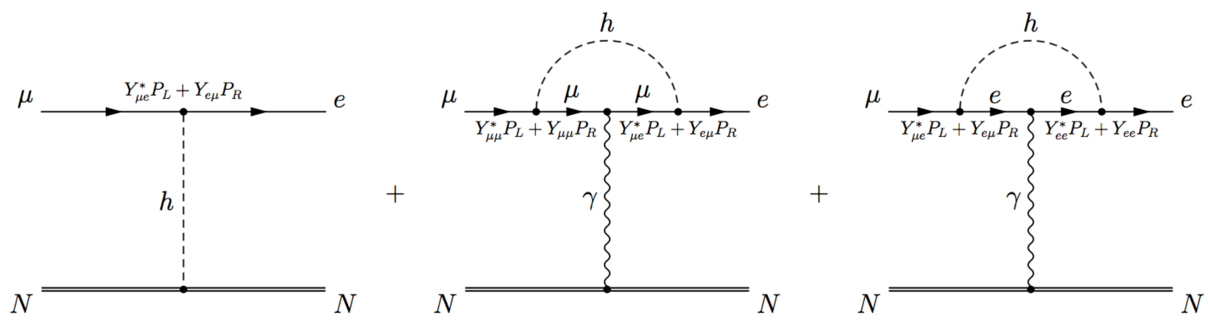

- As has been discussed, LFV higgs couplings will contribute

CLFV using taus

cLFV Experiments using taus

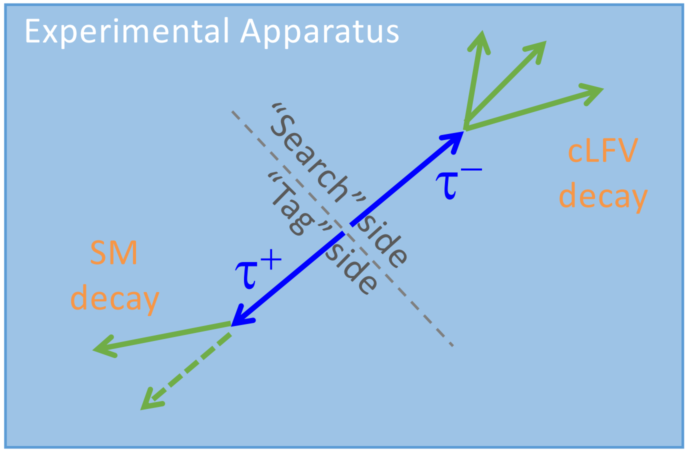

Sensitivity dominated by Belle & BaBar

cLFV Experiments using taus

Physics process	Cross section (nb)
$\Upsilon(4S) \to B\bar{B}$	1.2
$e^+e^- \to$ continuum	2.8
$\mu^+\mu^-$	0.8
$\tau^+\tau^-$	0.8
Bhabha ($\theta_{\mathrm{lab}} \geq 17^\circ$)	44
$\gamma\gamma$ ($\theta_{\mathrm{lab}} \geq 17^\circ$)	2.4
2γ processes [b]	~ 80
Total	~ 130

$\tau^+\tau^-$ production cross section ~ 1 nb

Latest results use 500-800 fb^{-1} ~ 500-800M $\tau^+\tau^-$ pairs

cLFV Experiments using taus

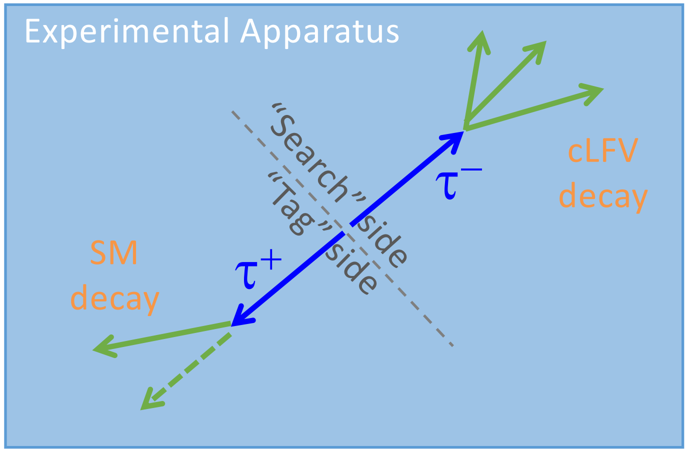

- Exploit (E,p) constraints available at e^+e^- collider
- On Search side: $m_{reco} = m_\tau$, $E_{reco} = E_{beam}$ (in CM)
- Employ excellent particle identification algorithms
- Additional requirements to suppress qq, $\mu\mu$, ee, $\gamma\gamma$

Some cLFV Results

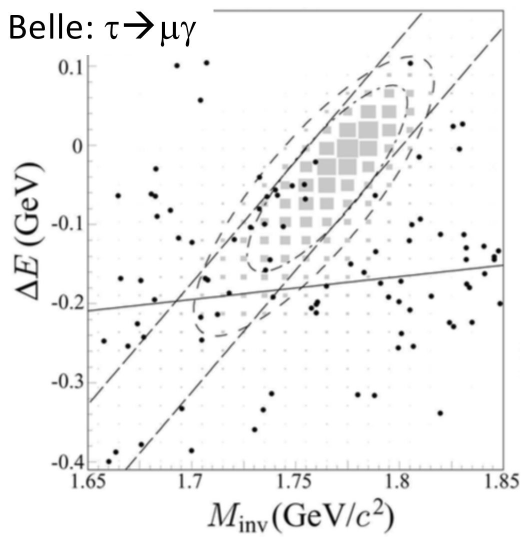

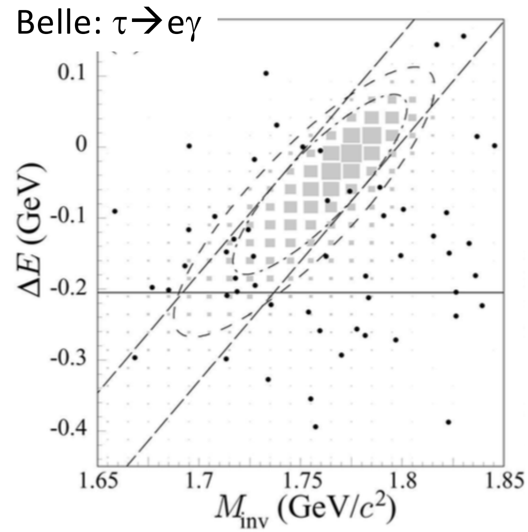

- Data gnal MC

  Inner (outer) ellipse : Signal (blinded) region

  - No significant excess is observed
  - $\tau \rightarrow e\gamma$, $\mu\gamma$ already observe background

Some cLFV Results

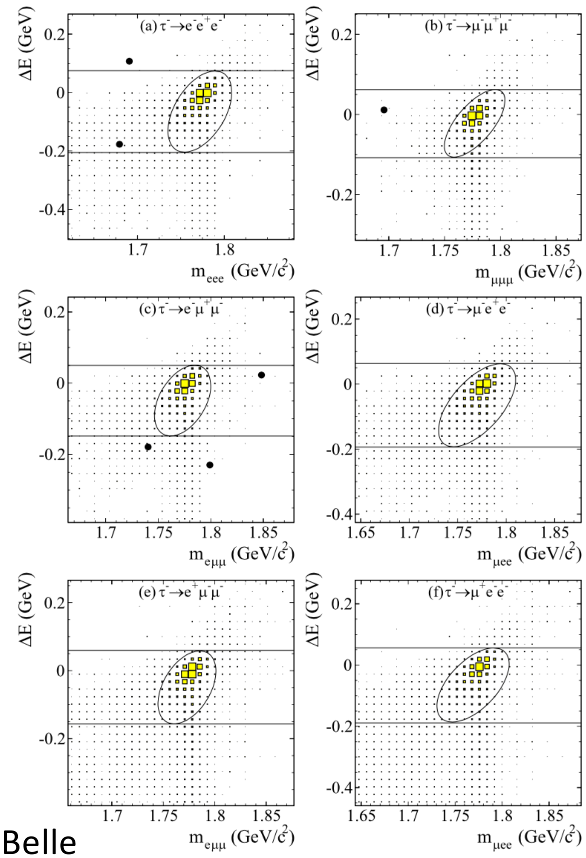

Belle

- Data

Signal MC

Ellipse = Signal Region

Solid lines : m_{reco} sidebands

- $\tau \rightarrow$ 3 leptons very clean
- No events in signal region

cLFV tau decays at LHCb

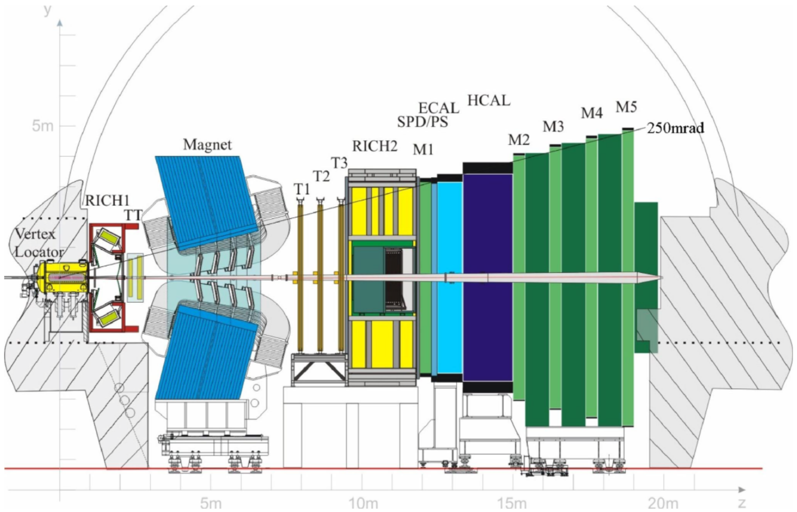

- Lots of τ from $b \rightarrow \tau \nu X$ and $c \rightarrow \tau \nu X$
- Effective cross section of 85 μb
- Competitive $\tau \rightarrow \mu\mu\mu$ sensitivity

cLFV Result

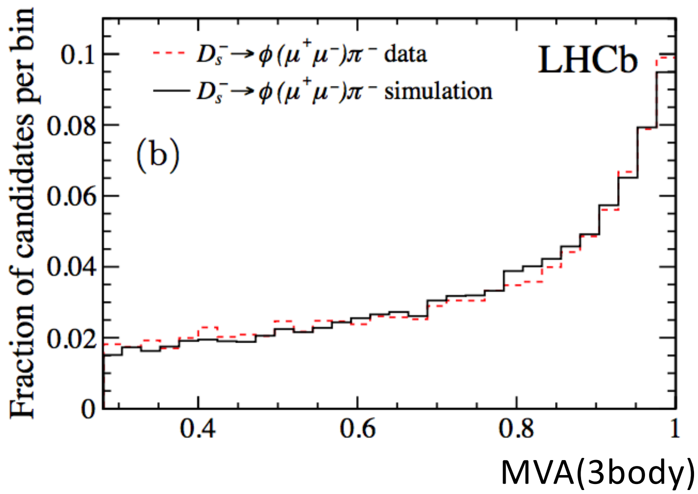

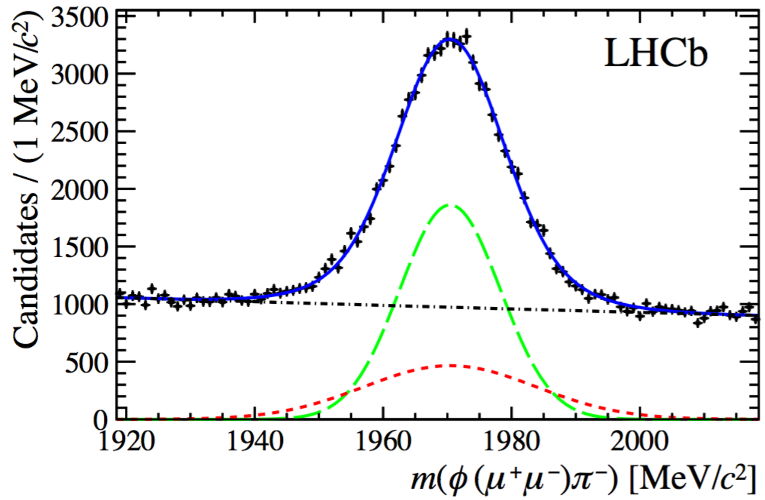

$$\mathcal{B}\left(\tau^- \to \mu^-\mu^+\mu^-\right) = \frac{\mathcal{B}\left(D_s^- \to \phi\left(\mu^+\mu^-\right)\pi^-\right)}{\mathcal{B}\left(D_s^- \to \tau^-\bar{\nu}_\tau\right)} \times f_\tau^{D_s} \times \frac{\epsilon_{\text{cal}}^{\text{R}}}{\epsilon_{\text{sig}}^{\text{R}}} \times \frac{\epsilon_{\text{cal}}^{\text{T}}}{\epsilon_{\text{sig}}^{\text{T}}} \times \frac{N_{\text{sig}}}{N_{\text{cal}}} \equiv \alpha N_{\text{sig}}\,,$$

- Normalized to $D_s \to \phi\pi \to (\mu\mu)\pi$

cLFV Result

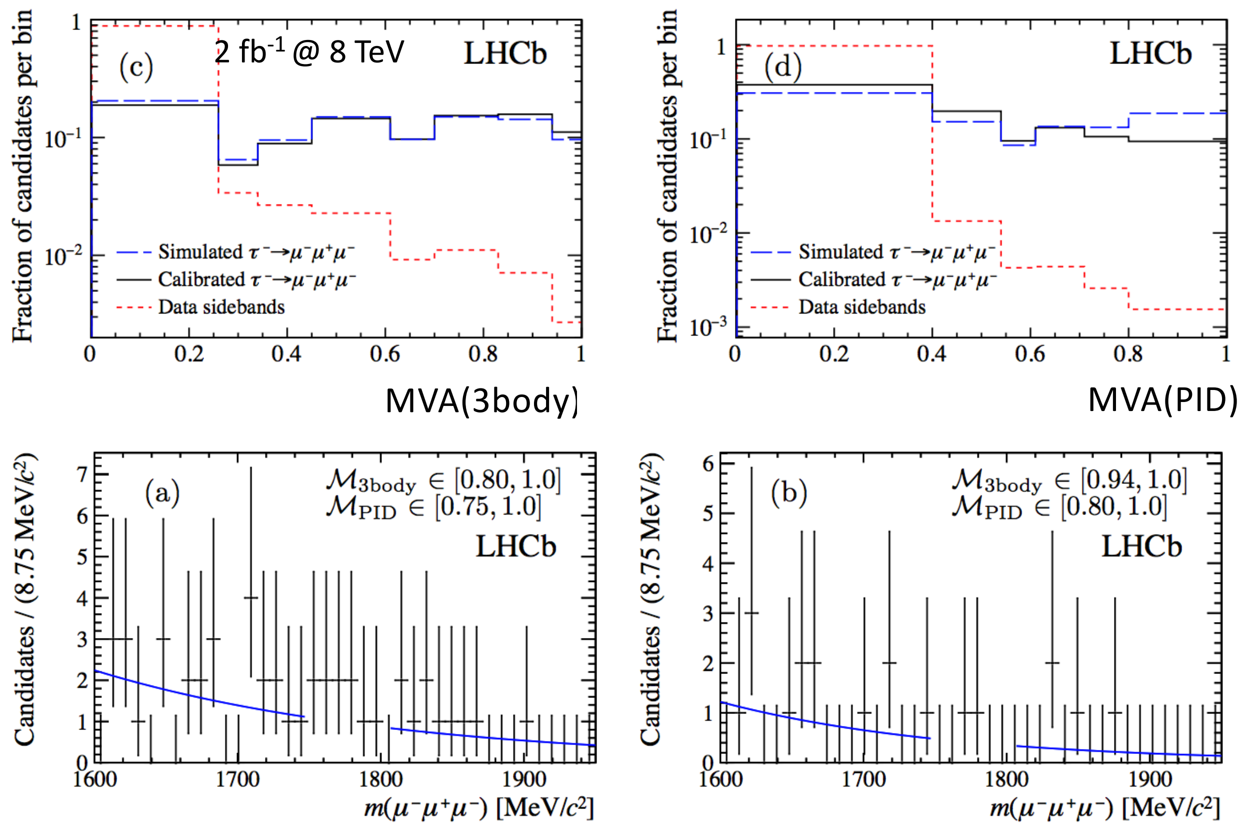

- 3D lhood fit ($M_{\mu\mu\mu}$, MVA_{3body}, MVA_{PID})

Most Recent HFAG Results

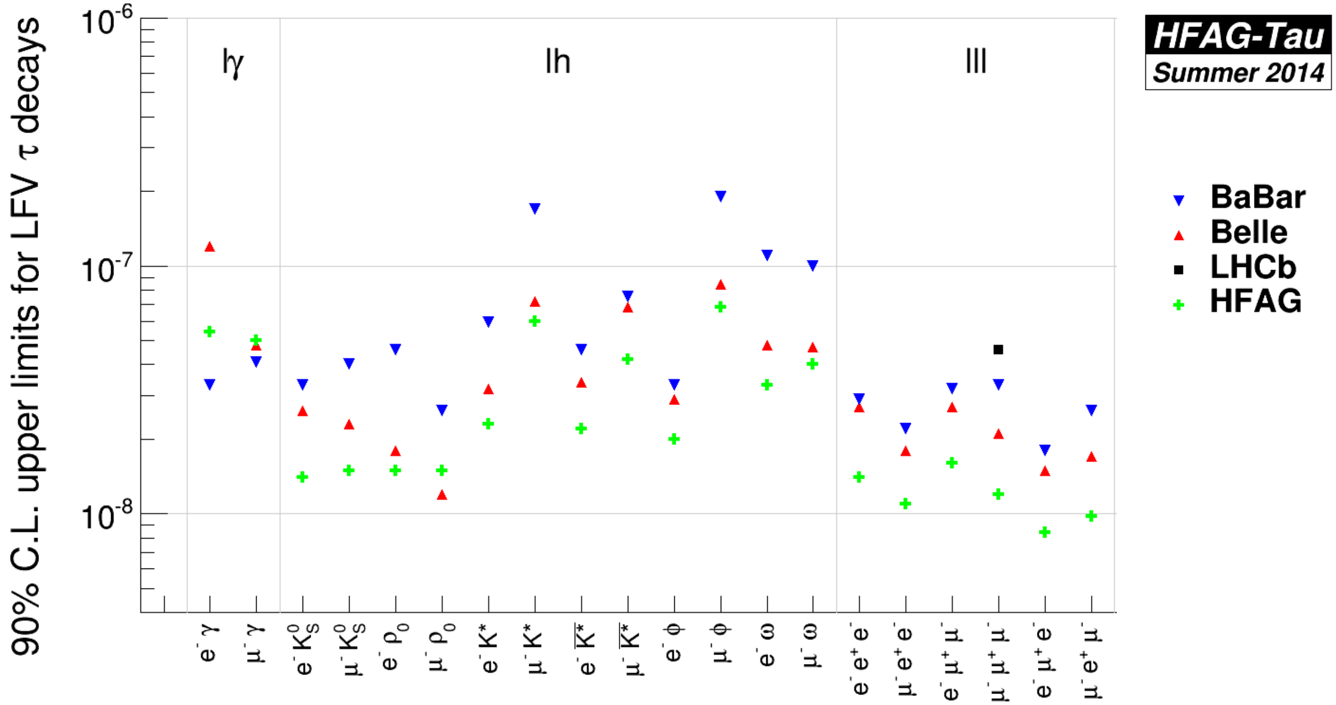

Future Sensitivity

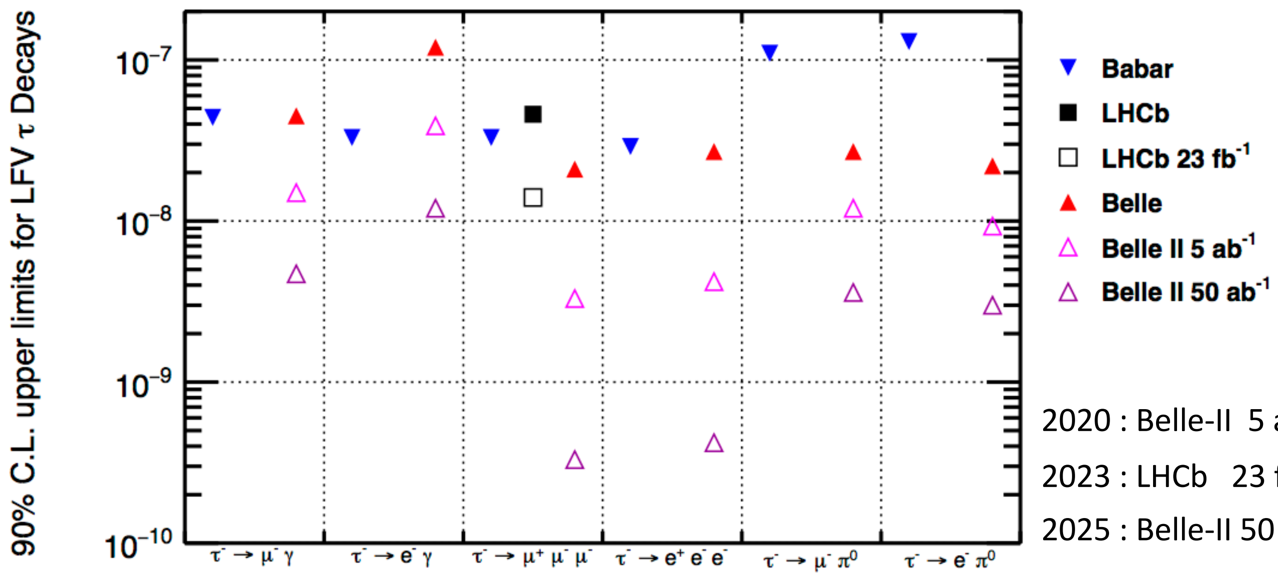

2020 : Belle-II 5 ab^{-1}

2023 : LHCb 23 fb^{-1}

2025 : Belle-II 50 ab^{-1}

LHCb $\tau \to \mu\mu\mu$ Results

Table 1: Terms entering into the normalisation factors, α, and their combined statistical and systematic uncertainties.

	7 TeV	8 TeV
$\mathcal{B}(D_s^- \to \phi(\mu^+\mu^-)\pi^-)$	$(1.32 \pm 0.10) \times 10^{-5}$	
$\mathcal{B}(D_s^- \to \tau^-\bar{\nu}_\tau)$	$(5.61 \pm 0.24) \times 10^{-2}$	
$f_\tau^{D_s}$	0.78 ± 0.04	0.80 ± 0.03
${\epsilon_{\text{cal}}}^{\text{R}}/{\epsilon_{\text{sig}}}^{\text{R}}$	0.898 ± 0.060	0.912 ± 0.054
${\epsilon_{\text{cal}}}^{\text{T}}/{\epsilon_{\text{sig}}}^{\text{T}}$	0.659 ± 0.006	0.525 ± 0.040
N_{cal}	$28\,200 \pm 440$	$52\,130 \pm 700$
α	$(7.20 \pm 0.98) \times 10^{-9}$	$(3.37 \pm 0.50) \times 10^{-9}$

$$\mathcal{B}(\tau^- \to \mu^-\mu^+\mu^-) = \frac{\mathcal{B}(D_s^- \to \phi(\mu^+\mu^-)\pi^-)}{\mathcal{B}(D_s^- \to \tau^-\bar{\nu}_\tau)} \times f_\tau^{D_s} \times \frac{\epsilon_{\text{cal}}^{\text{R}}}{\epsilon_{\text{sig}}^{\text{R}}} \times \frac{\epsilon_{\text{cal}}^{\text{T}}}{\epsilon_{\text{sig}}^{\text{T}}} \times \frac{N_{\text{sig}}}{N_{\text{cal}}} \equiv \alpha N_{\text{sig}} ,$$

LHCb $\tau \rightarrow \mu\mu\mu$ Results (2fb^{-1} @ 8TeV)

Table 3: Expected background candidate yields in the 8 TeV data set, with their uncertainties, and observed candidate yields within the τ^- signal window in the different bins of classifier response. The classifier responses range from 0 (most background-like) to +1 (most signal-like). The first bin in each classifier response is excluded from the analysis.

$\mathcal{M}_{\mathrm{PID}}$ response	$\mathcal{M}_{\mathrm{3body}}$ response	Expected	Observed
0.40 – 0.54	0.26 – 0.34	39.6 ± 2.3	39
	0.34 – 0.45	32.2 ± 2.1	34
	0.45 – 0.61	28.7 ± 2.0	28
	0.61 – 0.70	9.7 ± 1.2	5
	0.70 – 0.83	11.4 ± 1.3	7
	0.83 – 0.94	7.3 ± 1.1	6
	0.94 – 1.00	6.0 ± 1.0	0
0.54 – 0.61	0.26 – 0.34	13.6 ± 1.4	8
	0.34 – 0.45	12.1 ± 1.3	12
	0.45 – 0.61	8.3 ± 1.0	13
	0.61 – 0.70	2.60 ± 0.62	1
	0.70 – 0.83	1.83 ± 0.60	5
	0.83 – 0.94	2.93 ± 0.72	6
	0.94 – 1.00	2.69 ± 0.63	3
0.61 – 0.71	0.26 – 0.34	13.5 ± 1.4	7
	0.34 – 0.45	10.9 ± 1.2	11
	0.45 – 0.61	9.7 ± 1.2	12
	0.61 – 0.70	3.35 ± 0.69	2
	0.70 – 0.83	4.60 ± 0.89	5
	0.83 – 0.94	4.09 ± 0.81	4
	0.94 – 1.00	2.78 ± 0.68	1
0.71 – 0.80	0.26 – 0.34	7.8 ± 1.1	6
	0.34 – 0.45	7.00 ± 0.99	8
	0.45 – 0.61	6.17 ± 0.95	6
	0.61 – 0.70	1.57 ± 0.56	2
	0.70 – 0.83	2.99 ± 0.72	0
	0.83 – 0.94	3.93 ± 0.81	0
	0.94 – 1.00	3.22 ± 0.68	1
0.80 – 1.00	0.26 – 0.34	5.12 ± 0.86	3
	0.34 – 0.45	4.44 ± 0.79	6
	0.45 – 0.61	3.80 ± 0.78	5
	0.61 – 0.70	2.65 ± 0.68	2
	0.70 – 0.83	3.05 ± 0.67	2
	0.83 – 0.94	1.74 ± 0.54	2
	0.94 – 1.00	3.36 ± 0.70	3

Data are consistent with Background expectations

LHCb $\tau \rightarrow \mu\mu\mu$ Results (1fb^{-1} @ 7TeV)

Table 2: Expected background candidate yields in the 7 TeV data set, with their uncertainties, and observed candidate yields within the τ^- signal window in the different bins of classifier response. The classifier responses range from 0 (most background-like) to +1 (most signal-like). The first bin in each classifier response is excluded from the analysis.

$\mathcal{M}_{\text{PID}}$ response	$\mathcal{M}_{\text{3body}}$ response	Expected	Observed
0.40 – 0.45	0.28 – 0.32	3.17 ± 0.66	4
	0.32 – 0.46	9.2 ± 1.1	6
	0.46 – 0.54	2.89 ± 0.63	6
	0.54 – 0.65	3.17 ± 0.66	4
	0.65 – 0.80	3.64 ± 0.72	2
	0.80 – 1.00	3.79 ± 0.80	3
0.45 – 0.54	0.28 – 0.32	4.22 ± 0.78	6
	0.32 – 0.46	8.3 ± 1.1	10
	0.46 – 0.54	2.3 ± 0.57	4
	0.54 – 0.65	2.83 ± 0.63	8
	0.65 – 0.80	2.72 ± 0.69	5
	0.80 – 1.00	4.83 ± 0.90	7
0.54 – 0.63	0.28 – 0.32	2.33 ± 0.58	6
	0.32 – 0.46	8.3 ± 1.1	8
	0.46 – 0.54	2.07 ± 0.53	1
	0.54 – 0.65	3.29 ± 0.68	1
	0.65 – 0.80	2.96 ± 0.65	4
	0.80 – 1.00	3.11 ± 0.69	3
0.63 – 0.75	0.28 – 0.32	2.69 ± 0.62	1
	0.32 – 0.46	7.5 ± 1.0	5
	0.46 – 0.54	2.06 ± 0.53	3
	0.54 – 0.65	2.00 ± 0.55	5
	0.65 – 0.80	3.16 ± 0.66	2
	0.80 – 1.00	4.67 ± 0.84	2
0.75 – 1.00	0.28 – 0.32	2.19 ± 0.55	2
	0.32 – 0.46	3.38 ± 0.76	5
	0.46 – 0.54	1.52 ± 0.46	3
	0.54 – 0.65	1.28 ± 0.47	1
	0.65 – 0.80	2.78 ± 0.65	1
	0.80 – 1.00	4.42 ± 0.83	7

Data are consistent with Background expectations